

BIM-Based Seismic Loss Assessment for Instrumented Buildings

Sam Bahmanoo

A thesis

In the Department

Of

Building, Civil and Environmental Engineering

(BCEE)

Presented in Partial Fulfillment of the Requirements

For the Degree of Master of Applied Science at

Concordia University

Montreal, Quebec, Canada

August 2021

© Sam Bahmanoo, 2021

CONCORDIA UNIVERSITY

School of Graduate Studies

This is to certify that this thesis is prepared

By: Sam Bahmanoo

Entitled: BIM-Based Seismic Loss Assessment for Instrumented Buildings

and submitted in partial fulfillment of the requirements for the degree of

Master of Applied Science (Civil Engineering)

complies with the regulations of the University and meets the accepted standards with respect to originality and quality.

Signed by the final examining committee:

_____ Chair
Dr. Ashutosh Bagchi

_____ Examiner
Dr. Lucia Tirca

_____ Examiner
Dr. Mazdak Nik-Bakht

_____ Thesis Supervisor
Dr. Ashutosh Bagchi

Approved by _____
Dr. Michelle Nokken

August 31, 2021

Dr. Mourad Debbabi, Dean
Gina Cody School of Engineering & Computer Science

ABSTRACT

BIM-Based Loss Assessment for Instrumented Buildings

Sam Bahmanoo

A look at the most devastating earthquakes ever reported, emphasizes the essentiality of forecasting earthquake-induced loss of buildings with predictable seismic performances. This perspective is mostly adopted in performance-based earthquake engineering (PBEE) loss assessment frameworks. The current generation of PBEE framework developed by the Pacific Earthquake Engineering Research (PEER) center, PEER-PBEE (also known as FEMA P-58) is a state-of-the-art methodology among all the PBEE frameworks. It contains four stages of hazard analysis, structural analysis, damage analysis and loss analysis to predict the seismic loss estimation of buildings in terms of repair cost, downtime, and other decision variables. However, despite its numerous advantages, the quality of the PEER-PBEE framework can significantly be affected due to considerable sources of uncertainties. Lack of actual structural performance characteristics (structural analysis) and ineffective details of building components (damage analysis) are the main reasons identified by the previous studies to the incorporated uncertainties. Moreover, some attempts have been made before to employ innovative technologies such as seismic instrumentation and integrated BIM tools to tackle the associated uncertainties in structural and damage analysis, respectively. However, yet, no comprehensive systematic methodology has been dedicated to the full engagement of seismic instrumentation and integrated BIM tools in PBEE-based loss assessment frameworks. This objective of the thesis is to develop a systematic methodology to address the limitations associated with PEER-PBEE loss assessment framework by adopting innovative technologies such as seismic instrumentation of buildings and integrated BIM tools. For this purpose, a workflow of seismic loss estimation is developed for buildings with three main steps, including: (1) the measurement of structural dynamic response throughout an ambient vibration test and subsequent output-only system identification (SI), (2) experimental

structural analysis by both the model-based and nonmodel-based approaches (3) automated seismic loss analysis through the developed Application Programming Interface (API) tool in BIM platform (based on FEMA P-58 framework). Moreover, the full functionality of the proposed methodology is validated through a real case study located in Montreal, Canada.

Consequently, this study demonstrates the added values of the systematic utilization of seismic instrumentation as well as BIM-based API technology in seismic vulnerability assessment of buildings, which leads to a better interpretation of loss consequence predictions and subsequent decision-making process in disastrous situations.

Acknowledgments

I would like to acknowledge everyone who played a role in my academic accomplishments. First of all, my research supervisor, Dr. Ashutosh Bagchi, who supported me with his patient guidance and enthusiastic encouragement during the golden opportunity of developing this research effort. Secondly, my parents and my sister, who supported me with love and understanding. Without you, I could never have reached this current level of success.

I am also grateful to the members of my committee Prof. Lucia Tirca and Prof. Mazdak Nik-Bakht for their valuable time and effort.

Last but by no means least, I am also grateful to my dearest friends, Siamak Pejmanfar, Hassan Bardareh, Saman Namvarchi, Golnoosh Karimpourfard, Timir Baran Roy and so many others who have inspired me, believed in me, and supported me to achieve my goal.

Table of Contents

List of Figures	ix
List of Tables	xv
List of Abbreviations	xvi
CHAPTER 1 Introduction	1
1.1 Motivation and Background.....	1
1.2 Research Objectives	3
1.3 Thesis Organization.....	4
CHAPTER 2 Literature Review	5
2.1 Probabilistic Seismic Loss Estimation	5
2.2 Performance-Based Earthquake Engineering (PBEE) Approach	5
2.3 Second Generation PBEE Approach.....	9
2.3.1 Building Performance Model.....	10
2.3.2 Hazard Analysis	12
2.3.3 Structural Analysis.....	13
2.3.4 Damage Analysis	13
2.3.5 Loss Analysis	14
2.3.6 Decision Making.....	15
2.4 PBEE & Seismic Instrumentation	15
2.4.1 Model-based approaches.....	16
2.4.2 Nonmodel-based approaches	16
2.5 PBEE & Building Information Modeling	17
2.5.1 Impediments to attribution of building components characteristics into PBEE assessment; use of BIM in component-level loss assessment method	18
2.5.2 Obstacles in the estimation of building inventory quantities in PBEE assessment; use of BIM in component-level loss assessment method	19
2.5.3 Lack of visualization technology in PBEE assessment; use of BIM in component-level loss assessment method	20
2.5.4 Level Of Development (LOD) in BIM-based PBEE loss assessment.....	21
2.5.4.1 LOD definition	21
2.5.4.2 LOD for structural components.....	22
2.5.4.3 LOD for non-structural components	24

2.5.5	Application Programming Interface (API) in BIM-enable tools	25
2.5.5.1	Autodesk Revit API	25
2.5.5.2	DYNAMO Studio: A Revit API-based visual programming interface.....	27
2.6	Summary & Conclusion.....	28
CHAPTER 3	Proposed Methodology	29
3.1	Overview	29
3.2	Operational Modal Analysis (OMA)	30
3.2.1	Measurement of structural dynamic response.....	31
3.2.2	Output-only system identification (SI)	32
3.2.2.1	Frequency Domain Decomposition (FDD).....	32
3.3	Experimental structural analysis	33
3.3.1	Model-based approach	34
3.3.1.1	FE model calibration	35
3.3.1.2	Nonlinear response history analysis.....	36
3.3.2	Nonmodel-based approach.....	36
3.3.2.1	Experimental Response Spectrum modal analysis.....	37
3.3.2.2	Simplified experimental seismic analysis Dynamo algorithms	40
3.4	BIM-based seismic loss analysis.....	45
3.4.1	Loss analysis based on FEMA P-58 (in PACT software).....	46
3.4.2	Loss data visualization Dynamo algorithms	48
3.5	Summary	53
CHAPTER 4	Case study analysis.....	55
4.1	Overview	55
4.2	Case study specification	55
4.3	Experimental setup.....	56
4.3.1	Sensor specification	57
4.3.2	Sensor placement & AVT arrangements	58
4.3.3	Collection of the raw data	59
4.3.4	System identification and modal analysis.....	60
4.4	Experimental structural analysis for EDP determination.....	61
4.4.1	Model-based approach	62
4.4.2	Nonmodel-based approach.....	66
4.4.3	EDP result comparison between the proposed approaches.....	85
4.5	BIM-based seismic loss analysis.....	87

4.5.1	Loss analysis based on FEMA P-58 (in PACT software).....	87
4.5.1.1	Development of Building Performance Model	87
4.5.1.2	EDP acquisition for building performance model.....	91
4.5.1.3	Seismic loss analysis result	91
4.5.2	Loss data visualization Dynamo algorithms (results).....	98
4.6	Summary	111
CHAPTER 5	Summary and Conclusions.....	113
5.1	Summary	113
5.2	Contributions.....	114
5.3	Conclusions	117
5.4	Limitations and future work.....	118
CHAPTER 6	References	121
References	121
Appendix A - Publications	126

List of Figures

Figure 2. 1. HAZUS seismic loss estimation methodology for an individual building.....	7
Figure 2. 2. Overview of PEER-PBEE methodology and its mathematical equation.....	10
Figure 2. 3. A 3D image sample of Performance groups for a one-story building.....	11
Figure 2. 4. The classification of the eighteen different concrete flat slab– column connection joints, provided by FEMA P-58 database.....	19
Figure 2. 5. LOD definitions from LOD 100 to LOD 500, source: (NATSPEC, 2013).....	22
Figure 2. 6. The classification of seven different connection for steel columns, provided by FEMA P-58 database.....	23
Figure 2. 7. BIMForum 2020 LOD definition for steel framing columns (B1010.10.30) derived from (BIMForum, 2020).....	23
Figure 2. 8. The classification of twelve different candidates for sanitary sewerage piping, provided by FEMA P-58 database.....	24
Figure 2. 9. BIMForum 2020 LOD definition for sanitary sewerage piping (D2020.30) derived from (BIMForum, 2020).....	25
Figure 2. 10. A virtual 3D model of a complex building with the structural and non-structural building components in Autodesk Revit.....	26
Figure 2. 11. An overview of nodes and workflows in Dynamo Studio.....	28
Figure 3. 1. The overview and the scope of the proposed methodology.....	30
Figure 3. 2. The workflow of OMA in the proposed methodology.....	31
Figure 3. 3. The workflow of the structural analysis in the proposed methodology.....	34
Figure 3. 4. The overview of the proposed model-based approach.....	35
Figure 3. 5. The workflow of the proposed three-dimensional modal response spectrum analysis.....	37
Figure 3. 6. Schematic view of a three-dimensional simplified multi-degree-of-freedom building.....	38
Figure 3. 7. The workflow of simplified experimental seismic analysis by the Dynamo algorithms.....	41
Figure 3. 8. The visual script of the algorithm “A” adopted in the experimental structural analysis.....	42

Figure 3. 9. Code block module relationship defined in the algorithm “A” adopted for the experimental structural analysis.....	42
Figure 3. 10. The visual script of the algorithm “B” adopted in the experimental structural analysis	43
Figure 3. 11. Code block module relationship defined in the algorithm “B” adopted for the experimental structural analysis.....	44
Figure 3. 12. The workflow of the proposed BM-based seismic loss analysis based on FEMA P-58 framework	46
Figure 3. 13. Building performance model, containing vulnerable categories of components in PACT software along with the estimated loss data	48
Figure 3. 14. The overview of the developed Dynamo algorithms adopted for the BIM-based loss data visualization	49
Figure 3. 15. The visual script of the algorithm “FGVT” adopted for the BIM-based loss data visualization	50
Figure 3. 16. Code block module relationship defined in the algorithm “FGVT” adopted for the BIM-based loss data visualization	50
Figure 3. 17. The visual script of the algorithm “PGVT” adopted for the BIM-based loss data visualization	51
Figure 3. 18. Code block module relationship defined in the algorithm “PGVT” adopted for the BIM-based loss data visualization	52
Figure 4. 1. The Isometric view of EV Building, Concordia University (Source: Google Map) (left), typical floor plan of EV building at the lower stories (top right), typical floor plan for the higher stories (bottom right). The courtesy of the right pictures belongs to Concordia university.	56
Figure 4. 2. An overview of the “Sensequake Larzé” sensor developed by Sensequake Inc (Sensequake Larzé, 2021).....	57
Figure 4. 3. The layout of the sensor placements for AVT over EV building (courtesy of the pictures from left to right: Google Map, Concordia university).....	58
Figure 4. 4. The recorded raw data of EV building by the placed sensors for the first test setup, (Timir Baran Roy et al., 2019).....	59

Figure 4. 5. the first six natural frequencies and the corresponding mode shapes of EV building, (Timir Baran Roy et al., 2019).....	60
Figure 4. 6. An overview of the assumed directions for EV building project (Source: Google Map)	61
Figure 4. 7. An overview of the developed 3D model of EV building in Autodesk Revit with all the building components (left and top right), the isometric view of EV building (bottom right) (Source: Google Map).....	62
Figure 4. 8. The structural analysis model of EV building converged from Autodesk Revit into CSI ETABS software.....	63
Figure 4. 9. The first three mode shapes of EV building in CSI ETABS software after the calibration process: the first mode (left), the second mode (middle) and the third mode (right), (Bahmanoo et al., 2021).....	64
Figure 4. 10. Target spectra of Montreal area (class C) along with the scaled ground motions in the range 0.2T1 – 2T1 derived from (Wang, Pejmanfar and Tirca, 2019)	65
Figure 4. 11. Structural responses of EV building: peak story drift ratios (left) and peak floor absolute accelerations (right)	66
Figure 4. 12. An overview of the 3D model of EV building developed in Autodesk Revit.....	67
Figure 4. 13. The customized visual script of the algorithm “SMMIC” adopted in the experimental structural analysis for EV building	67
Figure 4. 14. The identification process of all the shear walls located at the second level of the building by code block module 1	68
Figure 4. 15. The identification process of all the structural columns located at the second level of the building by code block module 1	69
Figure 4. 16. The identification process of all the rectangles that represent the floor slab located at the second level of the building by code block module 1	69
Figure 4. 17. A sample of selected shear walls, structural columns and the floor slab located at the second floor of EV building.....	70
Figure 4. 18. The visual calculated centroid coordinates of the identified components at the second-floor level of EV building.....	70

Figure 4. 19. The calculated centroids for all the shear walls, structural columns, and the floor slab located at the second-floor level of EV building, respectively in Dynamo Studio (code block module 2)	71
Figure 4. 20. The transformation of the original coordinate system origin (around the center of the building) to the new coordinate system origin (top right)	72
Figure 4. 21. The transformation process of all the computed coordinates (at the second-floor level) to the new coordinate system origin in Dynamo Studio (code block module 3).....	73
Figure 4. 22. the collecting process of the material properties and physical dimensions of the identified components at the second-floor level of the building (code block module 4)	74
Figure 4. 23. The process of transferring all the collected information from the identified components at the second-floor level of the building to the relational database (code block module 5).....	75
Figure 4. 24. The customized visual script of the algorithm “MSOT” adopted in the experimental structural analysis for EV building.....	76
Figure 4. 25. The inputting process of the original and secondary coordinate values of EV building in Dynamo Studio from the relational database (code block module 1).....	77
Figure 4. 26. The formation process of the floor slabs at the second floor from with the corresponding input original (up) and secondary coordinates (bottom), respectively (code block module 2)	78
Figure 4. 27. The constructed floor slabs with the original (left) and secondary coordinates (right) in Autodesk Revit, respectively	79
Figure 4. 28. The identified movements of the second-floor slab, imposed by the first mode shape at each corner	79
Figure 4. 29. The computing process of the horizontal movements of the C.M. between the original and the secondary (transformed) floor slabs at the second-floor level of EV building (code block module 3)	81
Figure 4. 30. The computing process of the in-plane rotation of the C.M. between the original and the transformed floor slabs at the second-floor level of EV building (code block module 3).....	82
Figure 4. 31. The exporting process of the computed mode shape values from Dynamo to the relational database (code block module 4).....	83

Figure 4. 32. The inputted target response spectra for Montreal (City Hall) defined by NBCC 2015	85
Figure 4. 33. Structural responses of EV building: peak story drift ratios (left) and peak floor absolute accelerations (right), (nonmodel-based approach)	85
Figure 4. 34. Peak story drift ratios of EV building: model-based approach (left), nonmodel-based approach (right).....	86
Figure 4. 35. Peak floor absolute accelerations of EV building: model-based approach (left), nonmodel-based approach (right)	86
Figure 4. 36. The developed details of the wall-partitions, HVAC system etc. demonstrated in EV building BIM model in Autodesk Revit.....	88
Figure 4. 37. The cumulative loss distribution of repair cost of EV building: model-based approach (left), nonmodel-based approach (right)	93
Figure 4. 38. Participation of the structural and non-structural components in the total repair cost: model-based approach (left), nonmodel-based approach (right)	93
Figure 4. 39. Decomposition of the total repair cost in the 10th percentile: model-based approach (top), nonmodel-based approach (bottom).....	95
Figure 4. 40. Decomposition of the total repair cost in the 50th percentile: model-based approach (top), nonmodel-based approach (bottom).....	96
Figure 4. 41. Decomposition of the total repair cost in the 90th percentile: model-based approach (top), nonmodel-based approach (bottom).....	97
Figure 4. 42. The inputting process of repair cost and repair time of the most vulnerable categories of components of EV building (at the 50 th percentile).....	99
Figure 4. 43. Automatic selection of the vulnerable groups of components in EV building, based on the matched category codes with the inputted loss (at the 50 th percentile).....	99
Figure 4. 44. The automatic assignment process of the vulnerable groups of components in EV building with the corresponding obtained repair cost, repair time and color code (at the 50 th percentile)	100
Figure 4. 45. The most contributed vulnerable categories of components of EV building (at the 50 th percentile)	101

Figure 4. 46. The most contributed vulnerable categories of components of EV building (at the 50 th percentile): traction elevator (D1014.011), wall partition (C3011.002a) and wall partition (C3011.001a)	101
Figure 4. 47. The most contributed vulnerable categories of components of EV building (at the 50 th percentile) along with the corresponding estimated repair cost and repair time	102
Figure 4. 48. the input process of the distributed repair cost and repair time of the most vulnerable categories of components among all the stories in EV building at the 50 th percentile (code block module 1)	103
Figure 4. 49. The most vulnerable categories of components of EV building (at the 50 th percentile): traction elevator (D1014.011), wall partition (C3011.002a) and wall partition (C3011.001a) ..	103
Figure 4. 50. Automatic selection of the vulnerable groups of components in EV building, based on the matched category codes with the inputted loss at the 50 th percentile (code block module 2)	104
Figure 4. 51. Th automatic assignment process of the most vulnerable group of components of EV building (at the 50 th percentile) with the corresponding repair cost and repair time portions associated with the 16 th story (code block module 3).....	105
Figure 4. 52. The automatic process of range identification between the considered vulnerable categories of components at the 50 th percentile (code block module 4).....	106
Figure 4. 53. the assignment workflow of the mapped groups of components of EV building in various pre-defined ranges adopted in code block module 5.....	108
Figure 4. 54. the automatic assignment process of the mapped group of components of EV building in corresponding ranges through the code block module 5 of the algorithm “PGVT” (BIM-based seismic loss visualization).....	109
Figure 4. 55. An overview of the most contributed vulnerable group of components of EV building at the 50 th percentile, sorted by the corresponding estimated repair cost between all the stories	110
Figure 4. 56. Another view of the most contributed vulnerable group of components of EV building at the 50 th percentile with the corresponding estimated repair cost and repair time at different stories	110
Figure 4. 57. An overview of the Traction elevators of EV building at the 50 th percentile, sorted by the corresponding estimated repair cost between all the stories	111

List of Tables

Table 2. 1. Fragility Group descriptions and the predictive demand parameter used in Figure 2.3 example	12
Table 4. 1. The first three natural frequencies and the corresponding mode shapes of EV building, (Timir Baran Roy et al., 2019).....	61
Table 4. 2. Seismic characteristics of the employed artificial ground motions derived from (Wang, Pejmanfar and Tirca, 2019).....	65
Table 4. 3. The identified movements of the second-floor slab, imposed by the first mode shape at each corner	80
Table 4. 4. The computed displacements and in-plane rotation of the C.M. of the second-floor slab in the first mode shape	82
Table 4. 5. The collected mode shape values of the first mode shape of EV building	84
Table 4. 6. The identified structural component fragilities used in PACT software for EV building	89
Table 4. 7. The identified non-structural component fragilities used in PACT software for EV building	90
Table 4. 8. Total repair cost & repair time of the model-based approach (10 th , 50 th and 90 th percentiles).....	92
Table 4. 9. Total repair cost & repair time of the nonmodel-based approach (10 th , 50 th and 90 th percentiles).....	92
Table 4. 10. The obtained repair cost and repair time (loss data) of the most vulnerable categories of components (at the 50 th percentile) for EV building	98
Table 4. 11. The most vulnerable group of components of EV building (at the 50 th percentile) with the corresponding repair cost and repair time portions associated with the 16 th story	105
Table 4. 12. Defined ranges of the predicted repair costs of the most vulnerable components of EV building (at the 50 th percentile).....	107

List of Abbreviations

American Institute of Architect	(AIA)
Application Programing Interface	(API)
Architectural, Engineering and Construction	(AEC)
Building Information Modeling	(BIM)
Center of Mass	(C.M)
Damage Sensitive Feature	(DSF)
Engineering and Visual Arts	(EV)
Engineering Demand Parameter	(EDP)
Federal Emergency Management Agency	(FEMA)
Fragility Group	(FG)
Fragility Group Visualization Tool	(FGVT)
Finite Element Model	(FEM)
Frequency Domain Decomposition	(FDD)
Hazards United States Multi-Hazard	(HAZUS-MH)
Intensity Measure	(IM)
Level of Development	(LOD)
Mechanical, Electrical and Plumbing	(MEP)
Mode Shape Obtaining Tool	(MSOT)
Multi Degree Of Freedom	(MDOF)
National Building Code of Canada	(NBCC)
National Institute of Building Science	(NIBS)
Operational modal analysis	(OMA)

Pacific Earthquake Engineering Research	(PEER)
Performance Assessment Calculation Tool	(PACT)
Performance-Based Earthquake Engineering	(PBEE)
Performance Group	(PG)
Performance Group Visualization Tool	(PGVT)
Power Spectral Density	(PSD)
Research Objective	(RO)
Seismic Force Resisting System	(SRFS)
Seismic Mass and Moment of Inertia Calculator	(SMMIC)
Single Degree Of Freedom	(SDOF)
Singular Value Decomposition	(SVD)
system identification	(SI)
Three Dimensional	(3D)
Two Dimensional	(2D)

CHAPTER 1 Introduction

This research study aims to enhance current seismic loss assessment frameworks of buildings by employing sensing-based measurements and Building Information Modeling (BIM) tools. Current frameworks are now mainly capable of predicting the seismic loss estimation of buildings in terms of repair cost, downtime, and other decision variables. However, major sources of uncertainties are yet associated with the application of them. Utilizing innovative technologies such as seismic instrumentation and integrated BIM tools not only facilitate to overcome the associated uncertainties, but also, enhance the loss consequence predictions of buildings and subsequent decision-making process. The following sections of this chapter cover the motivation and background, objectives of the research and the organization of the thesis.

1.1 Motivation and Background

Forecasting earthquake-induced loss of a building is a crucial challenge for its resilience (Xu et al., 2019b). In response to this, various studies have been dedicated to the application of performance-based earthquake engineering (PBEE) approach to develop effective seismic loss assessment frameworks of buildings. Among them, Recent efforts by the Pacific Earthquake Engineering Research (PEER) Center have developed a systematic methodology for seismic performance assessment of buildings which is an appropriate basis for seismic loss predications. The current generation of PBEE or PEER-PBEE has been also adopted by Federal Emergency Management Agency as FEMA P-58 framework. FEMA P-58 has been widely adopted in Architectural, Engineering and Construction (AEC) industry and contains four stages of hazard analysis, structural analysis, damage analysis and loss analysis for the purpose of estimating loss consequence predications of buildings into appropriate performance metrics such as economic losses, downtime and other decision variables (Fischinger, 2014; Xu et al., 2019b; Filiatrault and Sullivan, 2014; Christodoulou, Vamvatsikos and Georgiou, 2010). Despite all the benefits, some limitations exist within the FEMA P-58 framework mostly due to certain sources of uncertainties that significantly, affect the quality of the seismic loss assessment. (Porter, 2003) showed that, the significant contributors to the associated uncertainties in PEER-PBEE framework come from

structural and damage analyses. This is caused mostly, by two factors, lack of accurate structural performance characteristics of buildings (structural analysis) and lack of effective details of the building components (damage analysis) (Xu et al., 2019b; Cremen and Baker, 2018). For structural analysis, FEMA P-58 has adopted mostly, finite element (FE) method as a practical numerical analysis tool to obtain structural response data of building, however, FE model of a structure is generally constructed by the highly idealized engineering and design assumptions that would represent a different seismic behavior from the result of an actual structure. Hence, the calculated damage and loss consequence predictions from a FE model often would not be sufficiently precise and accountable to be considered for post-earthquake rehabilitation (Cremen and Baker, 2018; Ren and Chen, 2010). To overcome the aforementioned limitation, measured responses should be obtained and analyzed accordingly by using building instruments. For example, the investigation by a group of researchers from Stanford University in 2018, indicates the benefits of building instruments, by adopting actual responses in damage and loss consequence predications of FEMA P-58 framework. They also, proved that by increasing the number of building instruments as well as the number of instrumented floor levels, loss consequence predications tend to be decreased in errors (Cremen and Baker, 2018). Also, with respect to damage analysis, lack of effective information over potential building components at risk can be a key obstacle towards attributing the characteristics of damage properly. Thus, obtaining the required effective information for a refined component-level loss assessment method such as FEMA P-58 to evaluate the post-earthquake economic resilience of buildings yet remains a challenge (Xu et al., 2019b; Georgiou, Christodoulou and Vamvatsikos, 2014; Xu et al., 2019a). To tackle this challenge, adopting a powerful data management system such as BIM could be a great step towards visualizing both physical and functional characteristics of the potential building components at risk. Moreover, it would visualize the indications of performance measures derived from the predicted seismic damage and losses within the FEMA P-58 framework for post-earthquake building rehabilitation (Xu et al., 2019b; Bahmanoo et al., 2019). The methodology proposed herein aims to enhance the limitations of a refined component-level loss assessment method (PEER-PBEE) by employing sensing-based measurements and BIM technology.

1.2 Research Objectives

The aim of this thesis is to mitigate the substantial current limitations of PEER-PBEE systematic methodology by employing innovative technologies such as seismic instrumentation and integrated BIM tools, which can significantly impact the loss consequence predictions of buildings and subsequent decision-making process. The scope of this study is limited to three stages of “Operational modal analysis (OMA)”, “Experimental structural analysis” and “BIM-based loss analysis” to forecast the earthquake-induced loss of buildings based on PEER-PBEE assessment framework. For this purpose, a workflow of seismic loss estimation is proposed, where initially, the structural performance characteristics of a building are experimentally obtained. Next, the obtained structural characteristics are adopted in experimental structural analysis to compute structural responses and the caused physical damage in potential building components at risk. Finally, a BIM-based API tool is developed to intelligently collect and visualize the predicted damage and associated loss based on PEER-PBEE assessment framework. It is to be noted that the BIM-based API tools are referred to the developed algorithms in Dynamo Studio in Autodesk Revit software program (BIM software). Further information is provided through the Research Objectives list.

In order to achieve the aforementioned goal, the specific Research Objectives (RO) of this thesis are set and categorized as follows:

Research Objective #1 (RO 1): Determining the structural performance characteristics of a building based on Operational Modal Analysis (OMA), including measurement of structural dynamic response (ambient vibration test) as well as output-only system identification (SI).

Research Objective #2 (RO 2): Developing an experimental structural analysis workflow based on model-based approach, including FE model calibration and nonlinear time history analysis to obtain refined structural response parameters.

Research Objective #3 (RO 3): Developing an experimental structural analysis workflow based on nonmodel-based approach (i.e. simplified three-dimensional response spectrum modal analysis).

Research Objective #4 (RO 4): Developing the simplified experimental seismic analysis Dynamo algorithm to automate the nonmodel-based approach workflow, including extracting modal properties from OMA and performing experimental response spectrum modal analysis.

Research Objective #5 (RO 5): Performing seismic loss analysis using the refined structural response parameters from the adopted approaches (model-based and nonmodel-based) based on FEMA P-58 procedure.

Research Objective #6 (RO 6): Developing the Loss data visualization dynamo algorithm to visualize the predicated loss data in a more understandable fashion (color code scheme).

1.3 Thesis Organization

The thesis is organized into five chapters including this introduction chapter.

The other five chapters are organized as follows:

Chapter 2 *Literature Review*: this chapter reviews the latest literature over the concepts, techniques and methodological frameworks that are used in the research. The literature review comprises the information about the PBEE seismic loss assessment frameworks including PEER-PBEE, seismic instrumentation of buildings and BIM technology.

Chapter 3 *Proposed Methodology*: this chapter proposes the framework to enhance the limitations of the current generation PBEE loss assessment (PEER-PBEE) by employing sensing-based measurements and BIM technology.

Chapter 4 *Case study analysis*: this chapter presents a case study analysis over a building located in Montreal, Canada to investigate the rationality and accuracy of both adopted approaches in the proposed methodology.

Chapter 5 *Discussion and Conclusion*: this chapter summarizes the present work, future research, and the concluding remarks.

CHAPTER 2 Literature Review

2.1 Probabilistic Seismic Loss Estimation

A look at the catastrophic earthquakes in recorded history, explains even though some buildings can withstand a seismic event, yet they may need to be demolished due to not conforming to economic resilience demands or required functionality (Filiatrault and Sullivan, 2014). Therefore, quantitative and qualitative prediction of earthquake-induced loss of buildings is a vital step towards achieving high resilience against disasters (Xu et al., 2019b; Ranjbar and Naderpour, 2020). Nevertheless, loss estimation requires some probable damage descriptors that are characterized by seismic performance of buildings, translated into monetary losses and other meaningful units to decision-makers (Porter, Mitrani-Reiser and Beck, 2006; Cimellaro, Reinhorn and Bruneau, 2006). In response to this there have been numerous studies and efforts dedicated to performance-based earthquake engineering (PBEE) approaches that are formed from conceptual frameworks to a feasible set of procedures and notable innovations (Calvi, Sullivan and Welch, 2014; Fischinger, 2014).

2.2 Performance-Based Earthquake Engineering (PBEE) Approach

FEMA 273 (1997) and Vision 2000 report (SEAOC 1995) are known as the first generation PBEE pioneers to articulate the PBEE methodologies (Lee, 2005; Günay and Mosalam, 2013). In these documents, PBEE is defined as a design development procedure that satisfies the stated system performance, subjected to different levels of seismic hazard (Lee, 2005; Günay and Mosalam, 2013). With regards to Vision 2000, the system performance levels are identified as fully operational, operational, life safety, and near collapse, whereas hazard levels are defined as frequent, occasional, rare, and very rare events (Lee, 2005; Günay and Mosalam, 2013). The objective is to comply with public resilience requirements (e.g. hospital buildings) or owner intent in private properties (e.g. residential buildings) through the practical combination of performance and hazard levels in design (Lee, 2005; Günay and Mosalam, 2013). Subsequent developments in the first generation PBEE led to FEMA-356 (2000), where design criteria is demonstrated through a similar framework, but with some improvements on performance descriptions and hazard levels (Günay and Mosalam, 2013). The primary developments in FEMA-356 (2000) have focused on

the performance of different structural and non-structural elements in terms of element deformation and force acceptability criteria per different type of structural analysis (Günay and Mosalam, 2013). Yet, no global system performance and probability distribution are defined for the proposed element performance evaluation as well as lack of consistency in the process of deriving relationships between engineering demands and element performance criteria (Günay and Mosalam, 2013). Despite all the limitations of the first generation PBEE, FEMA 273 and FEMA-356 led major advancement in PBEE frameworks by providing quantitative performance metrics such as economic loss, casualty rate and downtime. However, these performance metrics are relatively similar in regional seismic loss assessment methods such as HAZUS methodology (Hazus, 2011), where reasonably accurate loss quantification of individual buildings can also be examined (Fajfar and Krawinkler, 2004). HAZUS-MH (Hazards United States Multi-Hazard) as a comprehensive seismic loss estimation tool which uses ArcGIS platform, developed under the agreements between the National Institute of Building Science (NIBS) and the Federal Emergency Management Agency (FEMA) (Ploeger, Atkinson and Samson, 2010; Gulati, 2006; Hazus, 2011, 2020). Following is Figure 2.1, which demonstrates the procedure of HAZUS seismic loss estimation for an individual building.

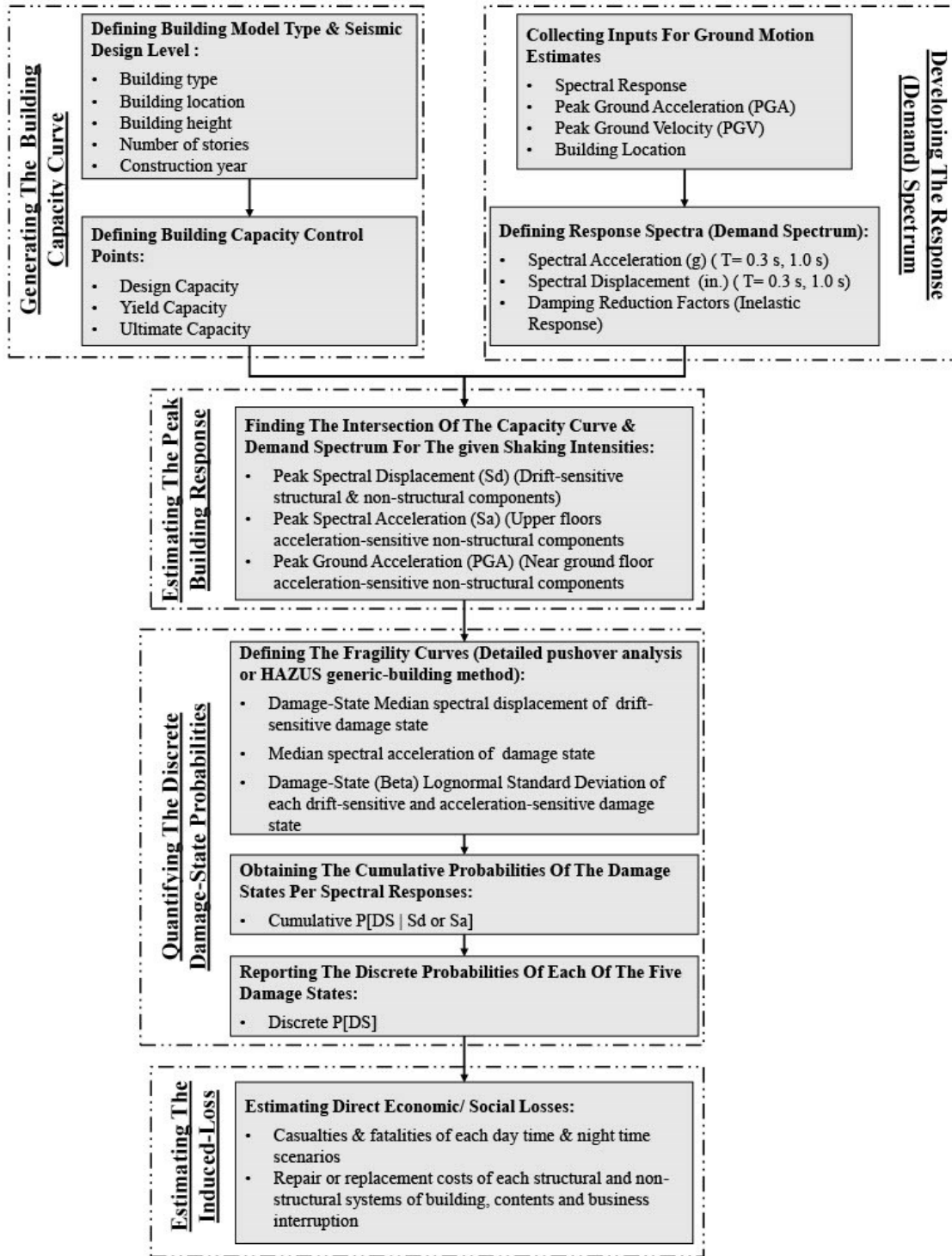


Figure 2. 1. Seismic loss estimation methodology for an individual building

The procedure of HAZUS seismic loss estimation of an individual building initiates with collecting and developing the building inventory information and the associated damage and loss parameters

through the AEBM extension of the HAZUS software. Next, depending on the site-specific location and related ground shaking parameters, deterministic or probabilistic ground motion maps are employed to identify the applicable demand spectrums (including damping-modified demand spectra for inelastic response). Subsequently, the following two components of HAZUS damage functions due to ground shaking are identified: (1) Capacity curve and (2) fragility curves. The building capacity curve is identified based on either pre-defined HAZUS building type or as the result of a detailed nonlinear analysis (static pushover) over the structural model of the building of interest. The fragility curves define the probable structural and non-structural damages to the target building based on given spectral responses of a building. These damages are calculated based on lognormal functions with the associated median values and standard deviations to express the probabilities of a physical damage through Slight, Moderate, Extensive and Complete damage states. As the result of utilizing these information through series of operations within the AEBM of HAZUS software, the probabilistic loss estimation of the building of interest is calculated. Ultimately, the loss estimation output contains the predicted structural and non-structural damage probabilities of the individual target building, casualties, building exposure and economic loss, that could be an essential asset for engineers and facility owners for the subsequent decision making process. (Gulati, 2006; Ploeger, Atkinson and Samson, 2010; Hazus, 2011).

Although HAZUS is one of the most commonly used techniques for predicting both the individual and regional seismic losses, major limitations exist within the body of this methodology: (1) HAZUS considers buildings as a Single Degree Of Freedom (SDOF) system, which causes significant uncertainties in financial loss analysis of a building, due to not having the accurate loss estimation of different stories; (2) The non-structural components of the HAZUS methodology are fairly general, which causes HAZUS approach to not reliably consider the financial losses of non-structural components within a building; and (3) The capacity spectrum method utilized in HAZUS methodology cannot practically account for the impact of ground motion features (such as near-field velocity pulses) on the induced-damage and losses of a building. Despite all the aforementioned drawbacks, HAZUS methodology is still practiced as relatively approximate loss analysis method of buildings. However, the current second-generation PBEE has been pursued by the Pacific Earthquake Engineering Research (PEER) Center to provide a much more precise and reliable solution in comparison with all the first-generation PBEE methods (Lu and Guan, 2017; Günay and Mosalam, 2013; Porter, 2003).

2.3 Second Generation PBEE Approach

The current second-generation PBEE or PEER-PBEE is framed as FEM P-58 (FEMA, 2012), estimates the performance of the whole system in terms of economic losses, downtime, environmental impacts, collapse risk, casualties and risk of building closure (Fischinger, 2014). PEER-PBEE framework consists of four distinct stages: hazard analysis, structural analysis, damage analysis, and loss analysis to provide indications of performance measures which could also be known as decision variables (Filiatrault and Sullivan, 2014). The first is hazard analysis, in which ground motion intensity is represented by intensity measure (IM) such as spectral acceleration at the fundamental period of the structure. With regards to the structural analysis phase as the second stage, the structural responses are estimated based on selected engineering demand parameters (EDPs), subjected to a given IM ($\rho[EDP|IM]$). It is noteworthy to mention that EDPs are classified as local parameters (such as member force or deformation) or global parameters (such as peak floor acceleration or peak inter-story drift ratio). The third stage is damage analysis phase, in which the structural responses given in terms of EDP ($\rho[DM|EDP]$) are applied to the set of fragility functions of structural and non-structural components of the concerned structure to estimate the probable damages in terms of DM. The last stage in the analysis is loss analysis phase, where the loss analysis is performed and the structural performance of the target structure in terms of decision variables (DV) are calculated using DMs ($\rho[DV|DM]$) (Porter, Mitrani-Reiser and Beck, 2006; Lee, 2005).

The aforementioned stages in PEER-PBEE's methodology are all formulated in an electronic calculation tool named, *Performance Assessment Calculation Tool* (PACT), which is provided by FEMA P-58 development team (FEMA, 2012). An overview of the four stages is demonstrated in Figure 2.2. With regards to "D" as the definition of the given building design and location, the objective of the methodology has demonstrated through the provided mathematical equation as the form of the triple integral which estimates the mean annual occurrence of a particular performance metric such as repair cost or other decision variables for a given "D". Note that the effects of inherent uncertainties are explicitly acknowledged through the various analysis stages (Filiatrault and Sullivan, 2014; Porter, 2003). Also, within the mentioned integral, the expression $\rho[X|Y]$ and $\lambda[X|Y]$ are referred to probability density and the occurrence frequency of X given Y. Highlights of PEER-PBEE methodology components are discussed briefly in each stage:

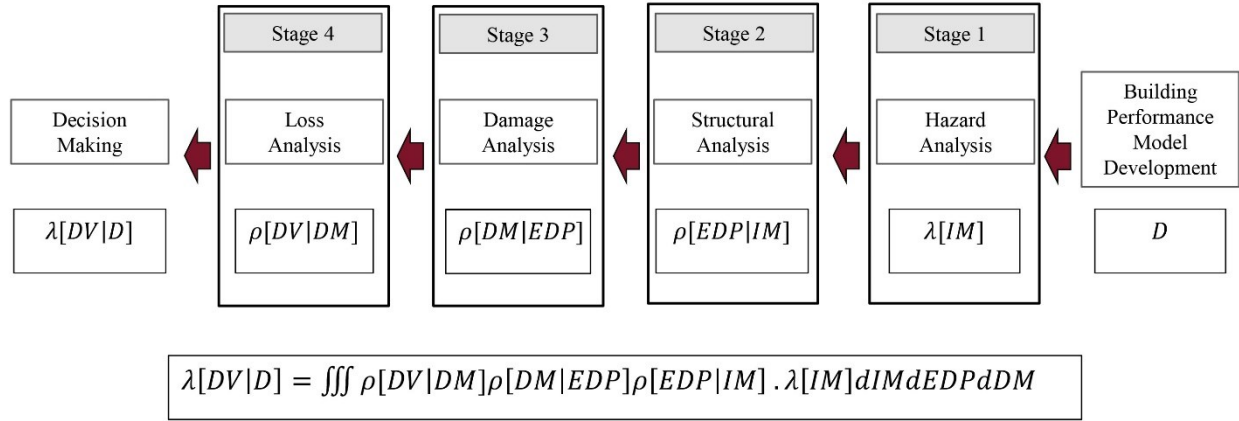


Figure 2.2. Overview of PEER-PBEE methodology and its mathematical equation

2.3.1 Building Performance Model

In order to collect the necessary data to define the target building assets at risk (partially denoted by design, D), developing the building performance model becomes so crucial. In fact, building performance model represents the essential sets of data to define the characteristics of the vulnerable building assets to the stated seismic activity. This includes definition of basic building data, population/occupancy models and all the vulnerable structural and nonstructural components that are categorized as different fragility groups and performance groups. Basic building data contains the overall layout of the target building (such as building location, number of stories, story height, floor area and so on) as well as the estimated replacement cost, time and quantities for embodied energy and carbon (FEMA, 2012).

Building population model is to identify the primary use of a building, defining the distribution of people using the facilities within the variation of time as well as defining and quantifying the nonstructural components and contents in the building. The main point of using building population models is to calculate casualties. It is noteworthy to mention that, in the absence of the inventory of the building assets, databases of normative quantities would be helpful for an approximate estimation of the non-structural components at risk, distributed in typical buildings of a certain size (FEMA, 2012; Hamburger, 2014).

Fragility specifications within the building performance model are defined and assigned per each category of all the vulnerable structural and non-structural components in the target building. A fragility group is a collection of components and assemblies that are not identical, but similar of

construction characteristics, probable modes of damage when subjected to earthquake as well as potential resulting consequences. Each fragility group of components is assumed to be dependent on the same type of demand parameter, subjected to the stated earthquake intensity. Moreover, each fragility group is identified and classified based on UNIFORMAT II described in NISTIR 6389 (Charette and Marshall, 1999) and assigned a fragility specification that expresses the component identification; detail information on component damage states; the predictive demand parameter that causes damage during response to earthquake shaking; median value per each damage state and uncertainty that parametrized through dispersion at damage onset; possible logical relationships between more than one damage states; and, consequence functions that predicts the possible losses at damage onset (Hamburger, 2014; FEMA, 2012).

Performance groups are the collection of components categorized under a fragility group that is subjected to the same demand parameters (such as peak inter-story drift ratio, peak floor acceleration, etc.) in a particular direction or floor level. Various units of measure associated with each fragility group are defined corresponding to the performance groups for the purpose of quantifying and estimating the existing components in a meaningful way for the subsequent damage and loss analysis processes (FEMA, 2012). Figure 2.3 shows a sample of performance groups for a two-story building that includes both the acceleration-sensitive components (e.g., HVAC Ducting) and story drift-sensitive components (e.g., Curtain walls and Masonry walls). Subsequently, Table 2.1 demonstrates the used fragility groups in Figure 2.3 with the corresponding Fragility classification Number and the predictive Demand Parameter used for damage assessment according to FEMA P-58 database.

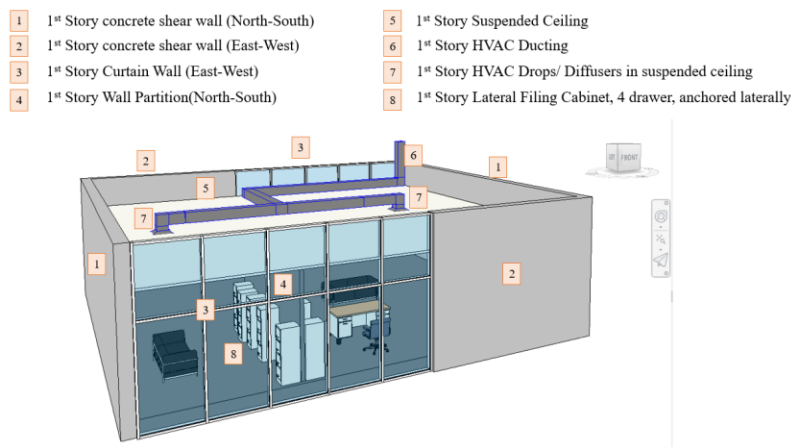


Figure 2.3. A 3D image sample of Performance groups for a one-story building

Performance Group Number	Fragility Classification Number (FEMA P-58)	Description	Demand Parameter
1	B1044.022	Rectangular low aspect ratio concrete walls 18"-24" thick with double curtain and heights 16' - 24'	Story Drift Ratio parallel to wall
2	B1044.022	Rectangular low aspect ratio concrete walls 18"-24" thick with double curtain and heights 16' - 24'	Story Drift Ratio parallel to wall
3	B2022.002	Curtain Walls - Generic Midrise Stick-Built Curtain wall, Config: Insulating Glass Units (dual pane), Lamination: Unknown, Glass Type: Unknown, Details: Aspect ratio = 6:5, Other details Unknown	Story Drift Ratio parallel to wall
4	C1011.001a	Wall Partition, Type: Gypsum with metal studs, Full Height, Fixed Below, Fixed Above	Story Drift Ratio parallel to wall
5	C3032.001d	Suspended Ceiling, SDC A, B, C, Area (A): A > 2500, Vert support only	Floor Acceleration
6	D3041.012b	HVAC Galvanized Sheet Metal Ducting - 6 sq. ft cross sectional area or greater, SDC C	Floor Acceleration
7	D3041.031b	HVAC Drops / Diffusers in suspended ceilings - No independent safety wires, SDC C	Floor Acceleration
8	E2022.125b	Lateral Filing Cabinet, 4 drawers, anchored laterally	Floor Acceleration

Table 2. 1. Fragility Group descriptions and the predictive demand parameter used in Figure 2.3 example

2.3.2 Hazard Analysis

Hazard analysis is the quantification of the intensity of earthquake ground shaking effects that evaluates the seismic hazard of a facility considering its seismic environment and design features (such as architectural, structural, and other features). The following types of assessments are recommended by FEMA P-58 to consider ground shaking hazard for the purpose of addressing induced-seismic building damages (FEMA, 2012; Porter, 2003):

- Intensity-Based Assessments
- Scenario-Based Assessments
- Time-Based Assessments

According to FEMA P-58, intensity-based assessments evaluate probable performance of a building through the selection of “N” number compatible ground motions to the target acceleration response spectrum within the determined period range. The shaking intensity is characterized by

pairs of ground motions, that are scaled compatibly with a 5% damped elastic acceleration response spectrum which itself, could be consistent with a building code. Scenario-based assessments evaluate probable performance of a building that is assumed to experience specific earthquake magnitude and distance relative to the building site. Time-based assessments evaluate performance of a building considering all probable earthquakes and the possibility of exceedance associated with each earthquake over a specific period of time (FEMA, 2012).

2.3.3 Structural Analysis

Structural analysis is used to estimate the uncertain structural response of a building to earthquake shaking in the form of engineering demand parameters (EDPs) that is associated with the given intensity measure (IM) and the building design. EDPs are typically peak values of story drift ratios in both two orthogonal directions as well as peak floor velocities, peak floor accelerations and residual drift ratio. According to FEMA P-58, the acquisition procedure of EDPs is typically through “(1) nonlinear response-history analysis; and (2) simplified analysis based on equivalent lateral force methods.”. Beyond the estimation of peak story drift ratios, peak floor velocities, peak floor accelerations and residual drift ratios, developing the collapse fragility curves is also essential for studying the structure-specific performance assessment. The process of defining the collapse fragility curve usually contains a median value, corresponding to the occurrence of collapse at the first mode spectral acceleration, a dispersion, identifying the potential collapse modes, the probability of the occurrence among the given collapse modes as well as possibility of fatalities and injuries correspond to each of them. The recommended framework in FEMA P-695; the analysis result through time-based assessment; SPO2IDA tool (provided as a practical electronic tool by FEMA P-58 collection); or, engineering judgment are employed to calculate the above median and dispersion values (Hamburger, 2014; FEMA, 2012; Porter, 2003).

2.3.4 Damage Analysis

The derived EDPs from the structural analysis are then used as the input to a set of fragility functions to characterize the various levels of physical damage, occurring in each fragility group in the form of discrete damage states. Each damage state represents a unique set of consequences defined relatively to particular performance measures (such as associated repair cost, repair time,

casualties and etc.), conditioned on structural response and building design. With regards to the fragility groups that have more than one damage state, possible logical relationships are defined between damage states such as: sequential, mutually exclusive, and simultaneous. Moreover, performance groups could be considered as having correlated or uncorrelated damage. Correlation of damage states represents the failure of one component along with simultaneous failure of all other components within the performance group. Correlated damage option significantly reduces computation effort but affects the dispersion in results. FEMA P-58 has developed and provided more than 700 fragility categories for the common structural and nonstructural components found in typical buildings and occupancies (FEMA, 2012; Porter, 2003).

2.3.5 Loss Analysis

The last stage in FEMA P-58 systematic methodology is to produce a probabilistic estimation of performance metrics (also referred to as decision variables, DV), conditioned on derived damage from the last stage and building design $p[DV|DM,]$. Decision variables represent the damage and resulting consequences of the facility in the form of performance measures such as repair cost, repair time, casualties, environmental impacts, and unsafe placarding which are greatest interest to stakeholders and decision makers. To assess many inherent uncertainties, affecting performance calculation, FEMA P-58 has utilized a Monte Carlo procedure to perform seismic loss calculation for a large number (hundreds to thousands) of realizations. As the result, a wide range of possible performance outcome is computed for the building, given a limited set of inputs and a single combination of each uncertain factor. In order to calculate the performance outcome in each realization, one should first consider the collapse susceptibility of the building, using collapse fragility function and structural analysis judgments. In the case of partial or total building collapse, the building would be assumed as a total loss with the most potential number of casualties and the full building replacement cost, time, and environmental impacts. If the building does not collapse in a given realization, the practicality of the building repair should be determined. FEMA P-58 has recommended the utilization of the maximum residual drift ratio combined with the building repair fragility to contemplate whether a damaged structure should be repaired or replaced. The threshold value set by FEMA P-58 is 50%. If the building has not experienced neither collapse nor irreparability in a given realization, the consequence functions associated with damage states in each component would indicate the performance measures. Since estimating the seismic

performance of real buildings deemed to be data-intensive and complex with explicit consideration of uncertainties, *Performance Assessment Calculation Tool* (PACT) is employed to perform the probabilistic calculations and accumulation of induced-losses. Furthermore, the indicated performance measures such as repair cost and repair time, derived from the provided consequence functions are adjustable through *Region Cost Multiplier* and *Date Cost Multiplier* fields in PACT and compatible with various cost index system (FEMA, 2012; Porter, 2003).

2.3.6 Decision Making

Performance assessment can provide useful information to facilitate risk-management decisions with estimating the exceedance frequency of various levels of DV. Performing such analysis for the existing or proposed facility, contemplate the safety level or satisfactory level of earthquake repair costs. Moreover, re-analyzing the same facility, considering the new design or retrofitted conditions would assess the efficiency of the taken decisions to meet performance objectives. It is also noteworthy to mention that various objectives and decision-making criteria could be satisfied, depending on the type of performance assessments. Intensity-based assessments are adopted to derive the probable building performance under Maximum Considered earthquake (MCE) or any other given intensity of response spectrum. Scenario-based assessments indicate the probability of induced-loss for specific earthquake scenarios such as buildings adjacent to active faults. Time-based assessments are usually conducted for cost-benefit analysis as indicate the average probable performance of buildings in a specific period of time (FEMA, 2012; Porter, 2003).

2.4 PBEE & Seismic Instrumentation

Although PEER-PBEE attempted to incorporate various sources of uncertainties into the performance estimation process at each stage, yet high sensitivity of damage and loss analysis to certain sources such as structural response may significantly impact the resulting performance metrics. (Porter, Beck and Shaikhutdinov, 2002) demonstrated that, the major contribution to the uncertainty of total repair cost comes primarily from the structural response and the physical damage determined through a deterministic sensitivity analysis. However, additional knowledge in actual response of structure can highly reduce the level of uncertainty. In response to this, innovative technologies such as seismic instrumentation of buildings can help to acquire actual

responses of structures and determine the associated damage with them. Moreover, it may reduce a major source of uncertainty in performance quantification of buildings and the related performance metrics such as repair cost, repair time and other relevant decision variables (Uma, 2007; Cremen and Baker, 2018; Bahmanoo et al., 2021).

Despite the few studies conducted recently, using sensing-based measurements of structural responses into PBEE methodologies to quantify the seismic performance of buildings (such as repair cost, downtime etc.), the full adoption of seismic instrumentation into PBEE frameworks is yet to come. Based on these studies, model-based and nonmodel-based approaches are the two main methodological approaches adopted to facilitate the seismic performance assessment of instrumented buildings and the associated seismic risk (Porter, Mitrani-Reiser and Beck, 2006; Cremen and Baker, 2018; Hwang and Lignos, 2018; Bahmanoo et al., 2021). It is noteworthy to mention that normally, the key difference between these two approaches is within the prediction of the probabilistic EDPs (structural response).

2.4.1 Model-based approaches

With regards to model-based approaches, (Porter, Mitrani-Reiser and Beck, 2006) proposed a similar loss estimation method to PEER-PBEE framework, except for the hazard analysis stage, in which the actual ground-motion time-history at the base of structure is acquired by the basement accelerograms. A reinforced concrete structure against the 1994 Northridge earthquake was adopted in that work to compute the resulting EDPs, using stochastic structural model and a nonlinear response history analysis. A Bayesian-Correlation method was then employed to refine the estimated EDPs along with the statistical structural model with due consideration of the nonlinearities of geometry and materials. Overall, it can be seen that, combining sensing-based measurements with model-based approaches not only leads to the estimation of more accurate story-based EDPs, but also, substantially reduces the related uncertainties in nonlinear building model validation.

2.4.2 Nonmodel-based approaches

(Çelebi et al., 2003) was perhaps one of the earliest studies, that adopted nonmodel-based approaches to quantify the story-based building EDPs for an instrumented building. Structural

response was recorded in the form of accelerations of a 24-story steel-frame building and translated into story drift ratios. Subsequently, FEMA 273-style performance levels such as 'Operational', 'Immediately Occupiable', 'Life Safety', and 'Collapse Prevention' (Council, 1997) and the associated drift limits with them were used to identify the possible exceedance of the computed drift ratios. Evidently, exceedance of a drift limit is presumed as the exceedance of the corresponding performance level. The main limitation of (Çelebi et al., 2003) work was that, the story drift ratios are obtained only at the consecutive instrumented floors. Whereas, in a related study, (Cremen and Baker, 2018) addressed how story-based building EDPs can be identified and correlated at non-instrumented floors, using statistical interpolation and resampling techniques. A notable significance of (Cremen and Baker, 2018) study was to adopt FEMA P-58 methodology to benchmark the loss consequence predictions of two reinforced concrete structures during the 1994 Northridge earthquake with various density of instrumentation. (Hwang and Lignos, 2018) presented a work on nonmodel-based approaches in rapid loss assessment of instrumented buildings, where wavelet-based damage-sensitive feature (DSF) along with minimal information on building geometry are utilized to quantify relatively precise story-based EDPs and the associated physical damages at a preferred shaking intensity.

2.5 PBEE & Building Information Modeling

With regards to HAZUS methodology and FEMA P-58 guideline as the most common and practical frameworks in PBEE application, awareness of elaborate details within a building will impact the quality of the seismic loss analysis. In the other words, inputting more detailed data leads to enhance the accuracy of the analysis as well as reducing the uncertainties. However, the acquisition of this information is a key obstacle in the application of PBEE assessment frameworks. Considering this, Building Information Modeling (BIM) could be an emerging paradigm in improving the accuracy of a seismic assessment (Xu et al., 2019a; Perrone and Filiatrault, 2017). BIM can be defined as an accurate virtual model of a building that is built digitally and contains the physical and functional characteristics of every detail of the building (Standard, 2010; Eastman et al., 2011). BIM as an intelligent 3D model-based process, supports building information data, required for decision making, throughout a building's whole life cycle, such as the phases of the design and construction to operation and maintenance or ultimately, deconstruction (Kolaric et al., 2018; Xu, Ma and Ding, 2014). Utilizing BIM technology not only

will enhance the exchange and interoperability of required building data (Xu et al., 2019a), but also, will help to overcome the following challenges in PBEE assessment frameworks: (1) inherent uncertainty in attribution of building component's characteristics, due to the lack of effective building information details. (2) uncertainty in the estimation of building inventory quantities, due to the lack of exact measurement data of the components. (3) Lack of visualization and misinterpretation of the estimated damage and loss data (Perrone and Filiatrault, 2017; Xu et al., 2019b). Moreover, adopting some commonly used BIM software programs such as Autodesk Revit would be a valuable step towards automating the workflows in PBEE assessment frameworks of buildings. This automation can be achieved using Application Programming Interface (API), that enables the user to develop customized tools and plugins or adding required features in Autodesk Revit (Kensek, 2014).

2.5.1 Impediments to attribution of building components characteristics into PBEE assessment; use of BIM in component-level loss assessment method

Nevertheless, because PBEE loss assessment methods are supposed to predict the seismic damage and losses of buildings, they demand comprehensive building information data. Specially, elaborate building input data becomes more essential when it comes to a component level loss assessment method like FEMA P-58. To render the component level loss analysis more comprehensive, FEMA has formulated an extensive database of component fragility specifications, which contains detailed documentation of fragility and consequence functions along with associated potential damage states. Among the 764 categories of components (including both structural and non-structural) provided by FEMA, only 55% of the total categories can be directly employed in the loss analysis without additional user-specified data. Thus, BIM can play a keynote roll to eliminate the inherent uncertainty in the remaining 45% of the FEMA component database (Xu et al., 2019a; b). To better demonstrate the necessity of attributed effective information in building components, Figure 2.4 shows eighteen different concrete flat slab-column connection joints, provided by FEMA P-58 database and updated in September 2016 (FEMA P-58, 2021). The classification of these components is based on slab specifications, such as the type of the slab, availability of shear reinforcing, the ratio of gravity shear (V_g/V_o) and the associated continuity reinforcement, etc. In the other words, the given data (e.g., slab type, reinforcement details, etc.) can lead the component to be determined from the corresponding 18

types of candidates. As a result, the perception of component characteristics can significantly, impact the seismic loss assessment. In relevant studies, Z. Xu et al demonstrated that BIM by providing the visual geometries, materials, construction details and potential damage conditions can significantly, enhance the classification of the FEMA component database as well as improving uncertainty in the corresponding seismic loss assessment. However, the employed BIM-based method in that study for obtaining the effective information data was partially automatic and the user still had to manually add the construction details and the potential damage properties for the building components (Xu et al., 2019a; b).

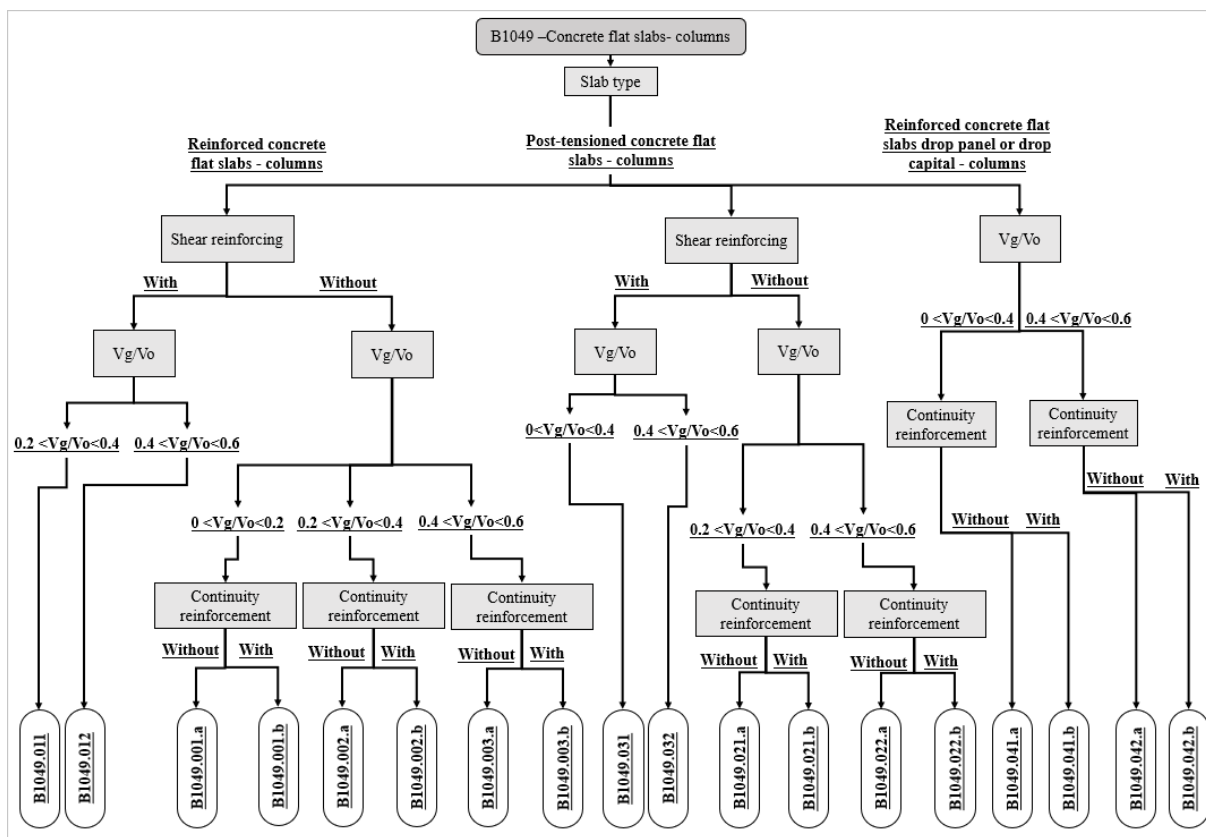


Figure 2.4. The classification of the eighteen different concrete flat slab– column connection joints, provided by FEMA P-58 database

2.5.2 Obstacles in the estimation of building inventory quantities in PBEE assessment; use of BIM in component-level loss assessment method

The importance of a precise estimation over the contents and the quantities of the vulnerable structural and non-structural components is evident, especially in a component level loss assessment method (e.g., FEMA P-58). However, recent studies show damage to nonstructural

elements causes much more losses and consequences than those attributed to structural elements, particularly in low-intensity seismic events. Therefore, providing a thorough realization of building information details is of vital importance to enhance the quality of the analysis and the associated uncertainties, in particular about non-structural elements. However, in the absence of detailed building-specific inventory, quantities should be determined based on given common nonstructural components, contents, and typical quantities (i.e., normative quantities) observed in similar-sized and occupied buildings. Therefore, employing BIM not only can avoid potential uncertainties brought by the normative quantities, but also, can lead to more accurate quantification of vulnerable contents and the corresponding quantities in a building (Xu et al., 2019a; b; Perrone and Filiatrault, 2017; Fema, 2012). In a recent study, (Xu et al., 2019a) utilized BIM to investigate the uncertainty in building seismic loss analysis due to the normative quantities of non-structural components. It was found that, establishing building information models that can achieve more practical and extractable information can highly improve the accuracy of the corresponding loss analysis (Xu et al., 2019a). Hereafter, they proposed a more improved loss assessment method inspired by FEMA P-58 and BIM technology, that uses ontology-based acquisitions to obtain exact quantities and measurements of components. However, a technical knowledge of ontology methods and semantic reasoning rules is demanded (Xu et al., 2019b).

2.5.3 Lack of visualization technology in PBEE assessment; use of BIM in component-level loss assessment method

Although, current practice of FEMA P-58 methodology focuses on the component level loss assessment in PBEE framework and deemed realistic, it could nevertheless be confusing to owners. This is mainly due to the implications of current loss analysis output format, that is somehow impossible to decipher. However, the resulting impediment can be resolved through adoption of available visualization technologies such as BIM in PBEE framework. Therefore, proper visualization capabilities not only can enhance the perception of the building's post-earthquake capacity for engineers, but also, can considerably improve the communication of performance implications to owners (Christodoulou, Vamvatsikos and Georgiou, 2010). Limited studies have been carried out on BIM, as a visualization tool for the seismic loss analysis of building components. Among them, (Christodoulou, Vamvatsikos and Georgiou, 2010) was one of the earliest studies, in which BIM, as a 3D/4D visualization was utilized to forecast the induced-

seismic loss data and the associated rehabilitation work. However, the damage predictions employed in that framework were not based on FEMA P-58 methodology, and not fully integrated with the BIM visualization (Christodoulou, Vamvatsikos and Georgiou, 2010). In a more recent study, (Xu et al., 2019b) combined BIM and FEMA P-58 to develop a visual loss prediction method for buildings. Two different visualization modes were employed in that study, named the absolute mode and the relative mode to demonstrate the spatial distribution of damage and losses among the components in a virtual walkthrough way. Moreover, the mapping algorithm uses plastic-hinge rotations to distribute the predicted damage states from group of components to the joint of each specific structural component (such as beams, slabs and columns). However, calculating the plastic-hinge rotations requires the explicit use of nonlinear response history analysis and consequently, a significant time commitment in model validation (Xu et al., 2019b).

2.5.4 Level Of Development (LOD) in BIM-based PBEE loss assessment

To better attribute the characteristics of damage and loss data in FEMA P-58, the detailing of structural and non-structural components available in building information models is required. Level of Development (LOD) is one of the most widely used metrics to evaluate the level of detail associated with various components in building information models. In the other words, effective information in seismic loss assessment can be a function of LOD associated with each component in building information models. Limited research has been conducted in this domain. Among them, (Xu et al., 2019a) established three different BIM models from the original model of a two-story steel moment frame office to investigate the influence of LOD diversity on building seismic loss assessment. The result noted that, diversity in LOD can affect the seismic performance of the entire building, which could lead to significant uncertainty in economical loss of both the structural and non-structural components (Xu et al., 2019a).

2.5.4.1 LOD definition

The American Institute of Architect (AIA) E202-2008 defines LOD as the extent to which each component, system, or assembly within building information models has been developed (Parrott and Bomba, 2010; Hong, Hammad and Akbarnezhad, 2019). Following is Figure 2.5, in which different LODs from LOD 100 to LOD 500 are demonstrated, based on (NATSPEC, 2013). It is

noteworthy to mention that, obtaining different level of detailed information, which could be either graphic or non-graphic is the main difference among different LODs of each component.


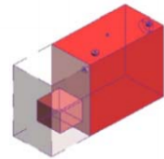



LOD 100 Conceptual	LOD 200 Approximate geometry	LOD 300 Precise geometry	LOD 400 Fabrication	LOD 500 As-built
				
The Model Element may be graphically represented in the Model with a symbol or other generic representation , but does not satisfy the requirements for LOD 200. Information related to the Model Element (i.e. cost per square metre, etc.) can be derived from other Model Elements.	The Model Element is graphically represented in the Model as a generic system, object, or assembly with approximate quantities, size, shape, location, and orientation.	The Model Element is graphically represented in the Model as a specific system, object, or assembly accurate in terms of quantity, size, shape, location, and orientation.	The Model Element is graphically represented in the Model as a specific system, object, or assembly that is accurate in terms of quantity, size, shape, location, and orientation with detailing, fabrication, assembly, and installation information .	The Model Element is a field verified representation accurate in terms of size, shape, location, quantity, and orientation.
	Non-graphic information may also be attached to the Model Element.	Non-graphic information may also be attached to the Model Element.	Non-graphic information may also be attached to the Model Element.	Non-graphic information may also be attached to the Model Element.

Figure 2.5. LOD definitions from LOD 100 to LOD 500, source: (NATSPEC, 2013)

2.5.4.2 LOD for structural components

With regards to structural components, characteristics derived from different LODs of each component can have either limited or significant effect on both the median and the uncertainty of the repair cost. Therefore, it is vital to determine the primary characteristics (attributes) of each structural component, which greatly affects the uncertainty of the seismic loss assessment (Xu et al., 2019a). The category of steel columns (B1031) is an example of structural component. As it can be seen in Figure 2.6, FEMA P-58 provides 7 types of steel connections, as the fragility group of steel columns (B1031). Among them, to identify each steel column base plate in the entire building, more effective information is required such as specific sizes and material details. However, according to LOD specification of Steel Framing Columns (Uniformat B1010.10.30) by BIMForum (BIMForum, 2020), a steel column with a LOD of 300 or higher contains all of the necessary details, required to determine the corresponding fragility and consequence function from

FEMA P-58 database. Figure 2.7 shows detailed descriptions of different LODs for steel framing column derived from (BIMForum, 2020).

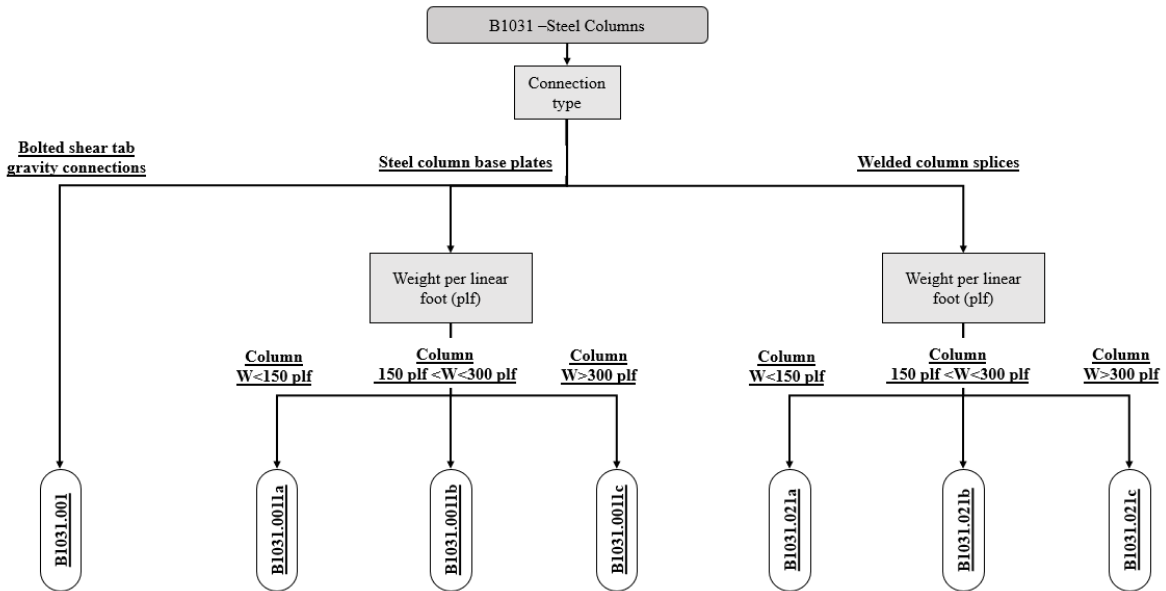


Figure 2.6. The classification of seven different connection for steel columns, provided by FEMA P-58 database


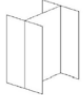

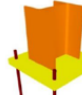
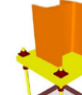
LOD 100	LOD 200	LOD 300	LOD 350	LOD 400
 <p>22 B1010.10-LOD-100 Floor Structural Frame (Steel Framing Columns), From Ikerd.com</p>	 <p>23 B1010.10-LOD-200 Floor Structural Frame (Steel Framing Columns), From Ikerd.com</p>	 <p>24 B1010.10-LOD-300 Floor Structural Frame (Steel Framing Columns), From Ikerd.com</p>	 <p>25 B1010.10-LOD-350 Floor Structural Frame (Steel Framing Columns) From Ikerd.com</p>	 <p>26 B1010.10-LOD-400 Floor Structural Frame (Steel Framing Columns), From Ikerd.com</p>
<p>Generic column element,</p> <p>Assumptions for structural framing are included in other modeled elements such as an architectural floor element that contains a layer for assumed structural framing depth or schematic structural elements that are not distinguishable by type or material.</p> <p>Assembly depth/thickness or component size and locations still flexible.</p>	<p>Model elements to include:</p> <ul style="list-style-type: none"> • Floor with approximate dimensions • Approximate supporting framing members • Structural grids defined accurately 	<p>Element modeling to include:</p> <ul style="list-style-type: none"> • Specific sizes of main vertical structural members modeled per defined structural grid with correct location and orientation 	<p>Element modeling to include:</p> <ul style="list-style-type: none"> • Actual elevations and location of member connections • Main elements of typical connections applied to all structural steel connections such as base plates, gusset plates, anchor rods, etc. • Any miscellaneous steel members with correct size, shape, orientation, and material. • Any steel structure reinforcement such as web stiffeners, sleeve penetrations, etc. 	<p>Element modeling to include:</p> <ul style="list-style-type: none"> • Welds • Coping of members • Cap pates • Washers, nuts, etc. • All assembly elements

Figure 2.7. BIMForum 2020 LOD definition for steel framing columns (B1010.10.30) derived from (BIMForum, 2020)

2.5.4.3 LOD for non-structural components

The sanitary waste piping (D2031) is considered as an example for non-structural components. Figure 2.8 shows the classification of sanitary waste piping provided by FEMA P-58. According to this classification, the attributes (such as coupling type and Seismic Design Category (SDC) etc.) can lead the component to be determined from the corresponding 12 types of candidates. Therefore, by employing LOD specification of sanitary sewerage piping (Uniformat D2020.30) by BIMForum (BIMForum, 2020), a sanitary piping with a LOD of 350 or higher contains all of the vital information, that is required to find the related fragility and consequence function in the FEMA P-58 database. Figure 2.9 shows detailed descriptions of different LODs for sanitary sewerage piping derived from (BIMForum, 2020).

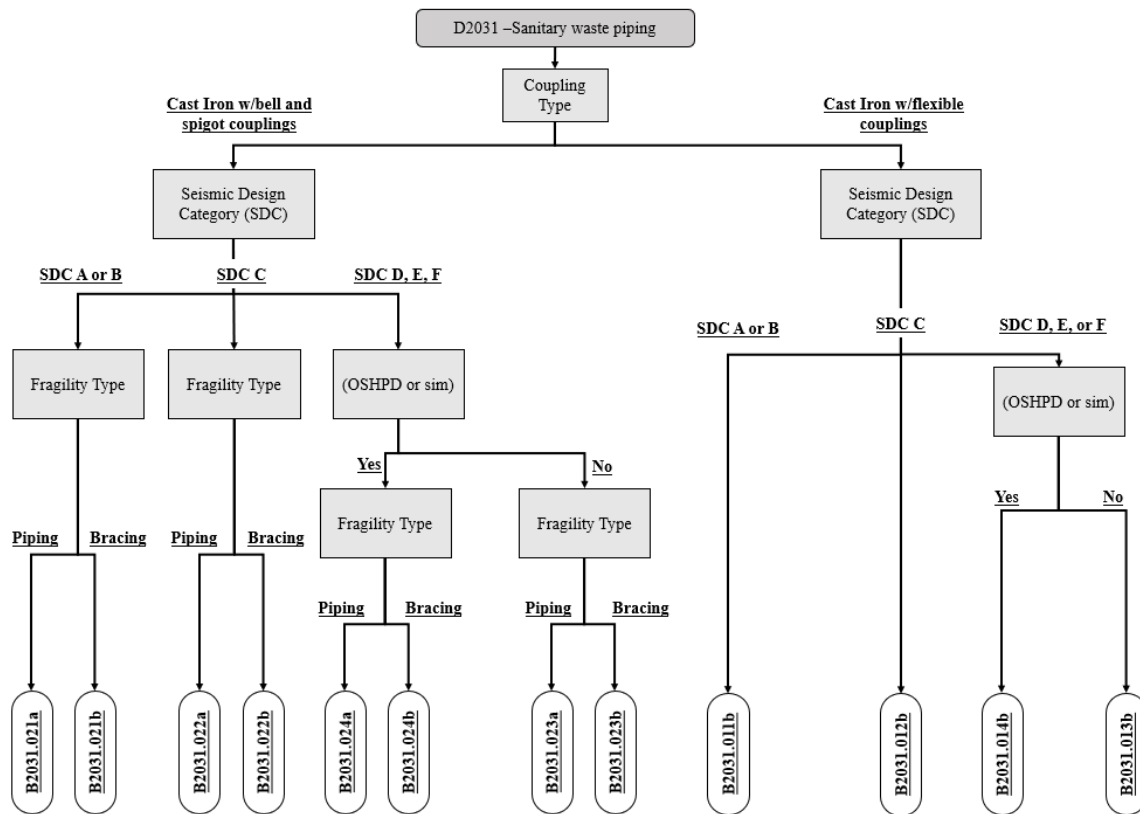


Figure 2.8. The classification of twelve different candidates for sanitary sewerage piping, provided by FEMA P-58 database



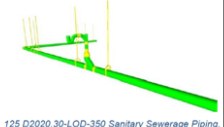
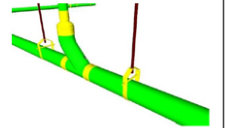
LOD 100	LOD 200	LOD 300	LOD 350	LOD 400
Not Defined	 <small>123 D2020.30-LOD-200 Sanitary Sewerage Piping. From bimfd.com</small>	 <small>124 D2020.30-LOD-300 Sanitary Sewerage Piping. From bimfd.com</small>	 <small>125 D2020.30-LOD-350 Sanitary Sewerage Piping. From bimfd.com</small>	 <small>126 D2020.30-LOD-400 Sanitary Sewerage Piping. From bimfd.com</small>
Diagrammatic or schematic model elements; conceptual and/or schematic layout/flow diagram; design performance parameters as defined in the BXP to be associated with model elements as non-graphic information.	Schematic layout with approximate size, shape, and location of mains and risers; shaft requirements modeled;	Modeled as design-specified size, shape, spacing, location, and slope of pipe, valves, fittings, and insulation for risers, mains, and branches; Approximate allowances for spacing and clearances required for all specified hangers, supports, vibration and seismic control that are to be utilized in the layout of all risers, mains, and branches; access/code clearance requirements modeled	Modeled as actual construction elements; Actual size, shape, spacing, location, connections, and slope of pipe, valves, fittings, and insulation for risers, mains, and branches; Actual size, shape, spacing, and clearances required for all hangers, supports, vibration and seismic control that are utilized in the layout of all risers, mains, and branches; Actual floor and wall penetration elements modeled. Actual access/code clearance requirements modeled	Supplementary components added to the model required for fabrication and field installation

Figure 2.9. BIMForum 2020 LOD definition for sanitary sewerage piping (D2020.30) derived from (BIMForum, 2020)

2.5.5 Application Programming Interface (API) in BIM-enable tools

Thanks to Application Programming Interface (API) capabilities, additional functionalities and interactive processing are developed that can lead to significant enhancement of interfaces in the commonly BIM-enable tools. As a result, various creative BIM extensions are developed through API facility that has reduced manual operation and improved automation in simulating the considerable amount of information associated with typical building components in BIM models. Moreover, adopting API implementations could dramatically boost the viability of conducting post-earthquake loss analysis of different buildings via BIM-enable tools (Jin and Gambatese, 2019; Oti et al., 2016; Kensek, 2014; Xu et al., 2019b; Yang, Koehl and Grussenmeyer, 2018).

2.5.5.1 Autodesk Revit API

Autodesk Revit is a well-known BIM software program utilized in the Architecture, Engineering and Construction (AEC) industry that enables the users to systematically access building information through a visualized database. Overall, Autodesk Revit incorporates three main workspaces of Revit architecture, Revit structure and Revit Mechanical, Electrical and Plumbing

(MEP) to digitalize the geometric and functional attributes of the entire building components with the associated parameterizations. Autodesk Revit is intended to establish a unified platform to support the theoretical and analytical workflows among the various workspaces. However, acquiring and parameterizing the seismic loss analysis data through the corresponding building components, require a considerable time investment (Yang, Koehl and Grussenmeyer, 2018). Figure 2.10 shows an example of a complex building with the associated architectural, structural and mechanical components in Autodesk Revit.

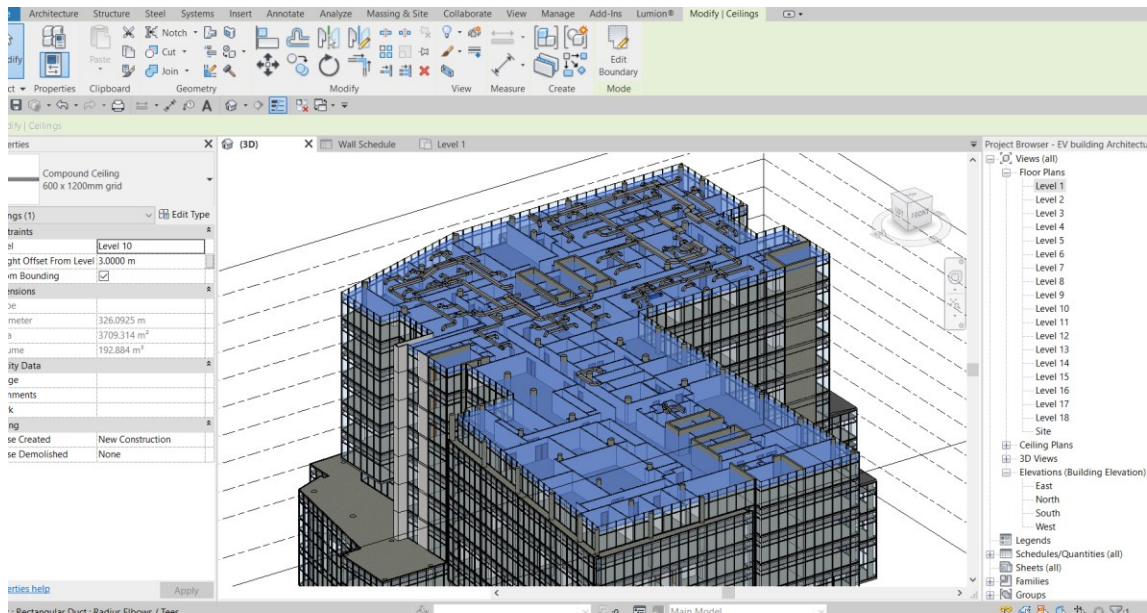


Figure 2.10. A virtual 3D model of a complex building with the structural and non-structural building components in Autodesk Revit

Autodesk Revit API is a widely used open API that enables users to develop programs or scripts to achieve a robust and efficient range of new functionalities in BIM environment. It provides an interactive environment that incorporates BIM parametric modelling and programming functions to extend the level of manipulation in Revit elements far beyond the existing features in this platform. Revit API is compliant with Microsoft.NET Framework languages, such as Visual C# or Visual Basic.NET, C#, or C++/CLI. Moreover, *Revit SDK*, *RevitLookup*, and *AddinManager* are also provided as additional tools to help in the development process (Jin and Gambatese, 2019; Yang, Koehl and Grussenmeyer, 2018; Oti et al., 2016; Kensek, 2014; Xu et al., 2019b). With regards to the advantages of employing algorithms and computational logics in Revit API, limited studies have utilized Revit API to facilitate seismic loss assessment of buildings through BIM

models. (Xu et al., 2019b) employed Revit API to systematically map the vulnerable categories of components defined in BIM model to the corresponding categories at FEMA P-58 database. The API-based mapping process was, nevertheless, relatively automatic in terms of sorting the components based on type and the elevation of stories, but also fully manual in identification of FEMA P-58 classification criteria and the corresponding components (Xu et al., 2019b). However, (Xu et al., 2019a) in another study conducted over the application of Revit API in FEMA P-58 loss analysis, attempted to automate the identification process between FEMA P-58 classification criteria and the corresponding components in BIM model, conditioned by the available attributes and LOD data (Xu et al., 2019a).

2.5.5.2 DYNAMO Studio: A Revit API-based visual programing interface

Dynamo Studio is an open-source visual scripting interface that enhances Revit's capabilities by making the Revit API easier to use. From the parametric modeling perspective of view, Dynamo Studio is inspired from Generative Components by Bentley and Grasshopper algorithmic plugin for Rhino. Dynamo Studio is designed to provide effective workflow interoperability and integrated automation into Revit for documentation, coordination and analysis purposes. Moreover, it enables the users to dynamically manipulate the modeling parameters and the associated data values derived from sensors or external analysis in different stages of project. With regards to visual characteristics of programing interface in Dynamo, the components with which users communicate are referred to as "nodes", which contains small scripts written in common textual programming language including C++ and Python. Each node is connected to the other nodes through the "connectors". A network of the connected nodes creates a "workflow". As the result of incorporating short algorithms through the sets of workflows, more customized and complex functionalities are achievable (Valinejadshoubi, Bagchi and Moselhi, 2019; Kensek, 2014; Bahmanoo et al., 2019). Figure 2.11 shows an overview of nodes and workflows in Dynamo Studio.

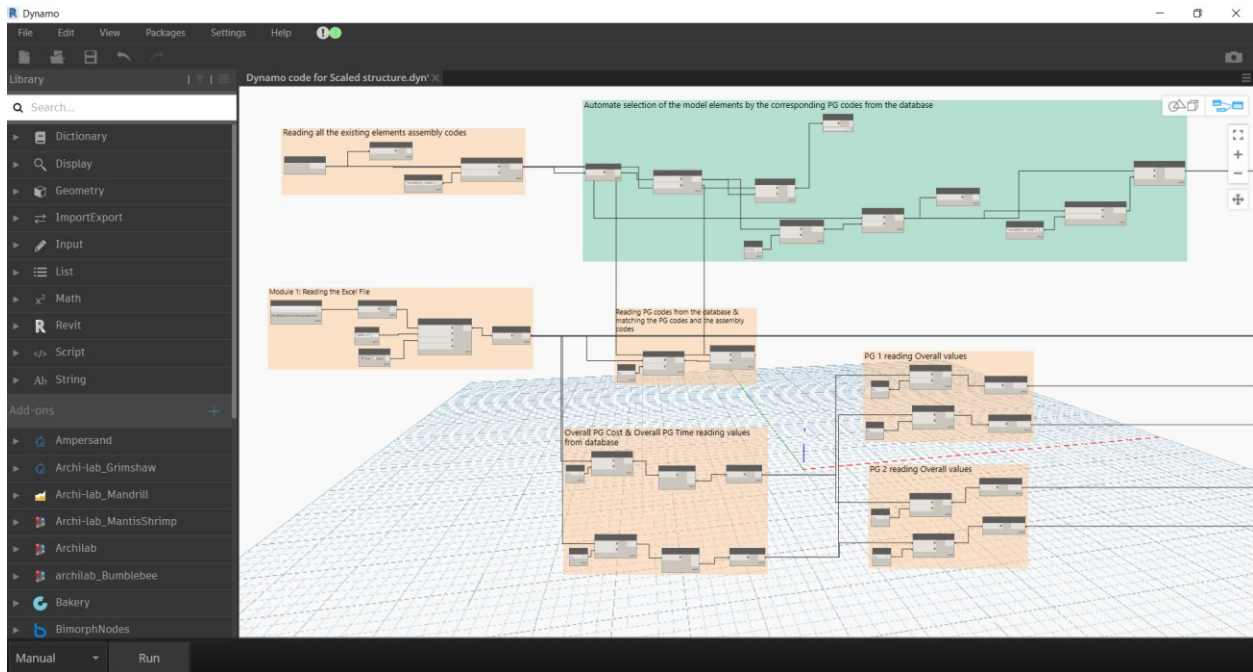


Figure 2.11. An overview of nodes and workflows in Dynamo Studio

2.6 Summary & Conclusion

This chapter reviewed the concepts, methods and technologies employed in the current body of research on probabilistic seismic loss assessment of buildings based on the most common and practical frameworks from Performance-Based Earthquake Engineering (PBEE) approach such as HAZUS methodology and FEMA P-58. Moreover, potential opportunities associated with utilizing more innovative technologies such as seismic instrumentation of buildings and Building Information Modeling (BIM) in PBEE assessment frameworks were also investigated.

It is found that, despite the many benefits of adopting PBEE loss assessment of buildings, some certain drawbacks on the acquisition, visualization and precision of loss data have caused significant uncertainties, that has raised considerable amount of research in the last few years. Some research addressed BIM implementation to overcome the aforementioned limitations, whereas some recommended seismic instrumentation as the solution, but, to the best of authors' knowledge, no comprehensive work was dedicated to the integration of BIM and sensing-based measurements within the PBEE assessment frameworks. In this study, to improve the practicality and reduce the associated uncertainties of PBEE assessment methodologies, a framework for employing BIM technology in seismic loss assessment of instrumented buildings is proposed.

CHAPTER 3 Proposed Methodology

3.1 Overview

The proposed methodology focuses on employing sensing-based measurements and BIM tools in PBEE assessment frameworks. With respect to section 2.4 and 2.5, major source of uncertainty in the predicted performance (e.g., economic) of PBEE assessment frameworks normally, occurs due to structural responses and the caused physical damage. PEER-PBEE's methodology defines the structural response of a building to an earthquake through the key response parameters (such as peak absolute floor acceleration, peak absolute floor velocity and peak story drift ratio), called EDPs. These response parameters are a function of structural characteristics of a building. In this chapter, at the first step, to identify the actual structural characteristics and modal properties of a building, a workflow of measurement of structural dynamic response as well as output-only system identification (SI) based on operational modal analysis (OMA) approach is proposed. Next, at the second step, to identify the key response parameters (EDPs) that are based on the actual (measured) modal properties derived from the first step, model-based approach and nonmodel-based approach, as the two main methodological approaches for the experimental structural analysis are proposed. The key difference between the model-based and nonmodel-based approach is the manner to compute the EDPs; the model-based approach uses finite element model (FEM), while the nonmodel-based approach is FEM free and is developed through a BIM-based API tool. Then, at the third step, initially, a workflow of performing a seismic loss analysis based on FEMA P-58 methodology in PACT software is proposed. Subsequently, another BIM-based API tool is developed to intelligently, collect the loss data from a database and visualize them through a color code scheme. Figure 3.1 shows the overview and the scope of the proposed methodology.

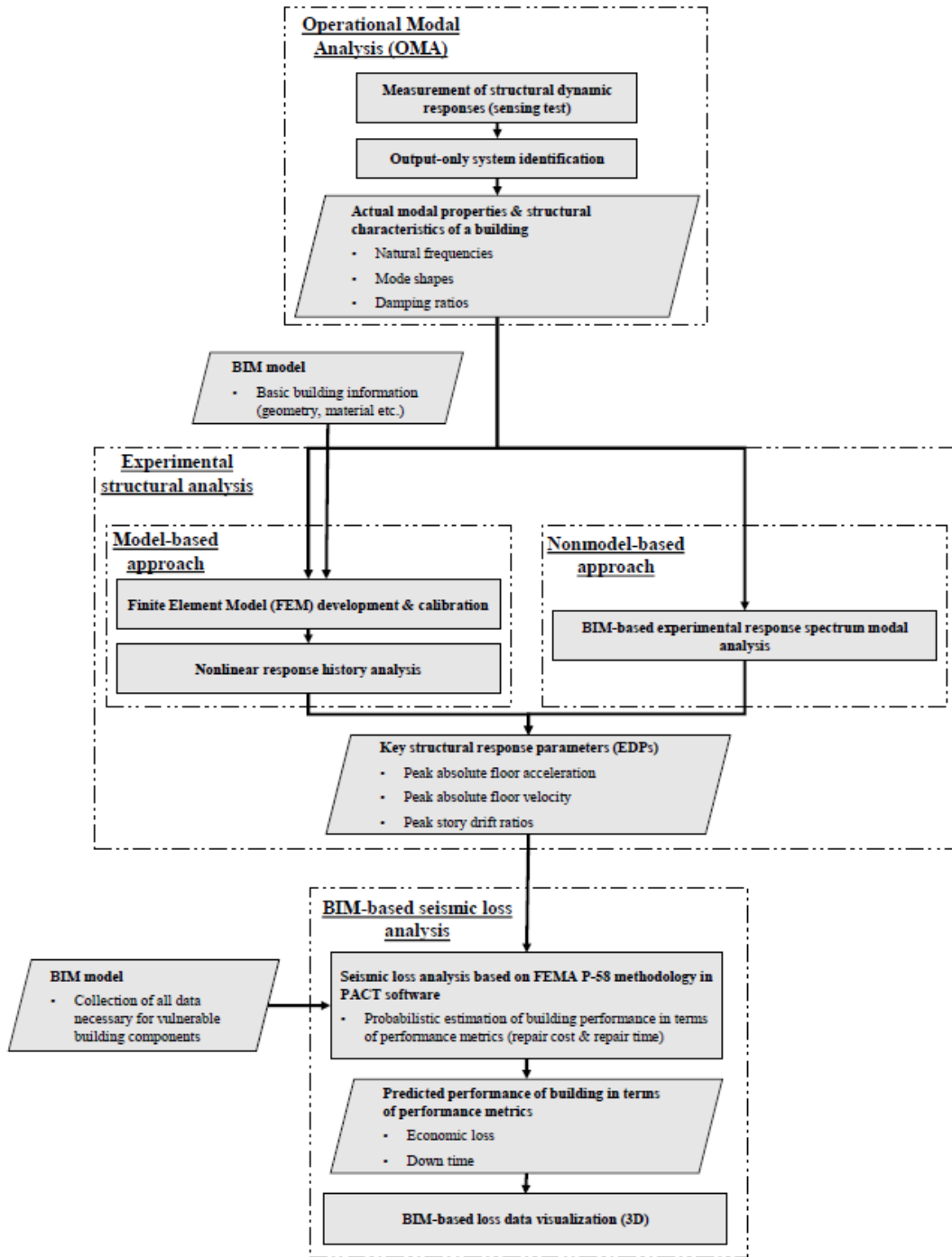


Figure 3. 1. The overview and the scope of the proposed methodology

3.2 Operational Modal Analysis (OMA)

The term "modal identification" refers to the process of determining the actual properties of structures based on experimental vibration tests and classified under the forced vibration tests (FVT)

and the ambient vibration tests (AVT). In contrast with FVT methods where the input excitation is measured and controlled, AVT is about analyzing the dynamic behavior of civil structures, subjected to immeasurable and uncontrollable operational loadings (such as traffic, wind and so on). Therefore, literature also refers to it as Operational Modal Analysis (OMA) or output-only modal analysis. As shown in Figure 3.2, to identify the actual properties of a structure, the workflow of OMA in this methodology contains measurement of structural dynamic response (sensing test) as well as output-only system identification (SI) (Mirshafiei, 2016; Sabamehr, 2018; Lim, 2016).

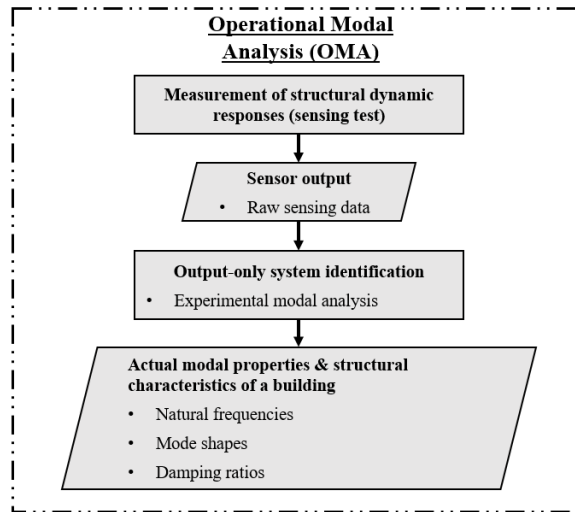


Figure 3. 2. The workflow of OMA in the proposed methodology

3.2.1 Measurement of structural dynamic response

With respect to the measurement of structural dynamic response under the OMA, the organization of sensor placements throughout the structure is of utmost importance. The optimal layout of all sensor locations is a matter of obtaining all the desired mode shapes of a structure from the test. In the other words, depending on the adequate number of the target mode shapes to be extracted, the placement of the sensors should be far away from the modal nodes to be able to detect the corresponding deformed shape of each particular mode. Normally, due to the lack of a sufficient number of sensors compared with the required measuring nodes or the enormous size of structures, multiple test setups are usually needed to perform AVT. Normally, in each setup, one or two sensors are required to be fixed in a common location between all the setups where associated deformation with each desired mode shape occurs (usually at roof corners of building). The fixed

sensors are referred as reference sensors, while the rest of sensors are called as roving sensors and are distributed uniquely in each setup to cover all the desired measurement nodes. It is noteworthy to highlight that the reference sensor serves as a link between the various test configurations, allowing the collected data to be merged and form the appropriate mode shapes. Moreover, the quality and accuracy of AVT to extract modal properties of a structure can be highly influenced by the sensing duration; much longer acquisition time contributes to a better performance. Apart from the duration of the test, the communication system between the sensors has a major impact on sensing results too. Sensors equipped with the radio communication system (radio antenna) can form a wireless chain, which helps all the test recordings have a same timing and be fully synchronized. Also, with respect to the Nyquist sampling theorem, the sampling frequency should be at least twice higher than the fundamental mode shape with the highest frequency among all the desired number of mode shapes(Mirshafiei, 2016).

3.2.2 Output-only system identification (SI)

The term “output-only system identification (SI)” refers to the process of identifying the operational dynamic response and characteristics of a structure from experimental data. Normally, the output of SI is a modal model of a structure that contains the natural frequencies of the structure along with the corresponding mode shapes and damping ratios. Output-only SI mainly classified under three groups of nonparametric methods that are mostly developed in frequency domain, parametric methods that are time domain-based methods and time-frequency domain which calculates time and frequency simultaneously. In this proposed methodology, the most common technique in frequency domain called, Frequency Domain Decomposition (FDD) is employed to compute the natural frequencies and the corresponding mode shapes of a structure (Sabamehr, 2018).

3.2.2.1 Frequency Domain Decomposition (FDD)

With respect to FDD, as a well-known used algorithm in frequency domain, the relationship between an immeasurable input $x(t)$ and the measurable output $y(t)$ can be expressed in Equation (3.1), where Singular value decomposition (SVD) is used to decompose the Power Spectral Density (PSD) matrix into its eigenproblem form:

$$G(w) = [U(w)][S(w)][U(w)]^H \quad (3.1)$$

With respect to Equation (3.1), G stands for PSD matrix, [S] is SVD matrix and [U] is the unitary matrix that contains the singular vectors. Moreover, H represents the Hermitian transformation. The FDD method begins with estimating the spectral densities among all the captured data for the purpose of assembling of PSD matrix, $G_{xy}(w)$. The reason behind this step is that the spectral density is a true indication of a signal's energy content (based on unit frequency), which can determine which frequencies influence the most energy to a signal. It is also noteworthy to mention that, only if the input signal is a white noise, so the peaks of the output PSD function equate to the system's natural frequencies. The PSD itself, is the estimated value of the product of all pairs of captured data's Fourier transforms, where each signal is divided into various sub-records with shorter duration and removed value operation, as shown in Equation (3.2). Moreover, the multiplication of pairs of discrete Fourier transforms utilized in this process should be averaged (Mirshafiei, 2016; Sabamehr, 2018).

$$G_{xy}(w) \approx \frac{1}{n} \sum_{a=1}^n X^a(w)Y^a(w) \quad (3.2)$$

With respect to Equation (3.2), the discrete Fourier transforms of corresponding time history records are X(w) and Y(w). Also, the number of sub records is n.

After estimating the output in PSD matrix, then the output PSD matrix should be decomposed by applying the SVD matrix. As the result of this process, the singular vectors represent the calculated mode shapes, and the singular values represent an approximation of how much each mode contributes to total energy at each frequency. The first singular vector gives an approximation of the corresponding mode shape for each resonant frequency based on the peaks on the first singular value plot (Mirshafiei, 2016; Sabamehr, 2018).

3.3 Experimental structural analysis

Experimental structural analysis refers to the process of developing numerical models to compute the structural responses of a building based on the experimental data. Since the actual structural characteristics and modal properties of a building are derived from the previous step, two different methodological approaches of model-based and nonmodel-based are proposed in this research to compute the key response parameters (such as peak absolute floor acceleration, peak absolute floor

velocity and peak story drift ratio), that are required to be prepared for the subsequent damage and loss analysis at the final step. In the other words, the experimental structural analysis (second step) is the linkage between the first and the third step of this methodology to derive the required engineering demand parameters (EDPs) (required for the subsequent loss analysis) out of the experimental modal model of a building. As demonstrated in Figure 3.3, the main difference between these two approaches is that numerical FEM model is utilized in model-based approach to compute the desired EDPs, while the nonmodel-based approach is free of FEM model employment. Thanks to the nonmodel-based approach, the explicit utilization of nonlinear building models as well as subsequent model validation processes that are inevitable part of the model-based approach can be avoided. On the other hand, the main common procedure of these two approaches is that BIM technology is used to facilitate the EDP estimation process.

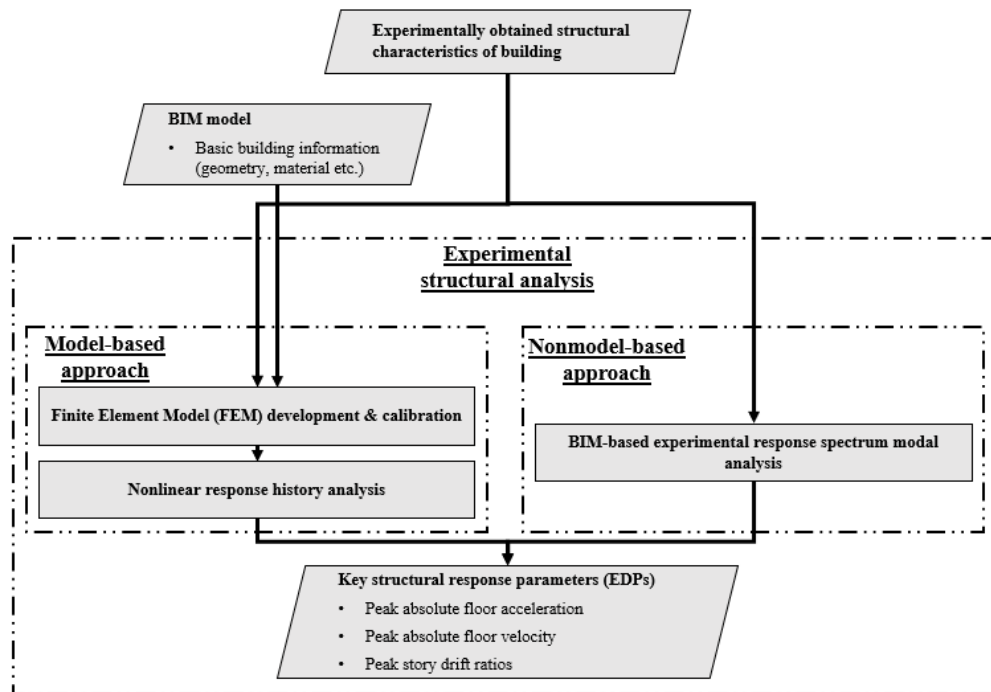


Figure 3. 3. The workflow of the structural analysis in the proposed methodology

3.3.1 Model-based approach

After extracting the dynamic characteristics of a structure through the operational modal analysis process at the previous step, experimental structural analysis can be performed. With respect to model-based perspective of view, initially, a Finite Element Model (FEM) of a structure is created

and then calibrated to reflect the actual building performance characteristics derived from the previous step (OMA). However, to reduce the usual time-consuming workload of FE model creation, a conversion function is used to form a highly detailed structural analysis model of the structure from the corresponding pre-existing BIM model. In this methodology, CSI ETABS and Autodesk Revit software programs are utilized to form the structural analysis model and BIM model, respectively, due to sufficient compatibility. Finally, a nonlinear time history analysis is performed over the calibrated model to produce the EDPs (e.g., peak absolute floor acceleration, peak absolute floor velocity and peak story drift ratio) (Figure 3.4).

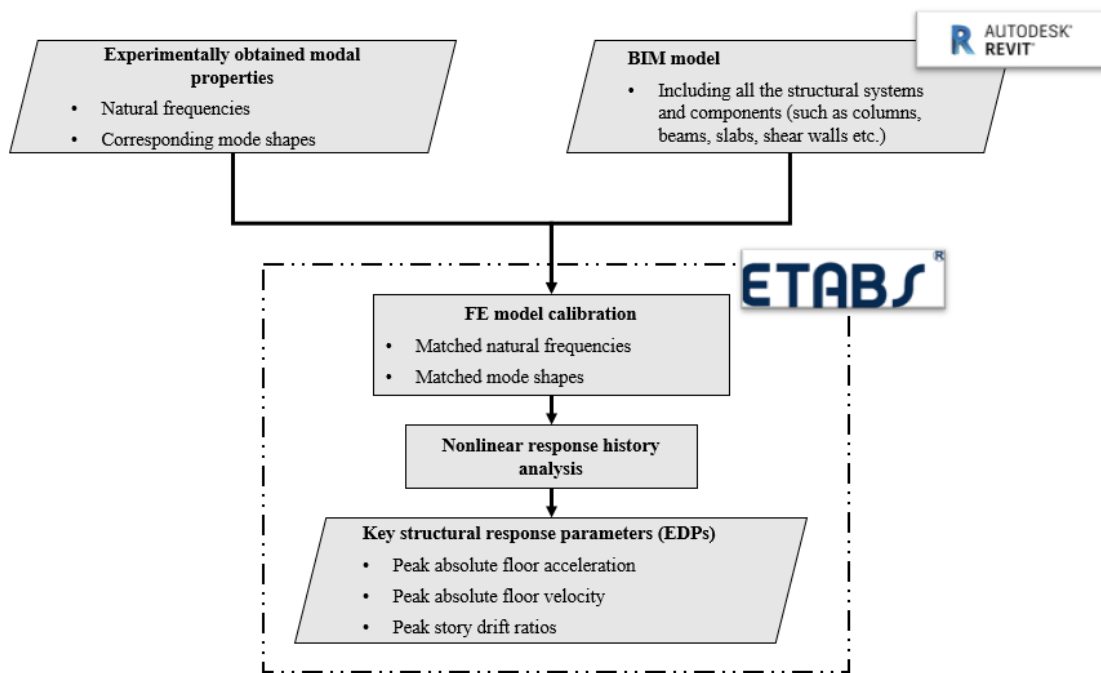


Figure 3. 4. The overview of the proposed model-based approach

3.3.1.1 FE model calibration

The FE method is often used in structural analysis of buildings. However, the accuracy of FE modeling is determined by a variety of variables, including element specification (type and size), geometry detail, material properties and boundary conditions. Moreover, analytical FE models are normally, constructed by the highly idealized engineering and design assumptions that would represent a different seismic behavior from the result of an actual structure. Thus, utilizing a correlated FE model of a structure based on extracted experimental modal parameters from ambient vibration tests is vital to provide the actual behavior of the structure. FE model calibration

entails adjusting the FE model's mass, stiffness, and damping parameters to compensate for identified inconsistencies between the analytical and experimental modal parameters (i.e. mode shapes, ϕ , and eigenfrequencies, λ) (Bagchi, 2005).

3.3.1.2 Nonlinear response history analysis

With regards to structural analysis, nonlinear time history analysis is performed over the calibrated FE model to estimate the structural response of a building to earthquake shaking. This process begins with collecting and scaling an adequate number of earthquake records with given earthquake intensities based on the National Building Code of Canada (NBCC) guidelines and building's location. Finally, the nonlinear time history analysis is performed to calculate the actual structural responses of the building. As the result, the EDPs (e.g., peak absolute floor acceleration, peak absolute floor velocity and peak story drift ratio) are available for the subsequent loss analysis at the final step.

3.3.2 Nonmodel-based approach

This section addresses the proposed framework to estimate the seismic behavior of a structure based on extracted experimental modal properties of OMA through a visual programming tool in a BIM software program (Autodesk Revit) called, Dynamo Studio. The major advantage of this framework compared to the model-based approach is to be free of FE modeling. Furthermore, the whole experimental seismic analysis framework is automated in a BIM environment platform. As demonstrated in Figure 3.5, a set of algorithms are developed based on Dynamo Studio (an API tool developed in Autodesk Revit as a BIM software) that are integrated with a relational database to perform three-dimensional modal response spectrum analysis based on extracted experimental modal properties from OMA. The structural input parameters required for the seismic analysis in this algorithm are derived from building's actual characteristics: building component geometry and material properties, natural frequencies, and the corresponding modal matrix. The geometry and material properties are mostly, extracted from building's BIM model which is constructed based on available technical drawings, while the natural frequencies and the corresponding mode shapes are derived from the performed OMA. Subsequently, various modules of this algorithm process the aforementioned input data and compute the required structural input parameters. Finally, the

derived structural input parameters are transferred automatically to the relational database, which is formulated based on a series of rapid and simple estimation of building's peak response from the properties of the response spectrum concept. As the result, the seismic response of the building is calculated without having to perform a response history analysis.

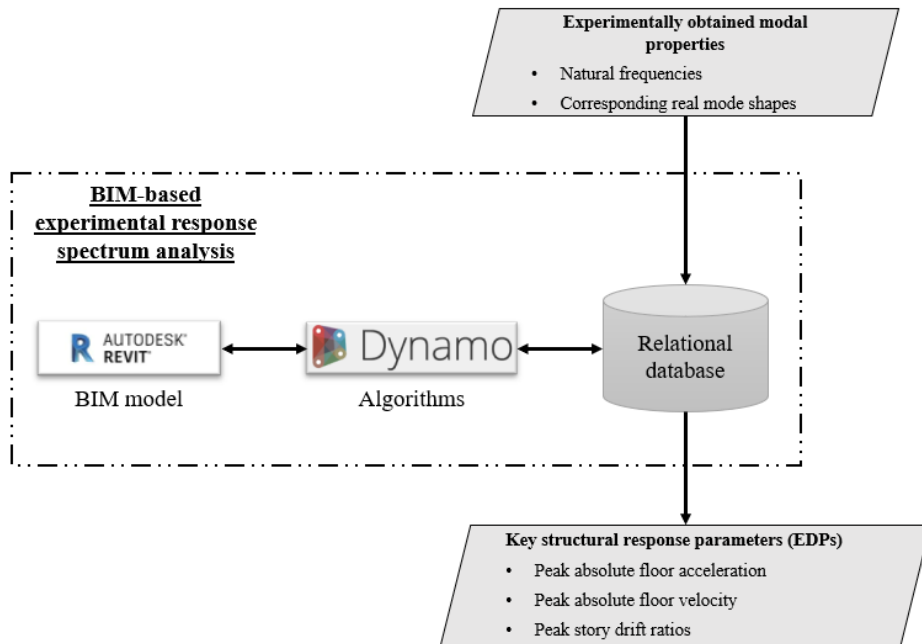


Figure 3. 5. The workflow of the proposed three-dimensional modal response spectrum analysis

3.3.2.1 Experimental Response Spectrum modal analysis

With respect to a simplified modal analysis, (i.e., response history analysis using modal decomposition) the simplest form of the equation of motion for three-dimensional simplified multi-degree-of-freedom buildings subjected to a horizontal seismic force can be carried out as following (Figure 3.6):

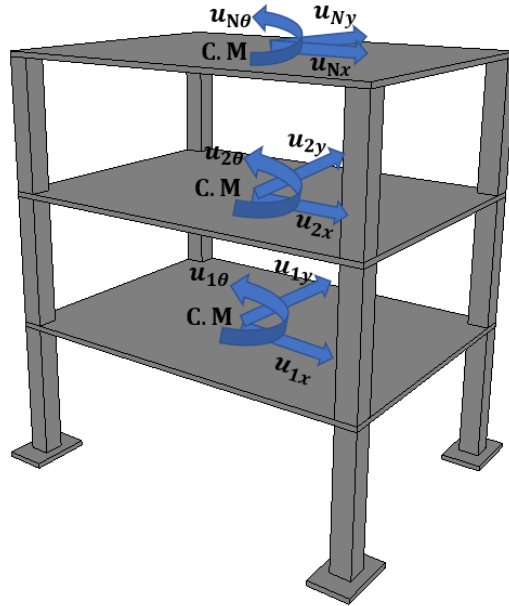


Figure 3. 6. Schematic view of a three-dimensional simplified multi-degree-of-freedom building

$$[M]\{\ddot{u}\} + [C]\{\dot{u}\} + [K]\{u\} = -[M]\{I\}a_g \quad (3.3)$$

Where the mass matrix is:

$$[M] = \begin{bmatrix} m_{1x} & 0 & \dots & \dots & \dots & \dots & \dots & \dots & \dots & \dots & \dots & 0 \\ 0 & m_{1y} & 0 & \ddots & \ddots & \ddots & \ddots & \ddots & \ddots & \ddots & \ddots & \vdots \\ \vdots & 0 & I_{o1} & 0 & \ddots & \ddots & \ddots & \ddots & \ddots & \ddots & \ddots & \vdots \\ \vdots & \ddots & 0 & m_{2x} & 0 & \ddots & \ddots & \ddots & \ddots & \ddots & \ddots & \vdots \\ \vdots & \ddots & \ddots & 0 & m_{2y} & 0 & \ddots & \ddots & \ddots & \ddots & \ddots & \vdots \\ \vdots & \ddots & \ddots & \ddots & 0 & I_{o2} & 0 & \ddots & \ddots & \ddots & \ddots & \vdots \\ \vdots & \ddots & \ddots & \ddots & \ddots & 0 & \ddots & 0 & \ddots & \ddots & \ddots & \vdots \\ \vdots & \ddots & \ddots & \ddots & \ddots & \ddots & 0 & \ddots & 0 & \ddots & \ddots & \vdots \\ \vdots & \ddots & \ddots & \ddots & \ddots & \ddots & \ddots & 0 & \ddots & 0 & \ddots & \vdots \\ \vdots & \ddots & \ddots & \ddots & \ddots & \ddots & \ddots & \ddots & 0 & m_{Nx} & 0 & \vdots \\ \vdots & \ddots & \ddots & \ddots & \ddots & \ddots & \ddots & \ddots & \ddots & 0 & m_{Ny} & 0 \\ 0 & \dots & \dots & \dots & \dots & \dots & \dots & \dots & \dots & \dots & 0 & I_{oN} \end{bmatrix}$$

$$\{u\} = \begin{Bmatrix} u_{1x} \\ u_{1y} \\ u_{1\theta} \\ u_{2x} \\ u_{2y} \\ u_{2\theta} \\ \vdots \\ \vdots \\ \vdots \\ u_{Nx} \\ u_{Ny} \\ u_{N\theta} \end{Bmatrix}$$

With respect to Equation (3.3), M refers to the diagonal matrix of the lumped mass and the moment of inertia of the building's floors about the vertical axis across the center of mass of each floor. The damping and stiffness matrices are represented by C and K, respectively. Although, the direction of earthquake forces is arbitrary, but the influence vector (I) is considered to obtain the effective earthquake forces parallel to the x and y axes. Moreover, it is assumed that each story of the building has rigid floor diaphragm(s), containing two translational and one rotational in plane degrees of freedom, which leads to 3N degrees of freedom (Considering N is the number of stories). As a result, the sway and torsional coupling effects are considered in the analysis.

Having extracted the relative horizontal displacement vector $\{u\}$ of all the building's floors from the performed OMA and employing Duhamel integral, the above equation of motion is solved without knowing the stiffness matrix (K). However, further modification needs to be performed over the extracted $\{u\}$ values prior to be used in the equation.

As a result, in each mode n:

$$\{u\}_n = q_n(t)\{\Phi\}_n \quad (3.4)$$

$$\ddot{q}_n + 2\xi_n\omega_n\dot{q}_n + \omega_n^2q_n = -\Gamma_n a_g \quad (3.5)$$

$$q_{n,max} = \Gamma_n S_{d,n} = \Gamma_n \frac{S_{a,n} g}{\omega_n^2} \quad (3.6)$$

$$\{u\}_{n,max} = q_{n,max} \{\Phi\}_n \quad (3.7)$$

$$\ddot{q}_n = \{\Phi\}_n \Gamma_n S_{a,n} \quad (3.8)$$

Where, $S_{a,n}$ and $S_{d,n}$ are the spectral acceleration and spectral displacement correspond to each natural period T_n , respectively. \ddot{q}_n is the absolute acceleration and Γ_n is also, the modal participation factor which is equal to:

$$\Gamma_n = \frac{\{\Phi\}_n^T [M] \{I\}}{M_n} \quad (3.9)$$

Moreover, as typically suggested in codes, the extracted mode shapes from the performed OMA are required to contribute a minimum cumulated of 90% to the response of the structure. This is examined through a parameter called, Modal participation mass ratio (%M) and is obtained from:

$$MPMR = \%M = \frac{\Gamma_n^2}{\sum(M_x)} \quad (3.10)$$

With respect to the Equations (3.4) to (3.10), peak values of actions $A_{n,max}$ due to $\{u\}_{n,max}$ are calculated in each mode. Finally, the peak structural response of each floor is determined by combining the peak modal contributions according to one of the modal combination rules such as ABSSUM, SRSS and CQC.

$$\text{ABSSUM: } A_{max} = \sum_{n=1}^N |A_{n,max}|$$

$$\text{SRSS: } A_{max} = \sqrt{\sum_{n=1}^N (A_{n,max})^2}$$

$$\text{CQC: } A_{max} = \sqrt{\sum_{i=1}^N \sum_{n=1}^N (\rho_{in} A_{i,max} A_{n,max})} \quad , \text{ where } \rho_{in} = \text{correlation coefficient}$$

3.3.2.2 Simplified experimental seismic analysis Dynamo algorithms

With the implementation of section 3.3.2.1 into the combination of the developed Dynamo algorithm and the corresponding relational database, simplified three-dimensional response spectrum modal analysis is performed. As the result, EDPs such as peak absolute floor accelerations, peak absolute floor velocities and peak story drift ratios are derived at each

building’s story. Figure 3.7 shows the workflow of simplified experimental seismic analysis by Dynamo algorithms, which includes: inputting the extracted modal properties (such as real mode shapes and the corresponding natural frequencies) from the performed OMA, calculating the required structural input parameters and performing the experimental response spectrum modal analysis. to perform this workflow in the proposed methodology, two main algorithms are developed in Dynamo. The first one is called “Seismic Mass and Moment of Inertia Calculator (SMMIC)”, which is shown as algorithm “A” and the second one is called “Mode Shape Obtaining Tool (MSOT)”, which is shown as algorithm “B”.

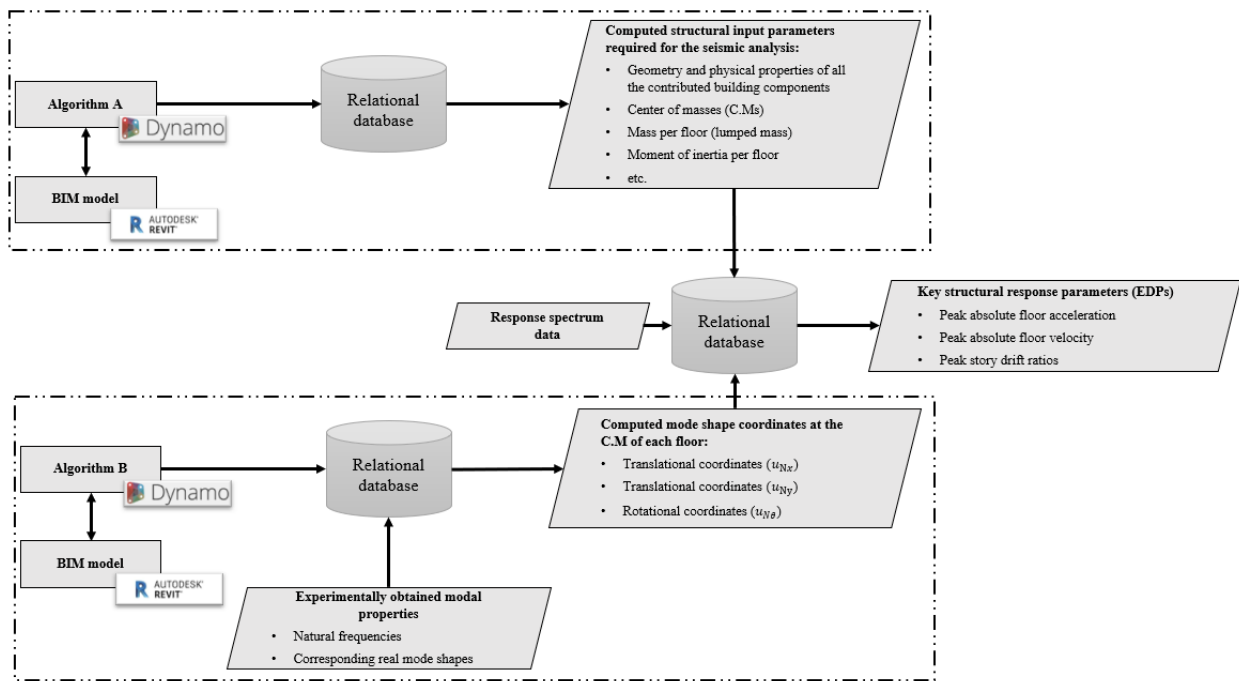


Figure 3. 7. The workflow of simplified experimental seismic analysis by the Dynamo algorithms

With respect to the algorithm SMMIC (also, known as algorithm “A”), all the required structural input parameters for the response spectrum modal analysis (such as coordinates of each floor’s center of mass, seismic weight, and moment of inertia) are automatically calculated. Visual script of Algorithm “A” and the relationship between its code block modules are demonstrated in Figure 3.8 and Figure 3.9, respectively.

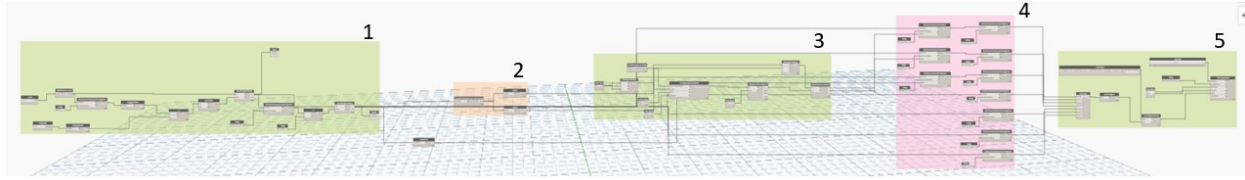


Figure 3. 8. The visual script of the algorithm “A” adopted in the experimental structural analysis

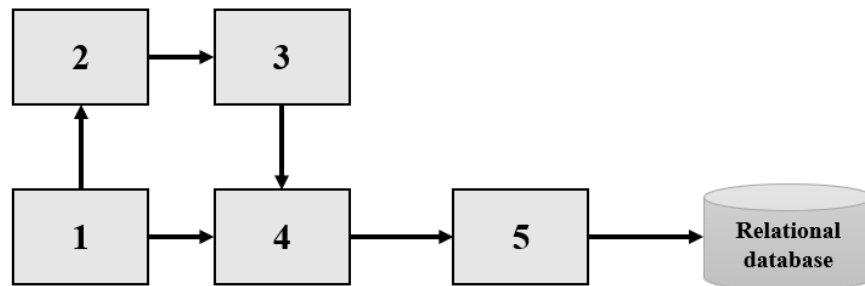


Figure 3. 9. Code block module relationship defined in the algorithm “A” adopted for the experimental structural analysis

- 1) This code block helps Dynamo to automatically select and sort all the existing categories of components in the corresponding constructed BIM model in Autodesk Revit that ultimately, impact the structural input parameters (such as seismic weight and moment of inertia of each floor).
- 2) In this code block the centroid of each element of the BIM model is calculated based on a global coordination. For example, the centroid coordinates of all the columns of each floor are calculated separately and listed.
- 3) This code block helps to automatically adjust and transform the orientation and the location of the whole BIM model’s coordinates based on the desired coordinate system origin.
- 4) At this code block, all the other required physical and functional parameters and properties of each category of components that, somehow contribute to the formation of structural

input parameters (such as center of mass, seismic weight, and moment of inertia per each floor) are collected and sorted.

- 5) This code blocks provide the automated connection and integration between Dynamo and the corresponding formulated relational database to transfer all the inputs that leads to the realization of structural input parameters for the experimental response spectrum modal analysis.

With respect to the conducted OMA, the extracted experimental mode shape coordinates are the result of the real mode shapes at the measured nodes. However, these measured nodes are typically located at the corners of the building. Therefore, no information is available at the center of mass (C.M.) locations in the extracted real mode shapes that can help to perform the seismic analysis. In response to this, the “MSOT” algorithm (also known as algorithm “B”) is developed in Dynamo to determine the real mode shape values (including two horizontal movements and one in-plane rotation) at the C.M locations from the corresponding measured nodes located at the corners of each floor. This is due to the assumption of rigid in-plane movement of each story. Visual script of Algorithm “B” and the relationship between its code block modules are demonstrated in Figure 3.10 and Figure 3.11, respectively.

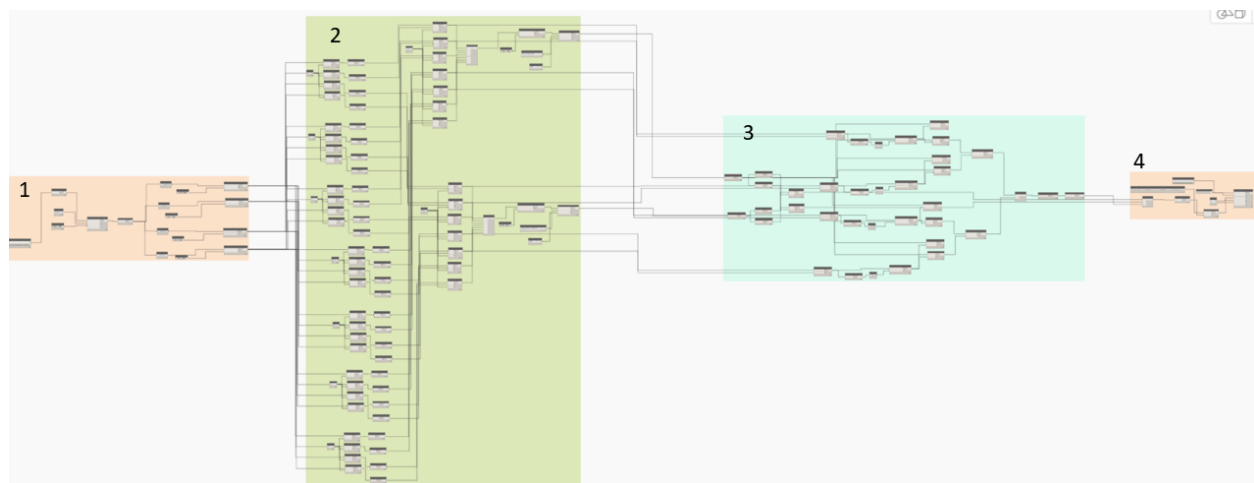


Figure 3. 10. The visual script of the algorithm “B” adopted in the experimental structural analysis

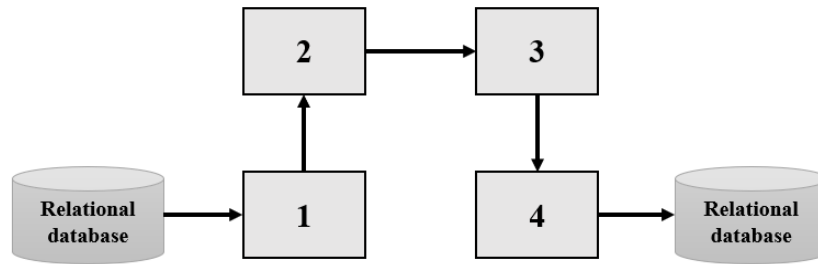


Figure 3. 11. Code block module relationship defined in the algorithm “B” adopted for the experimental structural analysis

- 1) At this code block, the extracted real mode shape coordinates at the measured nodes (corners) are automatically linked and imported in Dynamo from the relational database to form all the slab’s diaphragms. This process includes both the original and the secondary coordinates which represent the induced movements and rotations of each story at each mode shape.
- 2) This code block helps Dynamo to automatically read the imported coordinates and form the corresponding diaphragms of each story accordingly. This includes the actual location of the diaphragms and the secondary location of them according to the governed mode shape.
- 3) At this code block, the real mode shape matrix (including two horizontal movements and one in-plane rotation) at the C.M. location of each diaphragm is computed by comparing the initial and the secondary location and orientation of each diaphragm.
- 4) This code blocks provide the automated connection and integration between Dynamo and the corresponding formulated relational database to transfer the computed real mode shape matrix to the relational database to perform the experimental response spectrum modal analysis.

Eventually, through the automated linkage between the developed Dynamo algorithms and the corresponding relational database, the simplified three-dimensional response spectrum modal analysis is performed. In the other words, Employing the computed structural input parameters

from the BIM model, the extracted dynamic characteristics of the conducted OMA and the response spectra properties in the equation of motion (demonstrated in section 3.3.2.1), leads to finding the maximum relative displacement vectors at the C.M. locations. As the result of this process, the peak absolute accelerations, the peak absolute floor velocities, and peak story drift ratios of all the stories (also known as EDPs) can be all calculated accordingly and be sorted in the relational database.

3.4 BIM-based seismic loss analysis

With respect to the third step as the final step of this proposed methodology, a seismic loss analysis is proposed based on FEMA P-58 procedure, that utilizes the estimated EDPs from either of the demonstrated approach (model-based or nonmodel-based) at the previous step. Subsequently, another set of algorithms are developed based on Dynamo Studio (an API tool for BIM) that are integrated with a relational database to visualize the predicated loss data in a more understandable fashion (color code scheme). This workflow is demonstrated in Figure 3.12. Also, it is noteworthy to mention that, utilizing a BIM model with the high level of development (LOD) in both the structural and non-structural components dramatically, helps to identify the type and the quantities of the corresponding vulnerable components in the loss analysis.

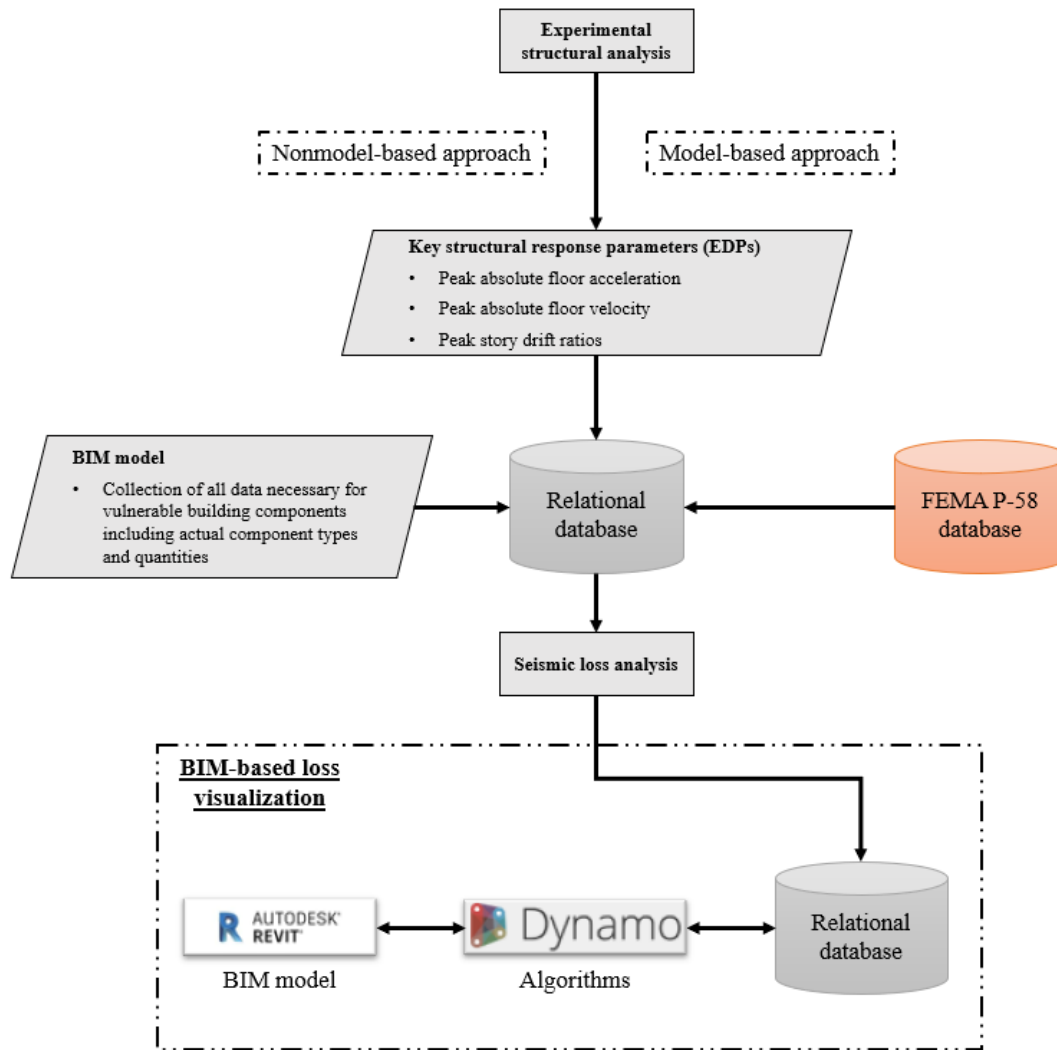


Figure 3. 12. The workflow of the proposed BM-based seismic loss analysis based on FEMA P-58 framework

3.4.1 Loss analysis based on FEMA P-58 (in PACT software)

As demonstrated in section 2.3, FEMA P-58 (FEMA, 2012) is the latest second-generation PBEE or PEER-PBEE which predicts the performance of a building at the component level based on economic loss, downtime and other decision variables. However, in order to derive these performance measures based on FEMA P-58 analysis, a procedure including of four stages: hazard analysis, structural analysis, damage analysis, and loss analysis needs to be respected. The conducted OMA and the subsequent experimental structural analysis methods (model-based and

nonmodel-based) proposed at the previous steps of this methodology sufficiently and precisely support the first two stages of FEMA P-58 (hazard and structural analysis) by providing the required EDPs. Moreover, by adopting a high LOD BIM model along with the FEMA P-58 extensive database of fragility specifications, comprehensive building information data can be provided, which leads to better identify the type and the quantities of all the vulnerable building components in the analysis. In the other words, this combination can efficiently, take care of the damage and loss analysis stages in FEMA P-58 procedure.

With respect to the aforementioned procedures, a building performance model within the PACT software needs to be assembled, which is a sorted data collection including all the vulnerable building structural and non-structural components. The choice of vulnerable components is normally, made through the FEMA P-58 fragility specification database. However, utilizing the BIM model of the building dramatically, reduces the associated uncertainties, as it includes a high extent of both the physical and functional characteristics of existing vulnerable components. Furthermore, all the estimated EDPs from the previous step should be inputted in the building performance model from the relational database. As the result of performing the loss analysis in PACT software, the seismic-induced loss of the building in terms of performance measures such as repair cost, repair time and other decision variables at the given earthquake intensities would be provided. However, under the FEMA P-58 methodology, there are no acceptance criteria related with the distribution of loss consequences. Therefore, in this methodology, 10th, 50th and 90th percentiles (90%, 50% and 10% chances of exceedance, respectively) from the cumulative loss distribution of repair cost and repair time are chosen as the benchmark within PACT software to better demonstrate the induced-seismic loss of all the vulnerable structural and non-structural components. The induced-loss data at each percentile includes the majority of the contribution to the induced-loss among all the vulnerable structural and non-structural categories of components as well as the corresponding repair cost and repair time of each category per each story. Finally, all the mentioned data are collected in the relational database. Figure 3.13 shows a sample of building performance model, containing vulnerable categories of components in PACT software along with the estimated loss data at the aforementioned percentiles.

- 10th Percentile
- 50th Percentile
- 90th Percentile

For example: 50th Percentile

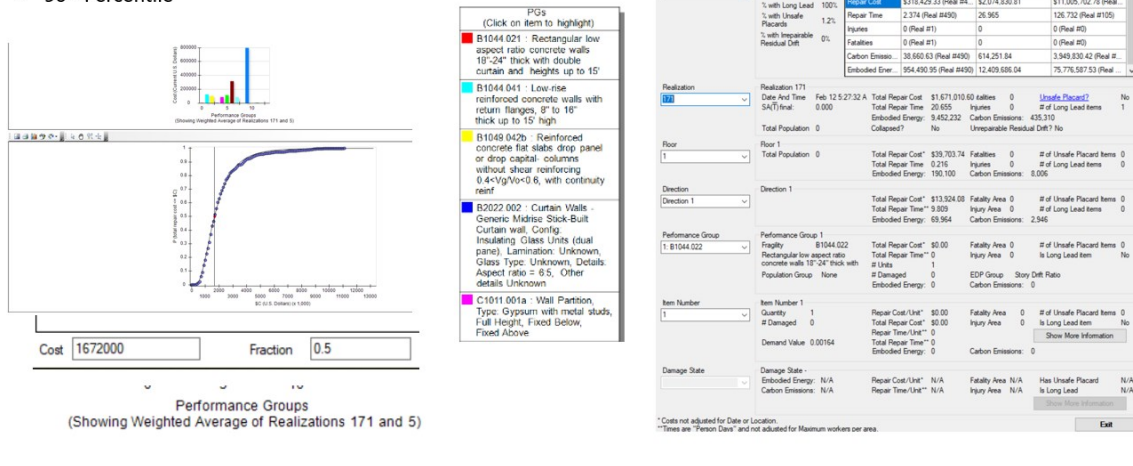


Figure 3. 13. Building performance model, containing vulnerable categories of components in PACT software along with the estimated loss data

3.4.2 Loss data visualization Dynamo algorithms

As demonstrated in Section 2.5.3, current practice of FEMA P-58 methodology is somehow confusing to facility owners due to implications of current loss analysis output format, which is somehow impossible to decipher. However, the resultant impediment can be overcome by incorporating accessible visualization technologies such as BIM, into the PBEE system, which also leads to significantly, improve the realization of performance consequences for the owners. In response to this, a combination of the developed Dynamo algorithms and the corresponding relational database is employed in this methodology to visualize the predicted performance measures such as repair cost and repair time with two different complementary strategies. Figure 3.14 shows the developed Dynamo algorithms, which are called “Fragility Group Visualization Tool (FGVT)” and “Performance Group Visualization Tool (PGVT)”, respectively. It is noteworthy to mention that, depending on the type of strategy, different standard format templates are developed in the relational database to collect and sort the induced-loss data, which also, helps the Dynamo algorithms to automatically read the required input parameters from the database and visualize them over the highly detailed spatial model in a color-coded fashion.

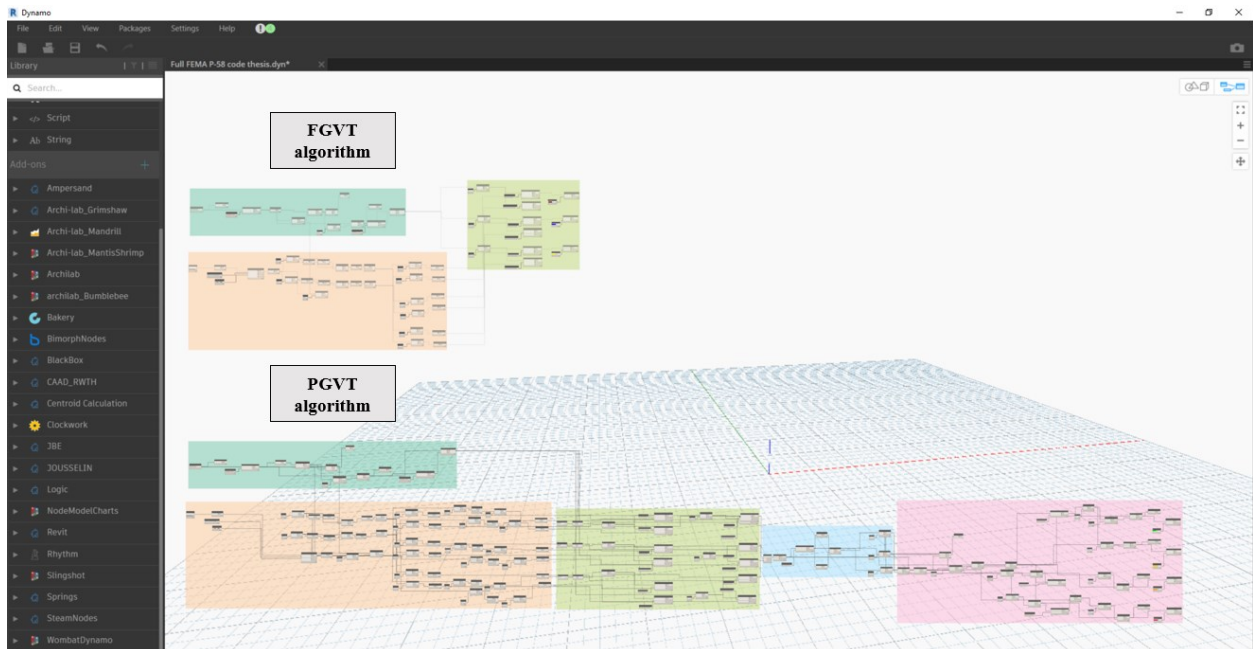


Figure 3. 14. The overview of the developed Dynamo algorithms adopted for the BIM-based loss data visualization

With respect to the “FGVT” algorithm, among all the introduced vulnerable categories of components by the performed seismic loss analysis, initially, categories with the most contribution to the induced loss in terms of repair cost and repair time in the whole building are automatically identified in the BIM model. Then, subsequently, all those vulnerable components with the common category in the entire building are automatically color coded based on the same color fashion presented in PACT software per each defined percentile. Moreover, the induced repair cost and repair time of the selected categories are automatically added to the corresponding component’s properties section in Autodesk Revit. Visual script of the “FGVT” algorithm and the relationship between its code block modules are demonstrated in Figure 3.15 and Figure 3.16, respectively.

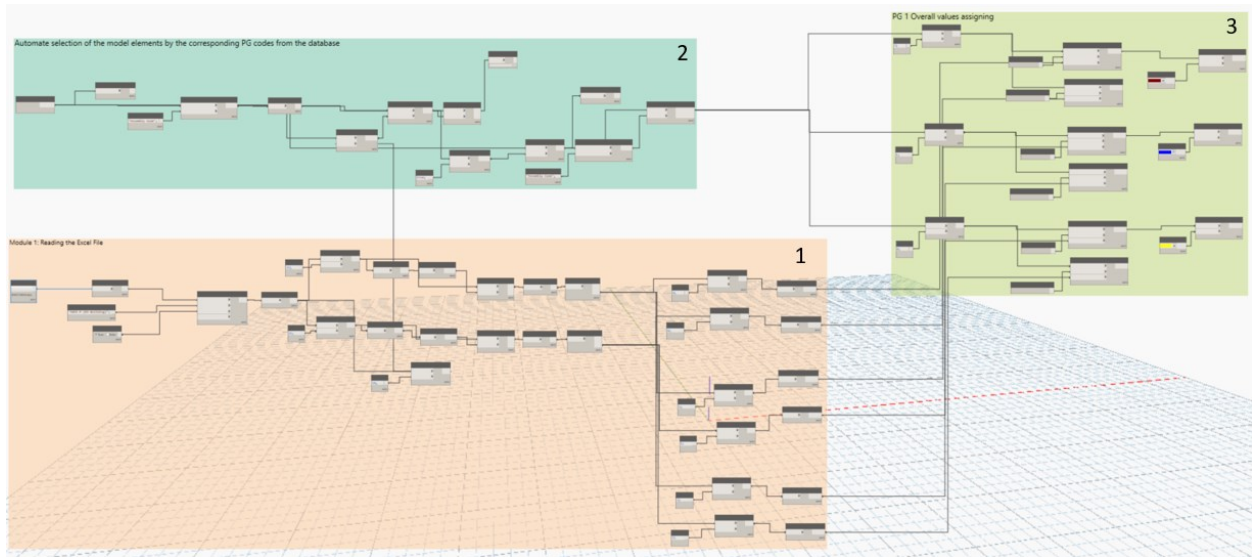


Figure 3. 15. The visual script of the algorithm “FGVT” adopted for the BIM-based loss data visualization

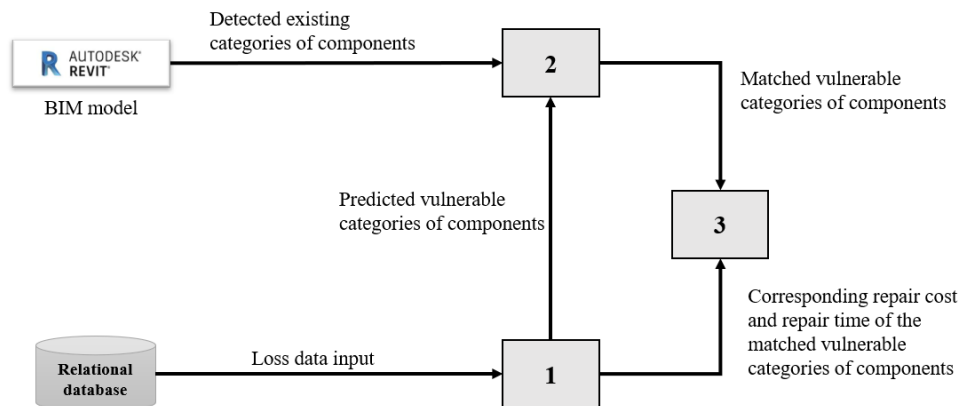


Figure 3. 16. Code block module relationship defined in the algorithm “FGVT” adopted for the BIM-based loss data visualization

- 1) This code block helps Dynamo to automatically, link with the relational database and input all the required information about the vulnerable categories of components, provided by the performed seismic loss analysis. This process includes the acknowledgment of the category code based on UNIFORMAT II described in NISTIR 6389 as well as the category’s contribution in the induced-loss in terms of repair cost and repair time per each percentile.

- 2) Next at this code block, Dynamo automatically selects and sorts all the components in the BIM model, having the matched category codes with the inputted seismic loss analysis output.

- 3) Finally, at this code block, all the group of components associated with the matched category codes in the entire building are automatically assigned with the corresponding repair cost and repair time of their categories. Furthermore, each group of components with the common category is color coded based on the same color fashion presented in PACT software at each defined percentile.

With respect to the “PGVT” algorithm, almost the same procedure as what already demonstrated at “FGVT” visualization is employed. However, unlike “FGVT” algorithm, which was only limited to the identification of categories and the corresponding contribution to the overall induced-loss (such as repair cost and repair time), “PGVT” is a story-based sensitive visualization. In the other words, “PGVT” algorithm can map the corresponding group of components of a category throughout different stories and accordingly, distribute the induced loss portion among them. Moreover, the estimated induced repair cost and repair time of each group of components with a common category and level are automatically, added to the corresponding component’s properties section in Autodesk Revit. Visual script of the “PGVT” algorithm and the relationship between its code block modules are demonstrated in Figure 3.17 and Figure 3.18, respectively.

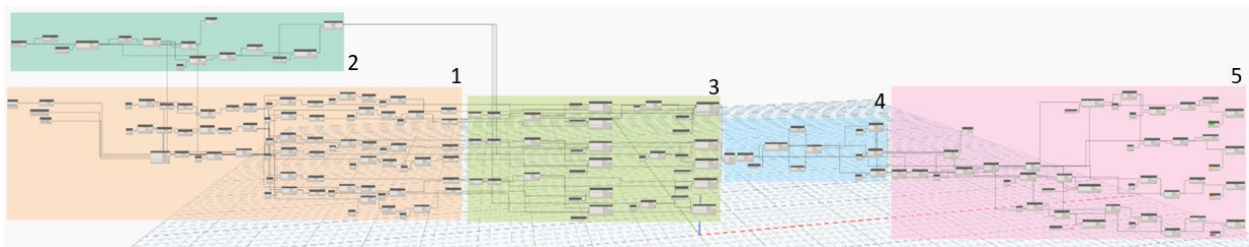


Figure 3. 17. The visual script of the algorithm “PGVT” adopted for the BIM-based loss data visualization

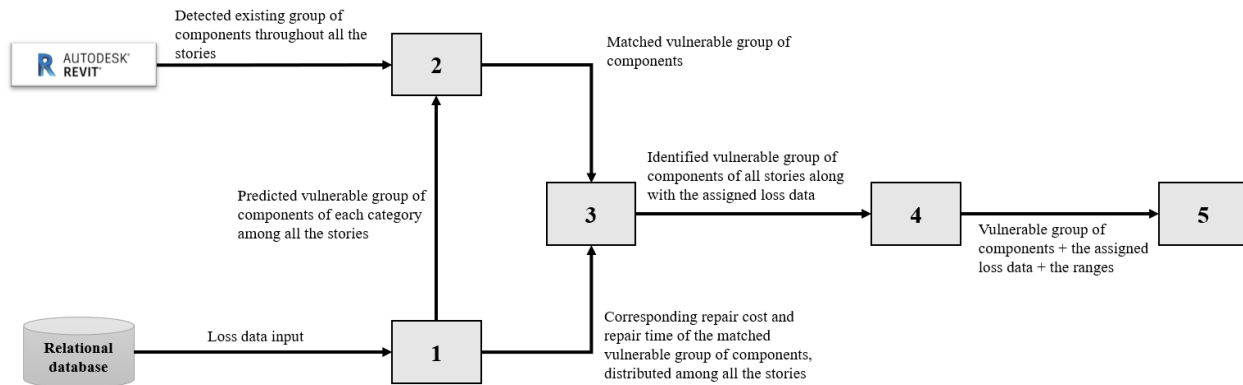


Figure 3. 18. Code block module relationship defined in the algorithm “PGVT” adopted for the BIM-based loss data visualization

- 1) This code block helps Dynamo to automatically, link with the relational database and input all the required information about the vulnerable categories of components, provided by the performed seismic loss analysis. This process includes the acknowledgment of the category code based on UNIFORMAT II described in NISTIR 6389 as well as the contribution of each group of components with the common category at each story in the induced loss in terms of repair cost and repair time per each percentile.
- 2) Next at this code block, Dynamo automatically selects and sorts all the components in the BIM model, having the matched category codes with the inputted seismic loss analysis output.
- 3) Next, at this code block, all the corresponding group of components located at various stories of the building are automatically assigned with the corresponding repair cost and repair time portions associated with their story.
- 4) Subsequently, the desired constrain functions are defined to initially identify the repair cost and repair time of all the contributed group of components in different stories for all the selected categories. Then, according to the distribution of all the repair costs or repair time, various ranges are automatically defined. For example, each range covers 1/3 of the whole organized ranges of the induced repair costs or repair time in a particular percentile.

Moreover, a color code scheme is also defined per each range corresponding to each percentile. It is also to be noted that, these ranges can be either limited only to all the group of components with a common category or it can be expanded to different categories simultaneously.

- 5) Finally, Dynamo sorts and maps all the group of components among the corresponding pre-defined ranges based on the corresponding portion of repair cost or repair time at each story. As a result, each group of components has its corresponding color code at each story.

3.5 Summary

In the absence of a comprehensive systematic methodology that can overcome the caused uncertainties in structural and damage analysis of the FEMA P-58 framework (as a PBEE framework), a systematic methodology was developed in this chapter to enhance the limitations of PEER-PBEE loss assessment framework. This methodology has utilized innovative technologies such as seismic instrumentation and integrated BIM tools embedded in FEMA P-58 framework. For this purpose, a workflow of seismic loss estimation was developed for buildings to first, experimentally obtain the actual performance characteristics of the structure through the operational modal analysis. This process includes the utilization of seismic instrumentation (sensing tests) as well as subsequent output-only system identification. Next, the derived structural performance characteristics were employed in the experimental structural analysis to obtain refined structural response parameters. These parameters are normally, peak absolute floor accelerations, peak absolute floor velocities and peak story drift ratios. To obtain these parameters, two main methodological approaches for the experimental structural analysis were proposed. The major difference between the proposed approaches is the manner to compute the structural response parameters (EDPs); the model-based approach uses FE model calibration and nonlinear response history analysis, while the nonmodel-based approach is FEM free and was developed through a BIM-based API tool to perform the simplified three-dimensional response spectrum modal analysis. The obtained EDPs were then, utilized in the seismic loss analysis based on FEMA P-58 framework to quantify the loss consequence predications of the building of interest into appropriate performance metrics such as economic losses, downtime, and other decision variables. Finally, another BIM-based API tool was developed with an integrated relational database to

collect and spatially visualize the predicted loss data. This BIM-based API tool was developed in Dynamo Studio in Autodesk Revit software program (BIM software) to visualize the predicated loss data in a more understandable fashion (color code scheme).

CHAPTER 4 Case study analysis

4.1 Overview

To investigate the functionality of the methodology outlined in the previous chapter, a case study analysis with detailed examination is performed over a building located in Montreal, Canada. The case study demonstrates the application of all the three main steps proposed in this research, including: (1) the measurement of structural dynamic response throughout an ambient vibration test and subsequent output-only system identification (SI), (2) experimental structural analysis by both the model-based and nonmodel-based approaches (3) seismic loss analysis by the developed BIM-based API tool (based on FEMA P-58 framework). The outcome of this case study clearly shows the efficiency of the proposed systematic seismic loss analysis framework among all other recent studies.

4.2 Case study specification

With respect to the case study, the building of interest is the 16-storey Engineering and Visual arts (EV Building) complex of Concordia University located in Montreal, Canada. The complex is a combination of two buildings (partially interconnected at some floors) with reinforced concrete structural system consisting of columns and flat slabs as the gravity load-resisting system. Also, reinforced concrete shear walls as well friction dampers are considered in this structural system as the seismic force resisting system (SRFS). However, due to the lack of adequate technical information about the friction dampers, the effect of these dampers is not considered in this study. The taller building with sixteen operational stories and a total height of 67.25 meters houses the Gina Cody school of engineering and computer science (Engineering building), whereas the other building (Visual Arts building) has eleven operational floors and a total height of 46.5 meters above the ground level. The Engineering building is 70 meters deep and 30 meters wide and the Visual Arts building is 40 m x 50 m. As shown in Figure 4.1, EV building is a high-rise irregular building containing high number of specialized labs (over 300 labs), conference and meeting room and student areas that could be considered as high-risk areas in a seismic event. Therefore, predicting the actual structural behavior and seismic performance of this building is of the crucial steps towards the risk mitigation of the major seismic events. Taking into account the

aforementioned information, EV building provides an opportunity to further exercise the methodology outlined in the previous chapter.

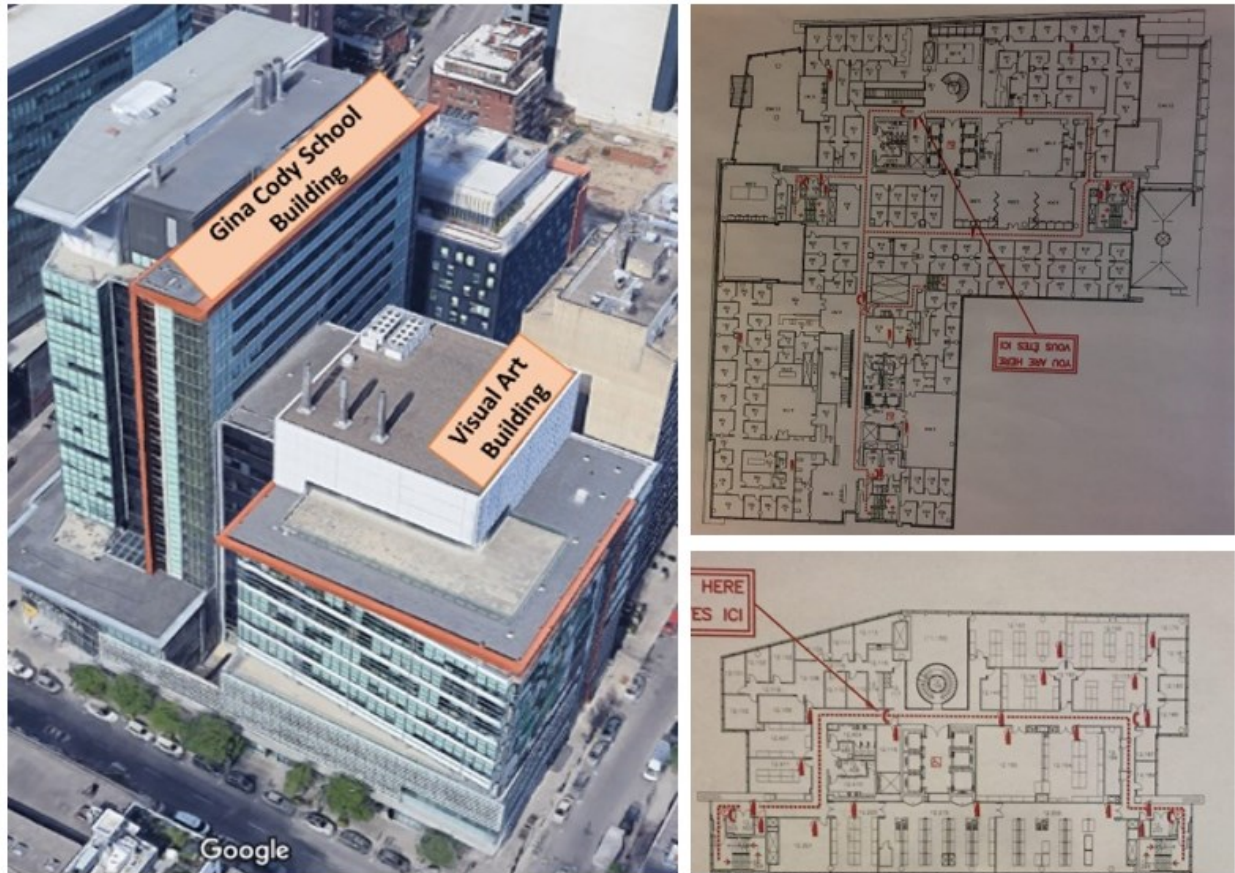


Figure 4. 1. The Isometric view of EV Building, Concordia University (Source: Google Map) (left), typical floor plan of EV building at the lower stories (top right), typical floor plan for the higher stories (bottom right). The courtesy of the right pictures belongs to Concordia university.

4.3 Experimental setup

As explained in Section 3.2, in order to derive the structural dynamic characteristics and actual behavior of a building, a successful ambient vibration test (AVT) is required to be conducted. Moreover, a successful AVT is a function of appropriate experimental setup, which includes using proper and effective sensing instruments (sensors), adopting adequate number of sensors and optimal placement of them based on desired sensing targets, duration of the test and so many other factors. Therefore, as a result, the acquired raw data from the sensors can efficiently be utilized in

subsequent processes to evaluate the actual dynamic characteristics of the building. The results of the experiments conducted by (Timir Baran Roy et al., 2019) have been utilized here to study the developed procedures of model-based and nonmodel-based for damage and loss estimation of EV building.

4.3.1 Sensor specification

With respect to the seismic instrumentation, a set of vibration sensors, called “*Sensequake Larzé*” developed by Sensequake Inc (Sensequake Larzé, 2021) were utilized to conduct the AVT on EV building. The “*Sensequake Larzé*” sensor (shown in Figure 4.2) is a combination of highly sensitive low noise triaxial velocity sensors (± 40 mm/s) and triaxial MEMS accelerometers ($\pm 2g$ and $\pm 6g$), specifically designed for ambient vibration monitoring. With respect to digital conversion, it has got 6 independent differential 32-bit channels and supports sampling rates within the range of 15 Hz to 488 Hz. It also can communicate with Wi-Fi, an optional cellular network and USB for different purposes. This sensor is manufactured with the storage of 16 GB, which is suitable to log a large amount of data. The power supply is also, through the internal lithium battery that can operate for more than 20 hours. Moreover, it is manufactured with 120 x 80 x 80 mm dimensions and 720 g weight to function within -30 to 50°C temperature range.



Figure 4. 2. An overview of the “*Sensequake Larzé*” sensor developed by Sensequake Inc (Sensequake Larzé, 2021)

4.3.2 Sensor placement & AVT arrangements

As described in section 3.2.1, the optimal layout of sensor locations to measure the structural dynamic response of a building is more a function of the number of available sensors as well as the nature of the desired mode shapes to be extracted. Therefore, due to the imposed limitation of available sensors and the enormous size of EV building, seven test setups were at least required to perform a successful AVT. With respect to the roving sensors at the first five test setups, a set of three “Sensequake Larzé” sensors were deployed over the floors with even numbers, starting from 2nd floor to 10th floor (i.e., 2nd, 4th, 6th, 8th and 10th) simultaneously. However, a reference sensor was always placed over the 16th floor to serve as a link between all the five test setups to merge the collected data. Then starting from the 12th floor to 16th floor, the number of the sensor reduced to two at each floor. However, still the reference sensor was kept at the 16th floor for the ramming two test setups. The duration of the test at each test setup was limited to 14 minutes and the sampling rate of 61 Hz. Figure 4.3 shows the layout of sensor placements at all floors. More information is available in (Timir Baran Roy et al., 2019)



Figure 4. 3. The layout of the sensor placements for AVT over EV building (courtesy of the pictures from left to right: Google Map, Concordia university)

4.3.3 Collection of the raw data

As a result of each test setup of the conducted AVT over EV building, a collection of raw data with a nature of acceleration and velocity are acquired. Normally the raw data are recorded and provided in three orthogonal directions. However, the acquired sensor data for EV building was limited to two in-plane orthogonal directions (X and Y) to represent the 2-degrees of freedom at each measuring nodes (corner joints). Consequently, with respect to the shape and height of EV building, fifty-seven measuring nodes were identified to be assigned with the acquired sensor data from different sensors for different setups to measure the global response of the building. More information regarding the conducted AVT over EV building is available in (Timir Baran Roy et al., 2019). Also, the following recorded raw data of all the four sensors at test setup number 1 is taken from the same source (Figure 4.4).

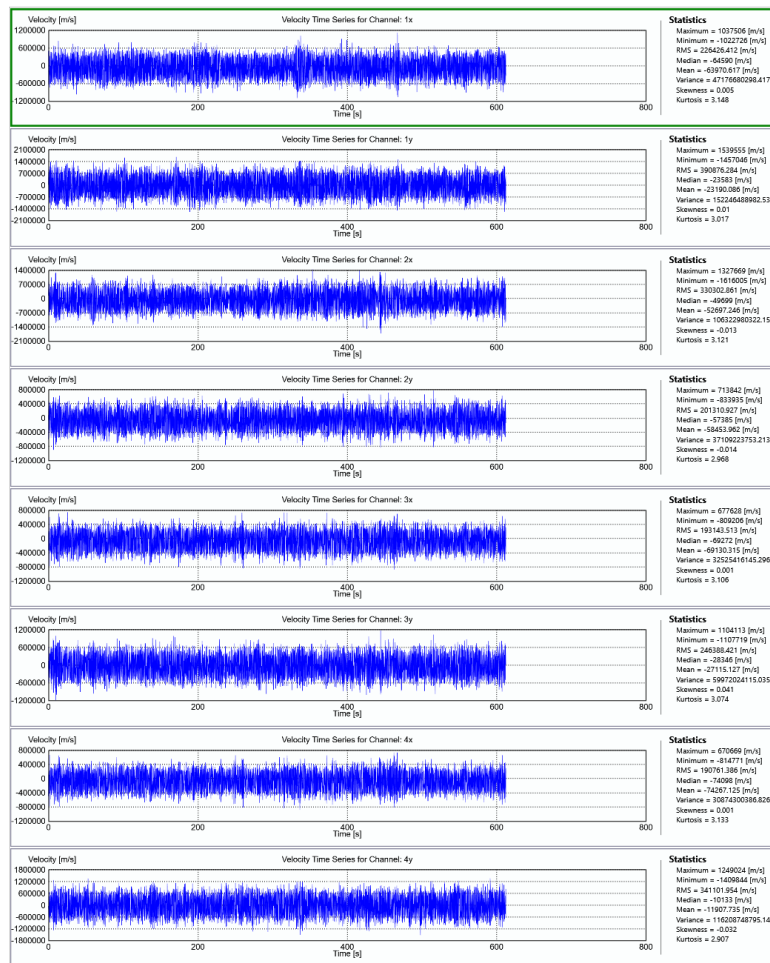


Figure 4. 4. The recorded raw data of EV building by the placed sensors for the first test setup, (Timir Baran Roy et al., 2019)

4.3.4 System identification and modal analysis

With regards to system identification, Frequency Domain Decomposition (FDD) technique was employed to extract the dynamic characteristics of EV building. For this matter, as already provided in (Timir Baran Roy et al., 2019), ‘*ARTEMIS Extractor Pro*’ software (Extractor, 1999) was utilized to estimate different natural frequencies and the corresponding mode shapes of EV building. This process includes estimating the output PSD matrix from the inputted sensor data and its subsequent decomposition by applying SVD matrix, which ultimately leads to manual selection of modal frequency values and the corresponding mode shapes using peak picking method. Figure 4.5 represents the first six natural frequencies and the corresponding mode shapes of EV building, derived from (Timir Baran Roy et al., 2019). However, with respect to the first lateral modes and the torsional mode as the most dominant vibration modes, this study is only limited to the first three mode shapes and the corresponding natural frequencies (Sabamehr, 2018).

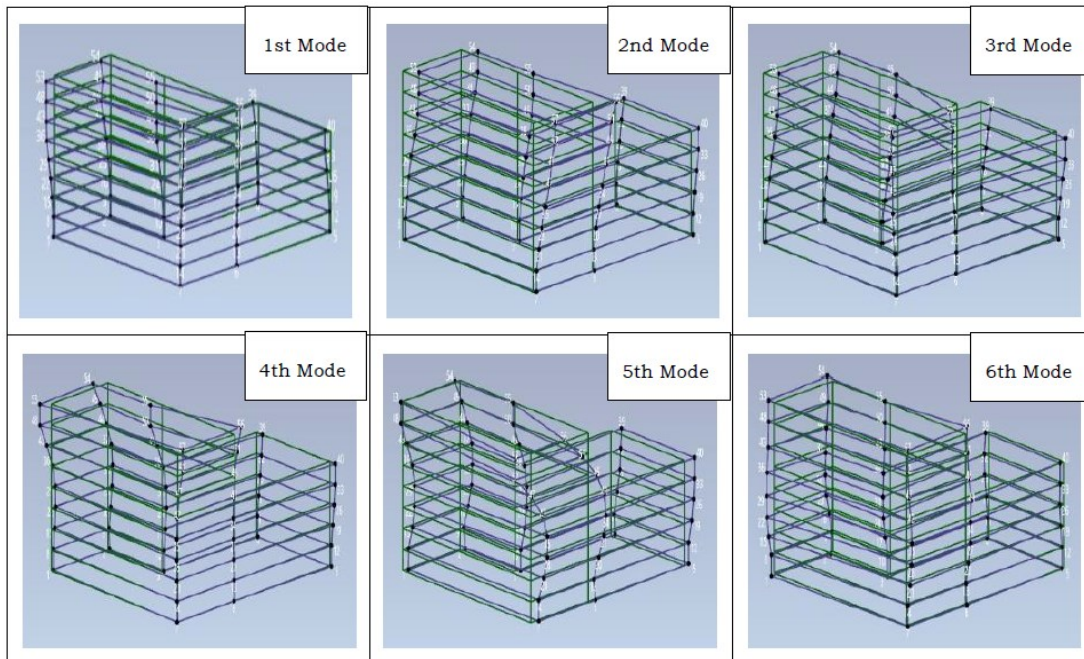


Figure 4. 5. the first six natural frequencies and the corresponding mode shapes of EV building, (Timir Baran Roy et al., 2019)

Table 4.1 provides the first three natural frequencies and the corresponding mode shapes of EV building derived from (Timir Baran Roy et al., 2019) . Direction X and Y are demonstrated in Figure 4.6.

Mode shape	Natural frequency (Hz)	Description
1 st Mode	0.66	Lateral mode in direction Y
2 nd Mode	0.75	Lateral mode in direction X
3 rd Mode	0.83	Torsional mode

Table 4. 1. The first three natural frequencies and the corresponding mode shapes of EV building, (Timir Baran Roy et al., 2019)

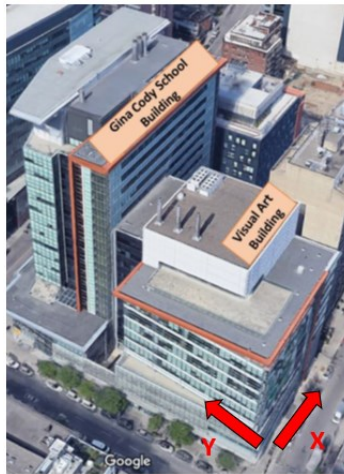


Figure 4. 6. An overview of the assumed directions for EV building project (Source: Google Map)

4.4 Experimental structural analysis for EDP determination

In order to compute the structural responses of EV building based on experimental data derived from the previous step, computational models have been developed. The structural responses of EV building computed from the developed computational models are represented by the key response parameters (such as peak absolute floor acceleration, peak absolute floor velocity and peak story drift ratio). For this purpose, model-based and nonmodel-based approaches have been utilized to develop different computational models of EV building and estimate the desired EDPs, independently. With respect to the model-based approach, a simplified numerical FE model of the building is developed and correlated to compute the desired EDPs, whereas the EDP estimation in nonmodel-based approach is free of FE modeling and based on a simplified three-dimensional experimental response spectrum modal analysis.

4.4.1 Model-based approach

To determine the desired EDPs by adopting model-based approach, initially, a highly detailed BIM model of EV building was constructed in Autodesk Revit software based on the available detail drawings. As shown in Figure 4.7, the developed 3D model of EV building in Autodesk Revit is highly capable of fitting all the structural system including the reinforced concrete column, concrete shear walls and the flat slabs at the proper locations according to the drawing plans. Subsequently, by using the CSI ETABS plug-in in Revit, the BIM model is converted to a structural analysis model with a conversion efficiency (Figure 4.8).

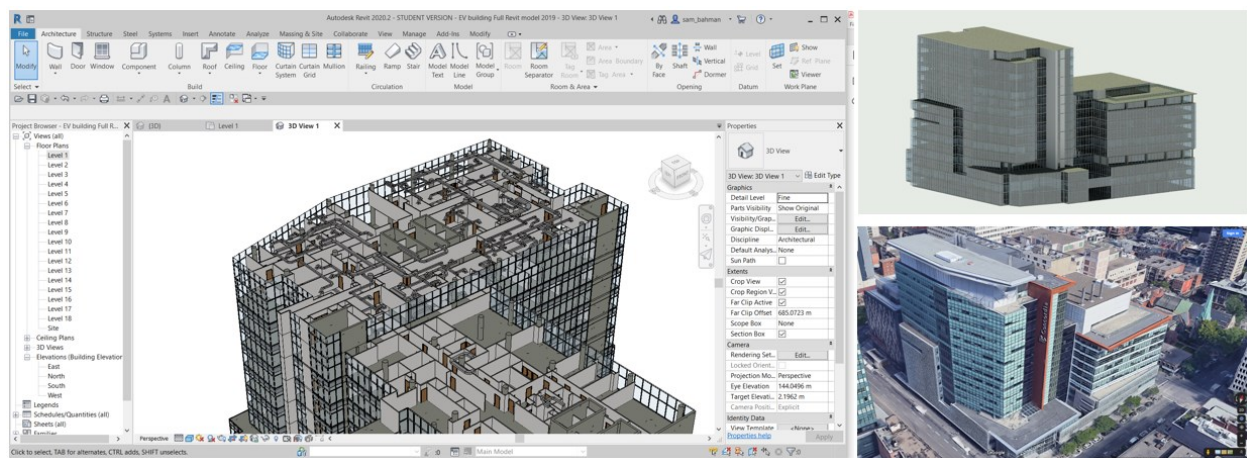


Figure 4. 7. An overview of the developed 3D model of EV building in Autodesk Revit with all the building components (left and top right), the isometric view of EV building (bottom right) (Source: Google Map)

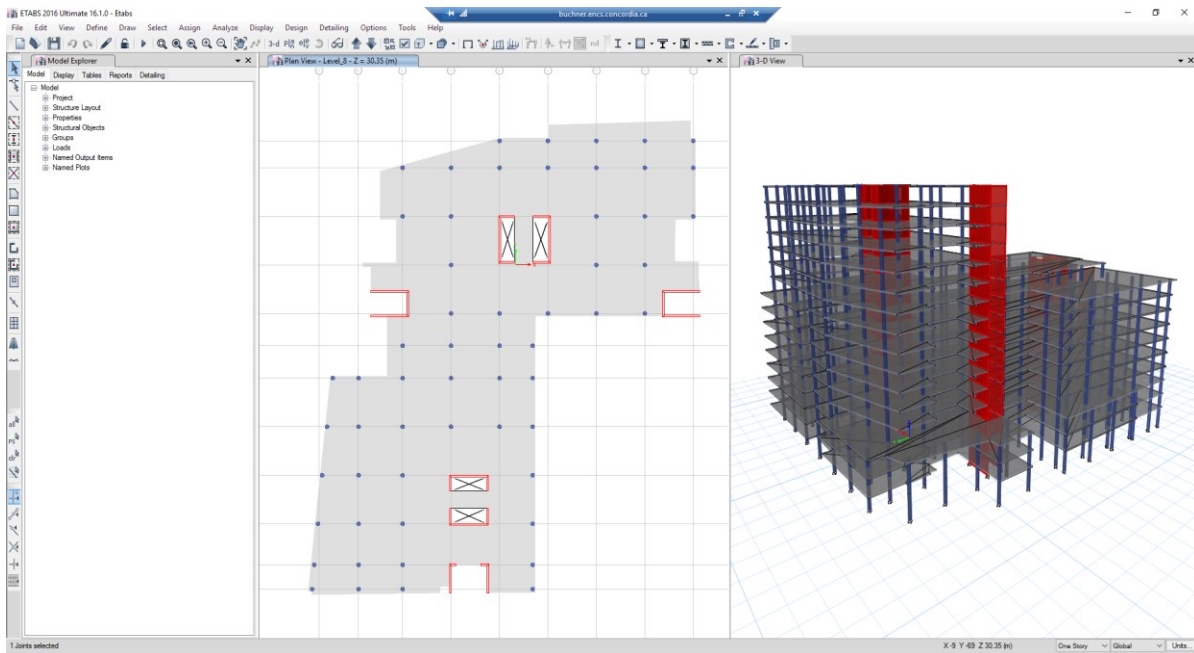


Figure 4. 8. The structural analysis model of EV building converged from Autodesk Revit into CSI ETABS software

After inputting the analytical FE model of EV building in CSI ETABS software, FE model calibration process was performed to compensate the identified inconsistencies between the analytical modal properties and the experimentally obtained modal properties. The main target in FE model calibration was to achieve the same first three experimentally obtained natural frequencies and the corresponding mode shapes within the analytical FE model. Although various FE model calibrating techniques could be adopted, iterative process was utilized to calibrate the FE model based on the derived structural performance characteristics from the operational modal analysis. As a result, the first three analytical and experimental natural frequencies and the corresponding mode shapes were matched with an acceptable precision. Figure 4.9 shows the first three mode shapes of EV building in ETABS software derived from (Bahmanoo et al., 2021) after the calibration process.

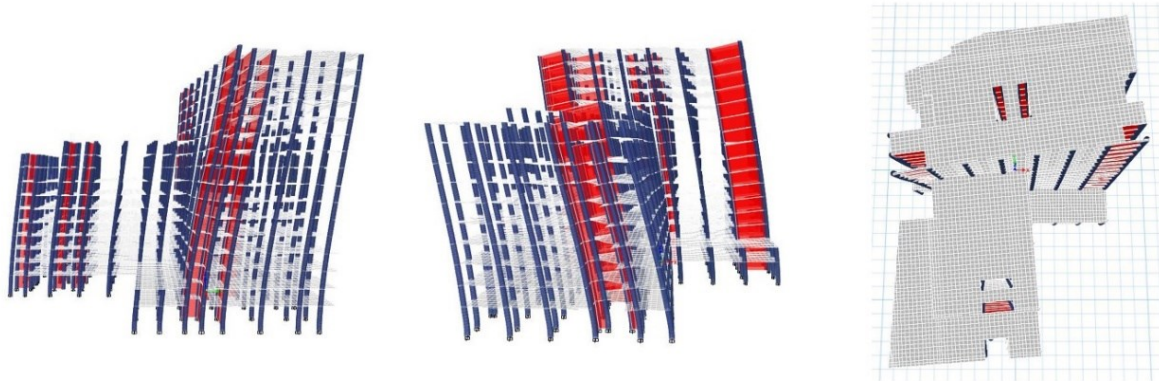


Figure 4. 9. The first three mode shapes of EV building in CSI ETABS software after the calibration process: the first mode (left), the second mode (middle) and the third mode (right), (Bahmanoo et al., 2021)

Eventually, to determine the desired EDPs (e.g., peak absolute floor acceleration, peak absolute floor velocity and peak story drift ratio), a simplified nonlinear time history analysis is performed over the calibrated FE model of EV building. For this purpose, initially, at the given intensity of Maximum Considered Earthquake (MCE) (2% probability of exceedance in 50 years), a collection of artificial ground motion records are derived from (Wang, Pejmanfar and Tirca, 2019) corresponding to the target spectra (site class C) in Montreal defined by NBCC 2015. This is mostly due to the lack of historical ground motions in Eastern Canada. These artificial records are considered with the magnitude of 7 along with the epicentral distances of 13.8 km to 50.3 km and the duration of about 20 seconds, which are available at www.seismotoolbox.ca (Atkinson and Goda, 2011). It is noteworthy to mention that due to the availability of a defined scenario-specific target spectrum, utilizing fewer pairs of ground motions than 11 records per suite is approved by NBCC 2015. Therefore, seven pairs of ground motions are selected among the collection of the records with the following seismic characteristics in Table 4.2 which was derived from (Wang, Pejmanfar and Tirca, 2019).

Event	Magnitude M_W	Station	PGA (g)	PGV (m/s)	PGV/ PGA	t_D (s)	t_p (s)	t_m (s)
M7C1-13.8	7.0	Simulated	0.727	0.370	0.052	7.180	0.120	0.244
M7C1-20.1	7.0	Simulated	0.653	0.396	0.062	6.012	0.140	0.296
M7C1-25.2	7.0	Simulated	0.386	0.187	0.049	7.320	0.060	0.243
M7C1-25.6	7.0	Simulated	0.339	0.194	0.058	7.846	0.160	0.266
M7C1-25.8	7.0	Simulated	0.293	0.178	0.062	7.308	0.080	0.282
M7C2-41.6	7.0	Simulated	0.229	0.144	0.064	7.614	0.140	0.306
M7C2-50.3	7.0	Simulated	0.151	0.075	0.051	8.744	0.160	0.277

Table 4. 2. Seismic characteristics of the employed artificial ground motions derived from (Wang, Pejmanfar and Tirca, 2019)

As shown in Table 4.2, PGA and PGV represent the peak ground acceleration and peak ground velocity, respectively. Also, t_D stands for the Trifunac duration, t_p shows the main period of ground motion record and t_m is the mean period. Figure 4.10 is also taken from (Wang, Pejmanfar and Tirca, 2019) which shows the scaled pairs of the records with respect to 2% in 50 years design spectra. Moreover, the mean spectrum of the considered records does not drop less than 90% of the design spectrum in the period range of $0.2T_1$ to $2.0T_1$.

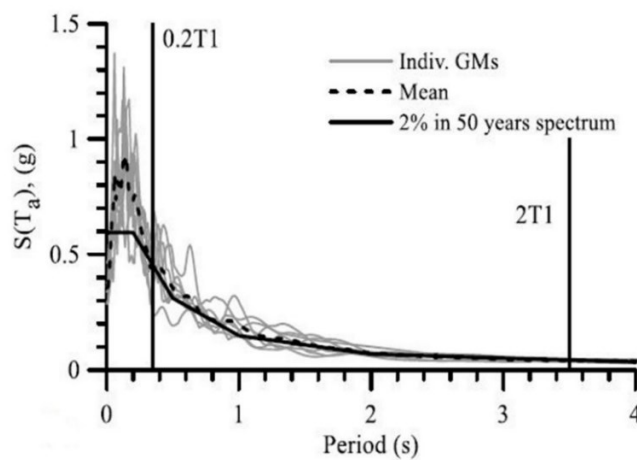


Figure 4. 10. Target spectra of Montreal area (class C) along with the scaled ground motions in the range $0.2T_1$ – $2T_1$ derived from (Wang, Pejmanfar and Tirca, 2019)

By applying the scaled pairs of ground motion at the corresponding horizontal directions of the structure (X and Y) as the seismic loads, nonlinear time history analysis is performed over the calibrated FE model. Also, it is noteworthy to mention that the nonlinearity perspective of the structural analysis was reflected more into the material properties of the structural elements than the geometry details or the connection behavior. Finally, as a result, the desired EDPs such as peak floor absolute accelerations and peak story drift ratios are obtained along both directions for the whole stories of the building. Figure 4.11 shows the obtained EDPs as well as the mean values and standard deviations (σ) of the obtained EDPs at both the X and Y directions.

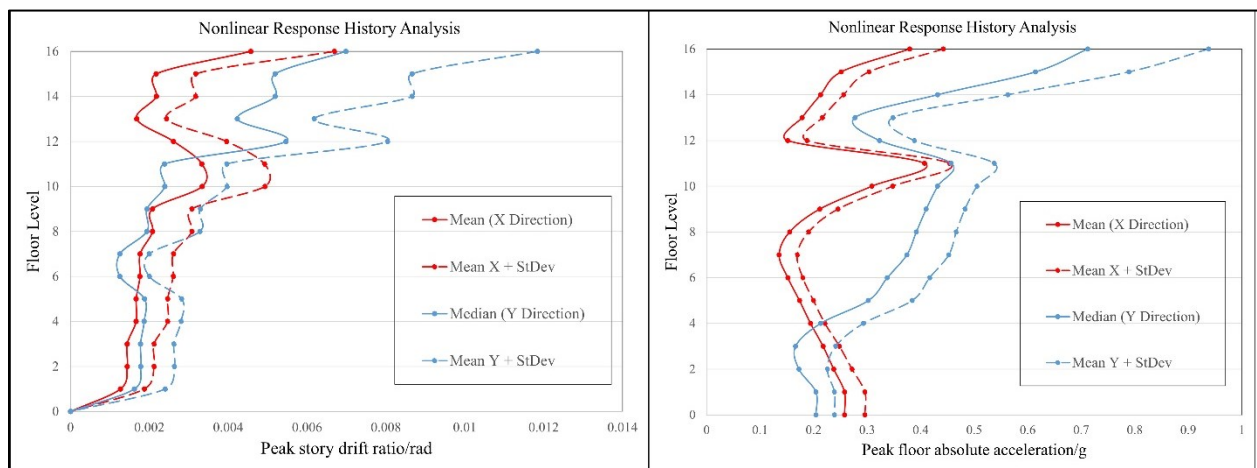


Figure 4. 11. Structural responses of EV building: peak story drift ratios (left) and peak floor absolute accelerations (right)

4.4.2 Nonmodel-based approach

As described in section 3.5.1.1, to determine the desired EDPs by adopting nonmodel-based approach, a BIM-based API tool is developed to perform a simplified three-dimensional experimental response spectrum modal analysis. For this purpose, the “SMMIC” and “MSOT” algorithms (also known as algorithm “A” and “B”, respectively) are developed in Dynamo Studio, which are integrated with a relational database to facilitate the automated process of EDP estimation. Therefore, to estimate the desired EDPs for EV building, initially, similar to the model-based approach, the 3D model of this building constructed in Autodesk Revit software earlier, which includes all the implemented structural and non-structural components and systems according to the provided drawing plans. Figure 4.12 shows the 3D model of EV building developed in Autodesk Revit with all the implemented details.

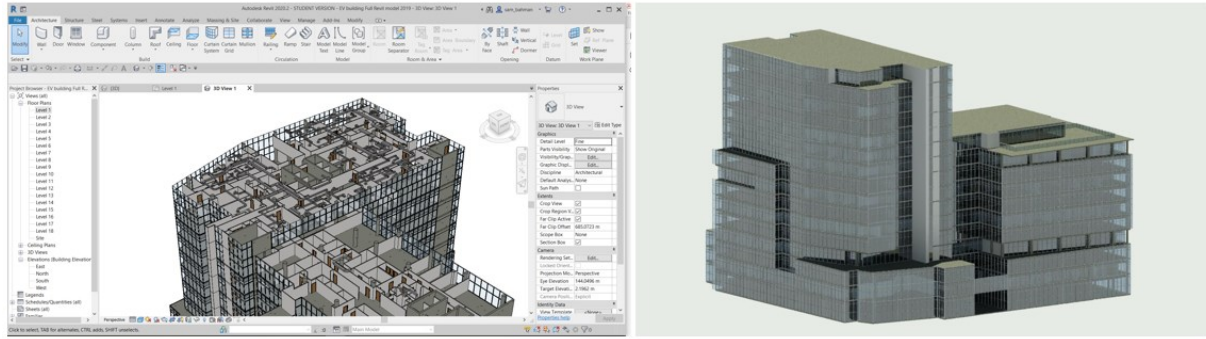


Figure 4.12. An overview of the 3D model of EV building developed in Autodesk Revit

As shown in Figure 4.12, apart from the non-structural components (Wall partitions, curtain walls and so on), the most contributed and dominant components in impacting the structural input parameters (such as coordinates of each floor’s center of mass (C.M.), seismic weight, and moment of inertia) are the reinforced concrete columns, concrete shear walls and the flat slabs at each floor. Therefore, to collect the physical and functional properties of each effective category independently, the main framework of the algorithm “SMMIC” is duplicated and customized in three similar workflows (Figure 4.13). By running the algorithm “SMMIC” over the 3D model of EV building, initially, Dynamo has acknowledged all the existing reinforced concrete columns, concrete shear walls and the flat slabs with various size and type at each floor.

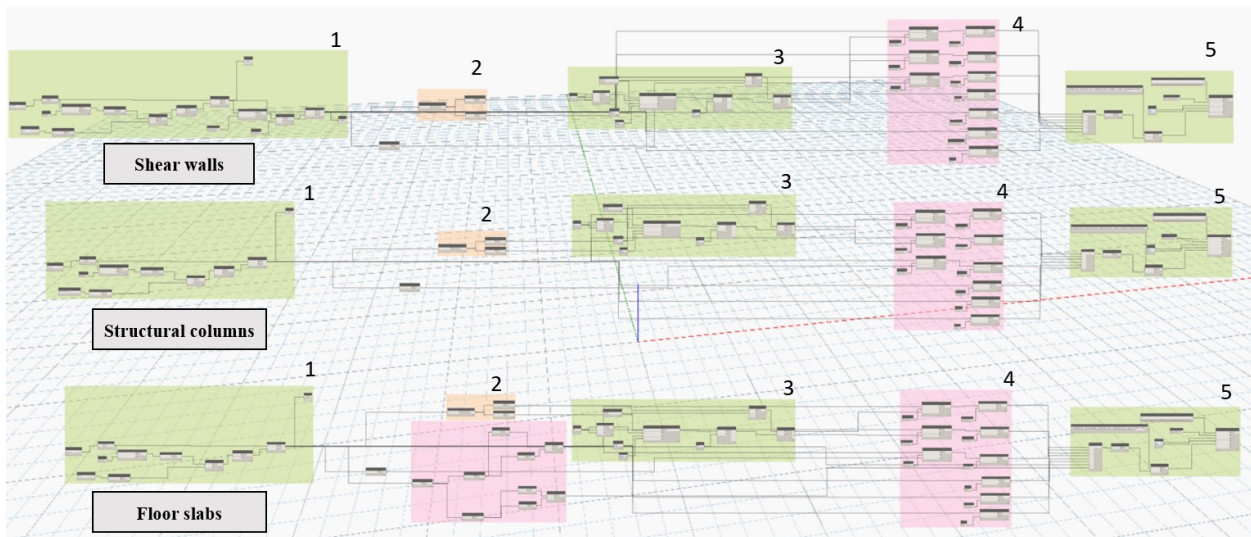


Figure 4.13. The customized visual script of the algorithm “SMMIC” adopted in the experimental structural analysis for EV building

To demonstrate the process of adopting algorithm “SMMIC” over the EV building BIM model, Figure 4.14 to Figure 4.16 show all the identified columns, shear walls and flat slabs located at the second level of the building by code block module 1, respectively. It can be seen that, among the 528 detected walls at the second level, 28 elements with the category code of B1044.011 constitute the target shear walls. Also, 77 structural columns are detected at this level. Same process should be repeated per each floor level. Also, it is to be noted that, the shape of the floor slabs at each level of EV building is irregular with alteration in mass distribution. For this purpose, each floor slab is broken down into several rectangles based on the geometry and mass distribution. Overall, 15 rectangles are identified for the second level that represent the floor slab together. Moreover, Figure 4.17 shows a sample of selected shear walls, structural columns and floor slabs located at the second floor of EV building.

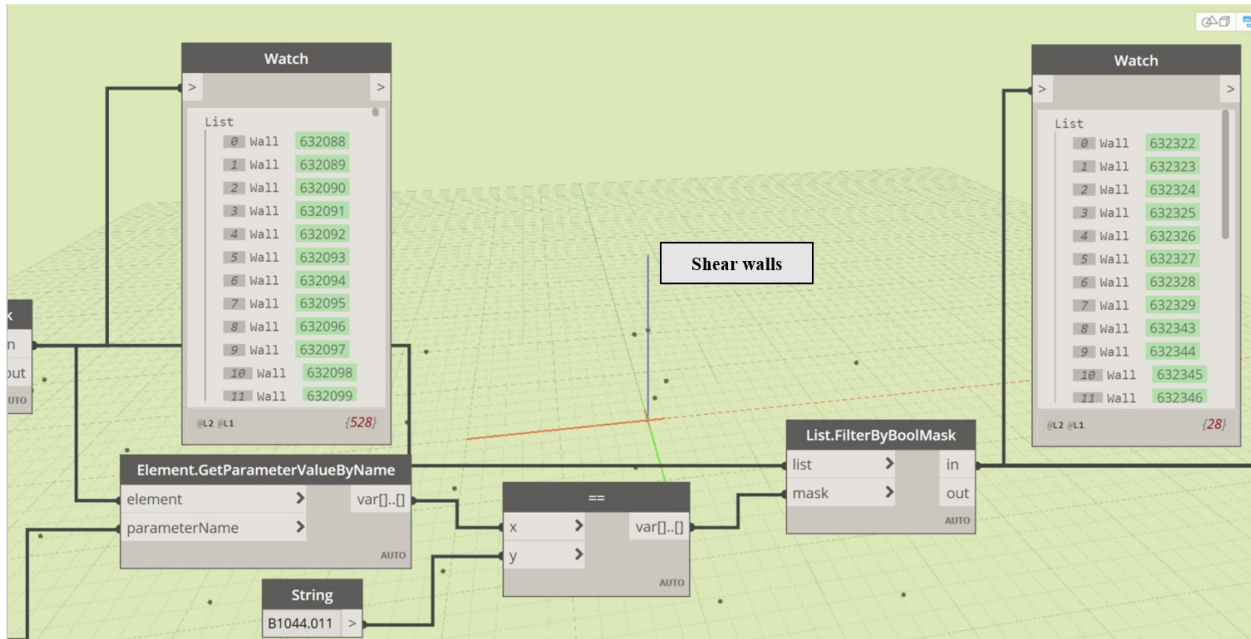


Figure 4. 14. The identification process of all the shear walls located at the second level of the building by code block module 1

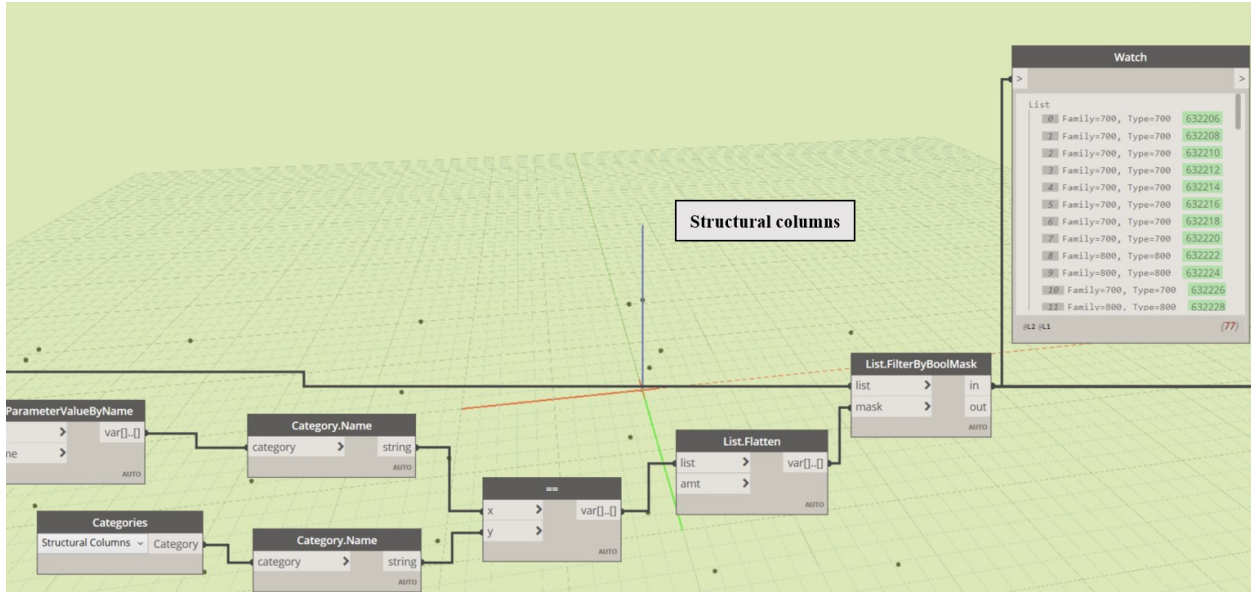


Figure 4. 15. The identification process of all the structural columns located at the second level of the building by code block module 1

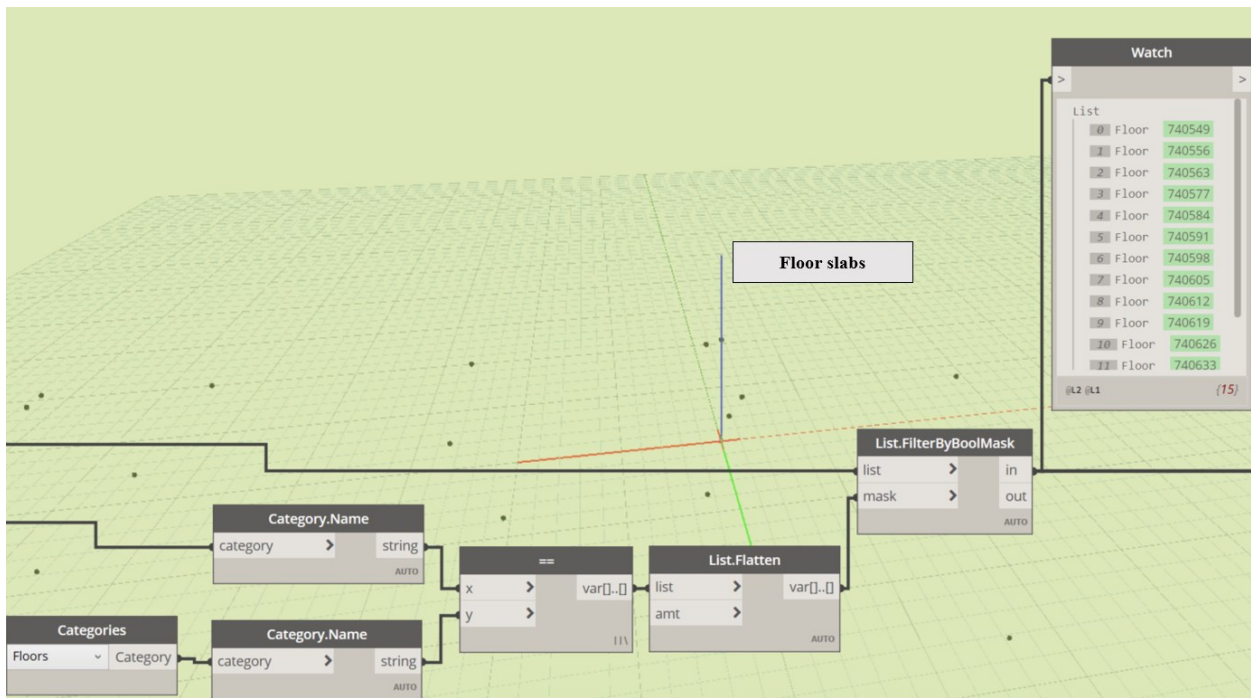


Figure 4. 16. The identification process of all the rectangles that represent the floor slab located at the second level of the building by code block module 1

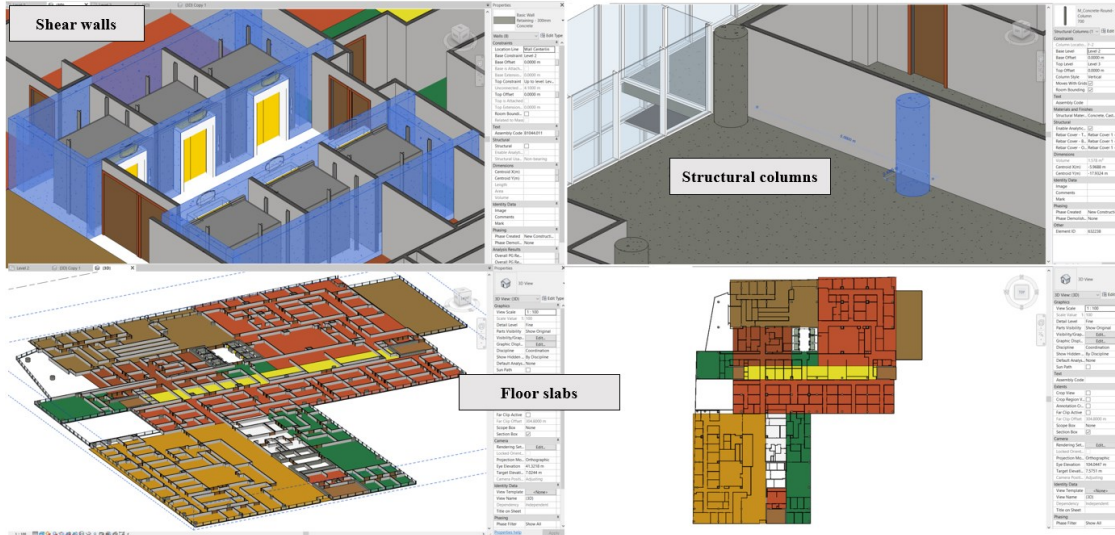


Figure 4.17. A sample of selected shear walls, structural columns and the floor slab located at the second floor of EV building

Next, the centroid coordinates of the identified components are computed and listed independently, based on a global coordination system by cod block module 2. Figure 4.18 shows the visual calculated centroid coordinates (X and Y coordinates) of the identified components per each category at the second-floor level. Figure 4.19 also, shows the calculated centroids for all the shear walls, structural columns, and the floor slab with its rectangles, respectively in Dynamo Studio (code block module 2). It is to be noted that, the centroid values will be translated finally into the relational database and are used to compute the C.M.s.

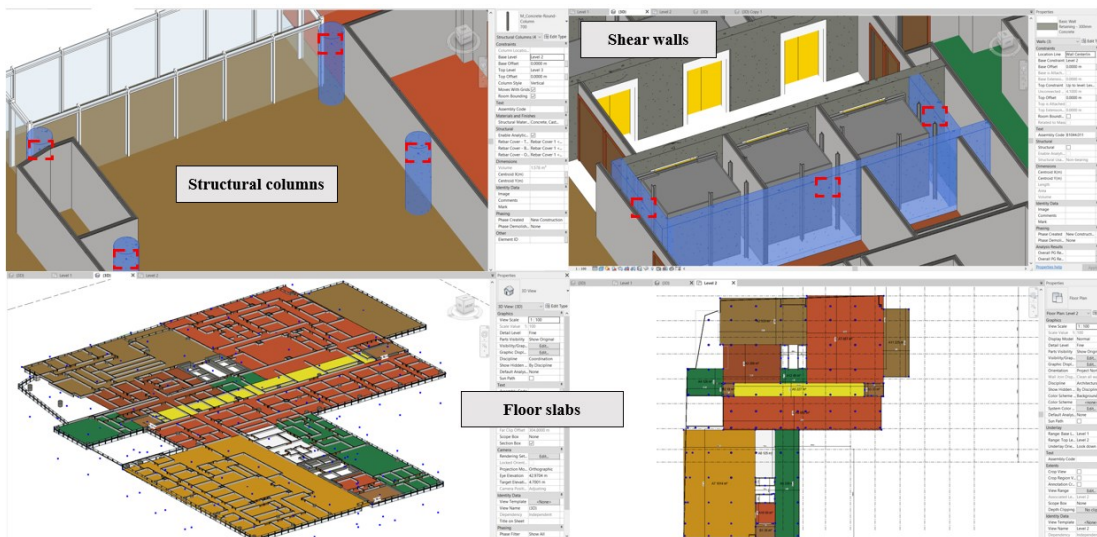


Figure 4.18. The visual calculated centroid coordinates of the identified components at the second-floor level of EV building

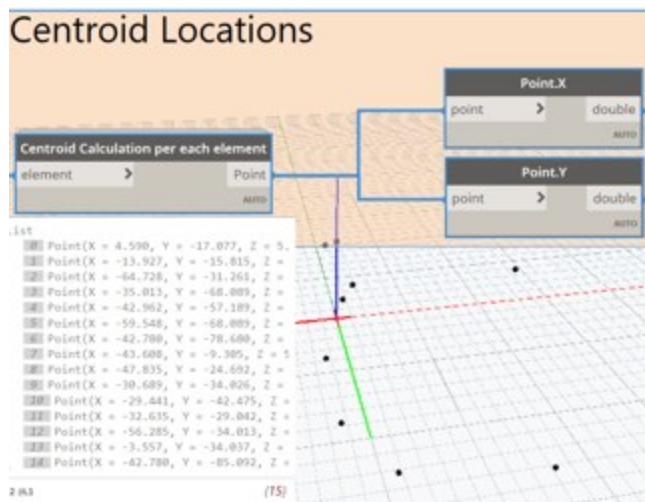
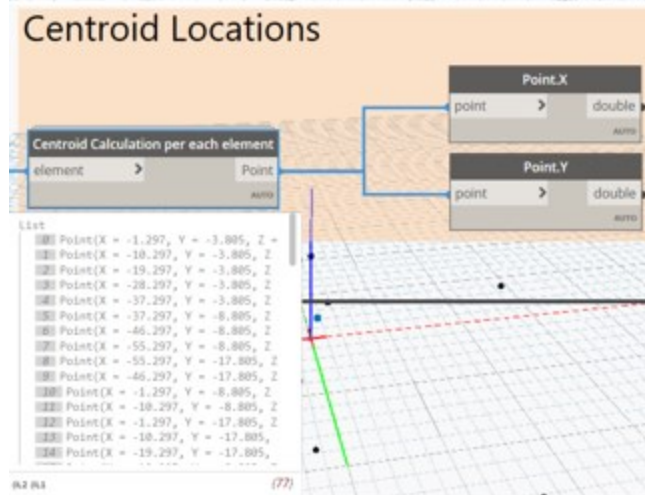
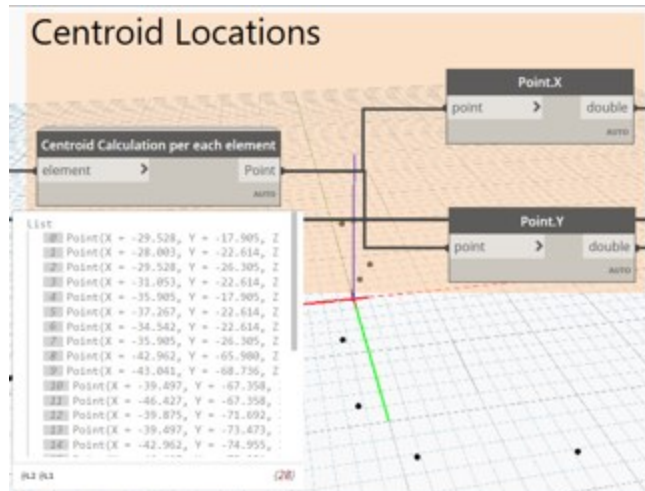


Figure 4. 19. The calculated centroids for all the shear walls, structural columns, and the floor slab located at the second-floor level of EV building, respectively in Dynamo Studio (code block module 2)

Subsequently, with respect to code block module 3, the orientation and the coordinates of the computed centroid of all the identified components in Dynamo are transformed based on a new coordinate system origin. As shown in Figure 4.20, originally the initial coordinate system origin was not located at a desired corner of the built 3D model. Therefore, by utilizing this code block module not only the whole 3D model coordinates are based on a new coordinate system origin (at the top right corner), but also, it facilitates to better understand the computed structural input parameters (such as each story's C.M.) by the user. Figure 4.21 shows the transformation of all the computed coordinates based on the new coordinate system origin in Dynamo Studio (code block module 3).

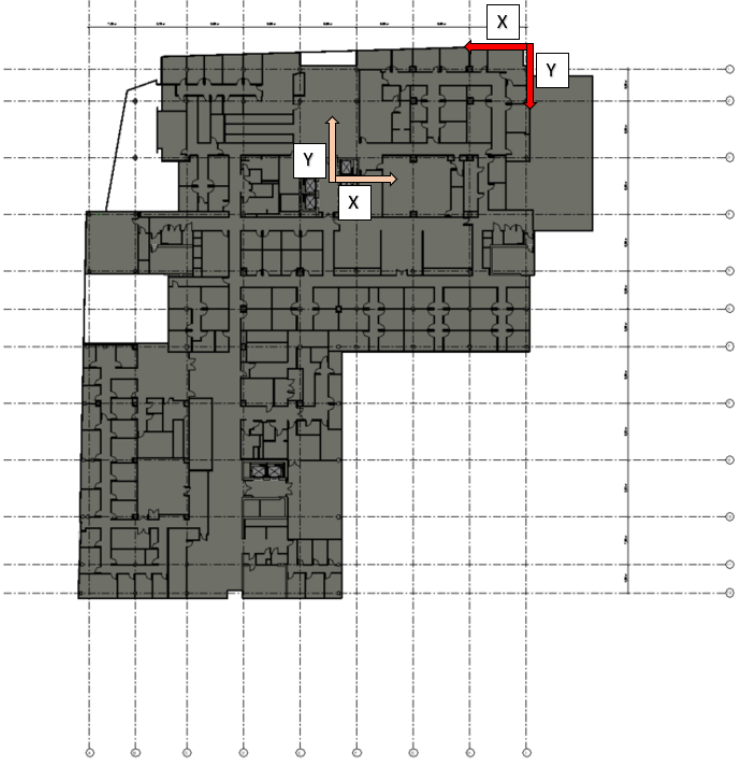


Figure 4. 20. The transformation of the original coordinate system origin (around the center of the building) to the new coordinate system origin (top right)

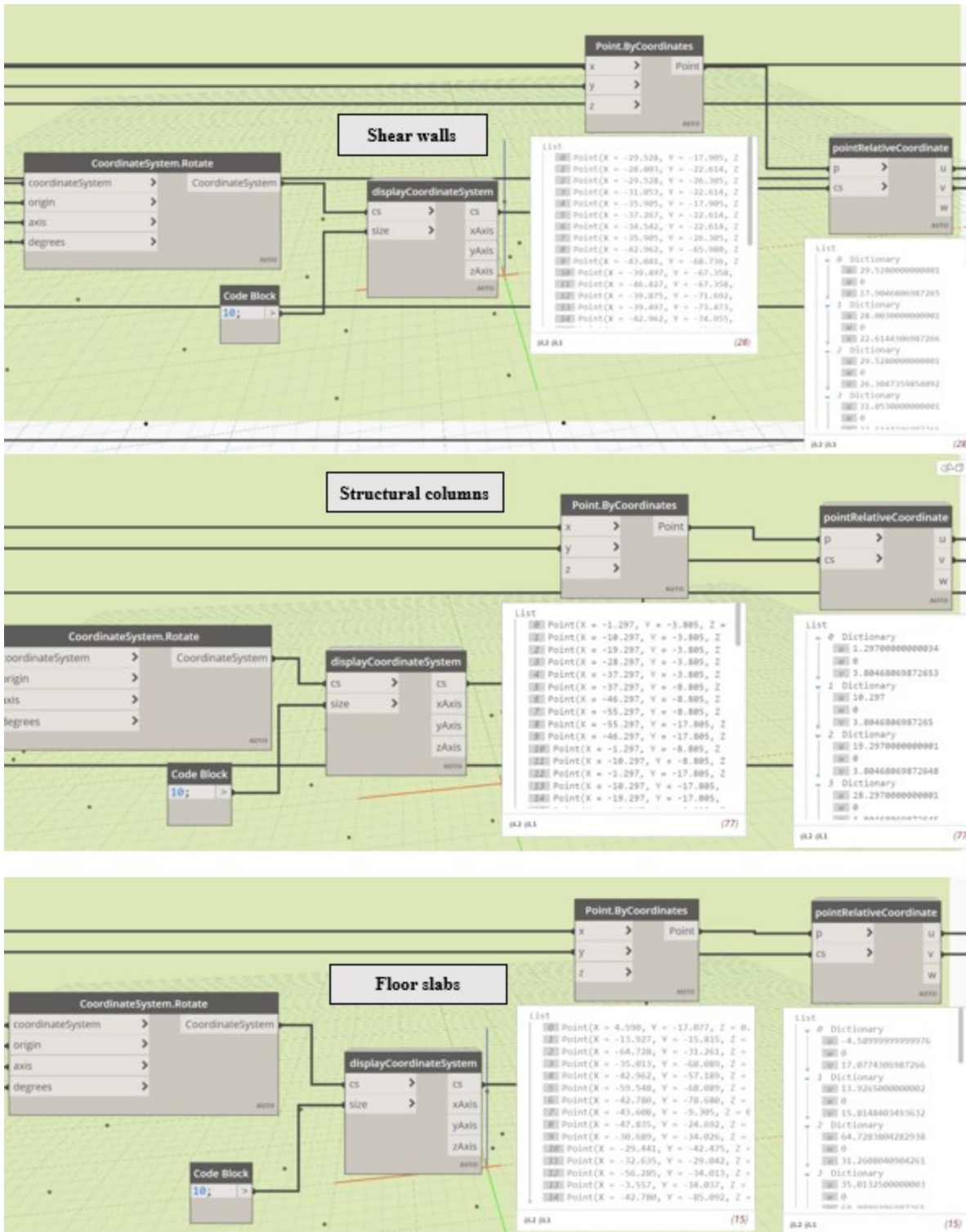


Figure 4. 21. The transformation process of all the computed coordinates (at the second-floor level) to the new coordinate system origin in Dynamo Studio (code block module 3)

Next, all the required physical and functional parameters and properties of the identified components are collected through code block module 4. Figure 4.22 shows the collected material

properties and physical dimensions of the existing columns in the 3D model. It is noteworthy to mention that these information are essential to calculate the structural input parameters such as coordinates of each floor's C.M., seismic weight, and moment of inertia.

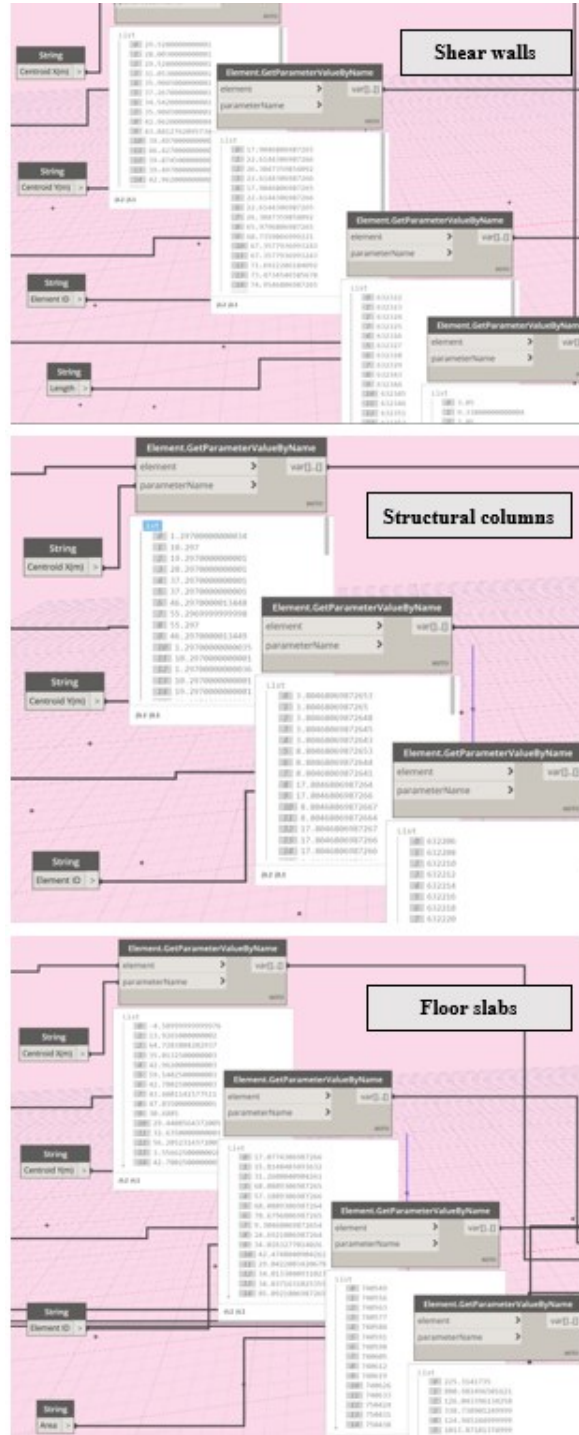


Figure 4. 22. the collecting process of the material properties and physical dimensions of the identified components at the second-floor level of the building (code block module 4)

Finally, all the collected information through the previous code block modules are automatically transferred to the formulated relational database which is integrated with Dynamo to compute the structural input parameters for the experimental response spectrum modal analysis. Figure 4.23 shows the process of transferring all the information through code block module 5 for all the categories. The whole process is repeated for all the floor levels to collect the required information to compute the structural input parameters utilized in the seismic analysis. The same cycle is repeated for all the floor levels of EV building.

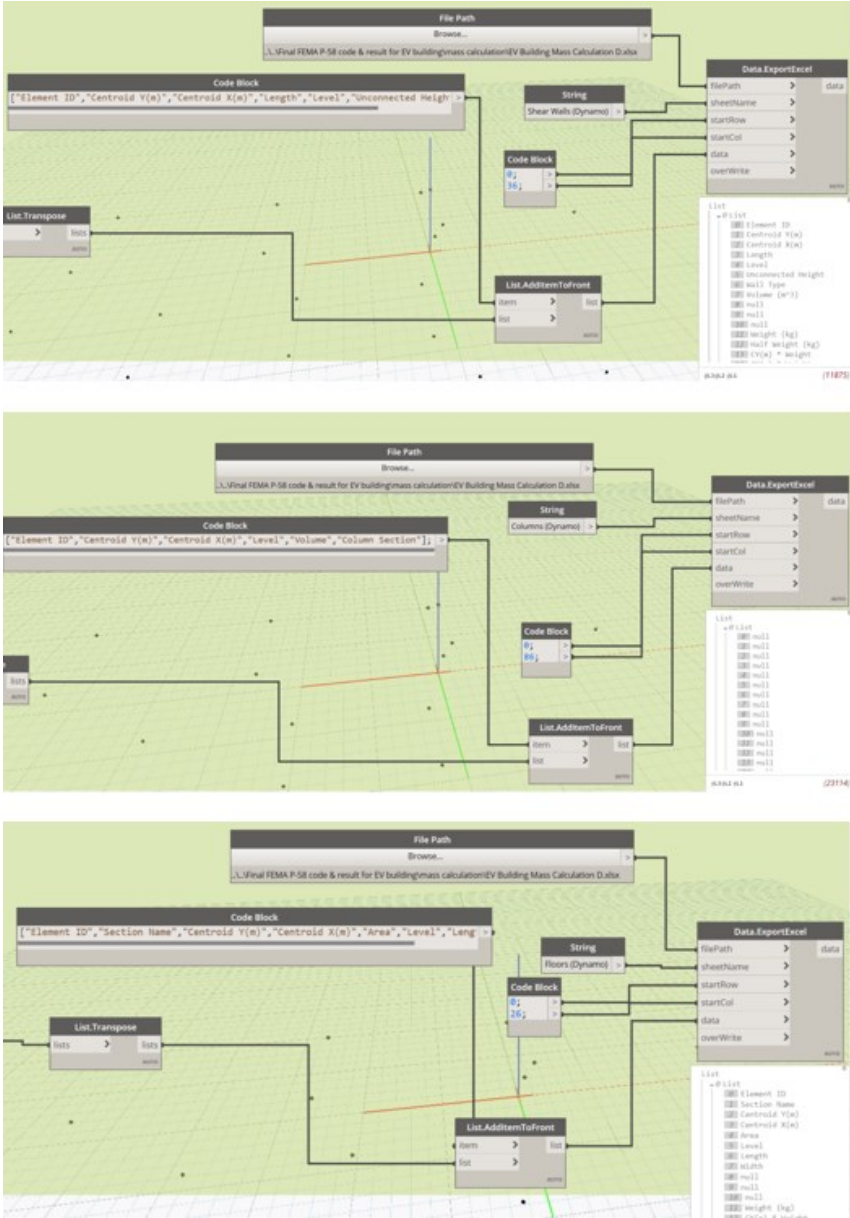


Figure 4. 23. The process of transferring all the collected information from the identified components at the second-floor level of the building to the relational database (code block module 5)

To accomplish the aforementioned procedure of the simplified three-dimensional experimental response spectrum modal analysis, Algorithm “MSOT” (also known as algorithm “B”) additionally, needed to be performed over the 3D model of EV building. The main purpose of running algorithm “MSOT” is to determine the real mode shape values (including two horizontal movements and one in-plane rotation) at the C.M. locations from the corresponding measured nodes located at the corners of each floor. To do this, the real mode shapes, and the corresponding natural frequencies, which are derived from the conducted OMA over EV building are required to be input. These information are the product of output-only system identification process at the OMA step. However, as mentioned in Section 4.3.4, the inputted mode shapes in this example, are the result of employing FDD technique in ‘*ARTEMIS Extractor Pro*’ software (Extractor, 1999). Therefore, although the output mode shapes are complex modes, still the normal modes can be estimated from the real part of experimental complex modes. This is due to two assumptions of considering classical damping as well as not having significant difference at the level of damping between different parts of EV building structure. This assumption can be validated by examining complex numbers corresponding to nodes at each particular mode shape to ensure that the difference between phase angles of various nodes remains close to zero or 180 degree (Mirshafiei, 2016). An overview of Algorithm “MSOT” is shown in Figure 4.24.

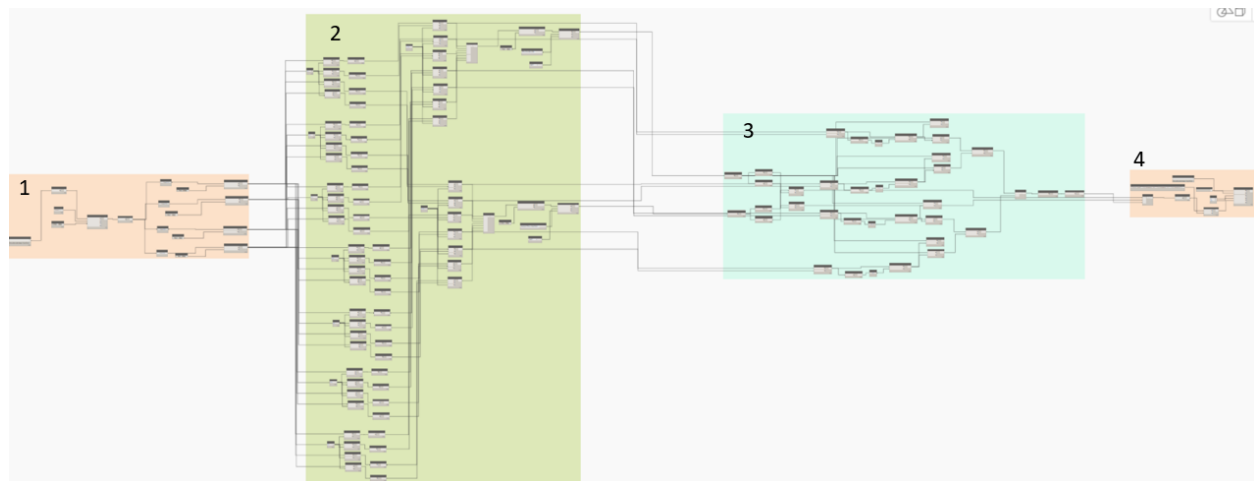


Figure 4. 24. The customized visual script of the algorithm “MSOT” adopted in the experimental structural analysis for EV building

To compute the mode shape values (including two horizontal movements and one in-plane rotation) at the C.M. location of each floor slab (diaphragm) from the corresponding measured

nodes located at the corners, algorithm “MSOT” should be applied. By running the algorithm “MSOT” over the EV building BIM model, the mode shape values of the C.M location are computed per each story level at each mode shape. Also, it is to be noted that, depending on the number of the measured nodes located at the corners of each floor, the shape of the floor slabs is formed. To demonstrate the application of this algorithm over EV building, the process of computing the mode shape values of the second-floor slab (at the C.M. location) at the first mode shape is as following:

initially, the actual coordinate values of the measured nodes for both the original and secondary location of the floor slabs at all the story levels are input in Dynamo Studio from the relational database. This process is performed through the code block module 1 (Figure 4.25).

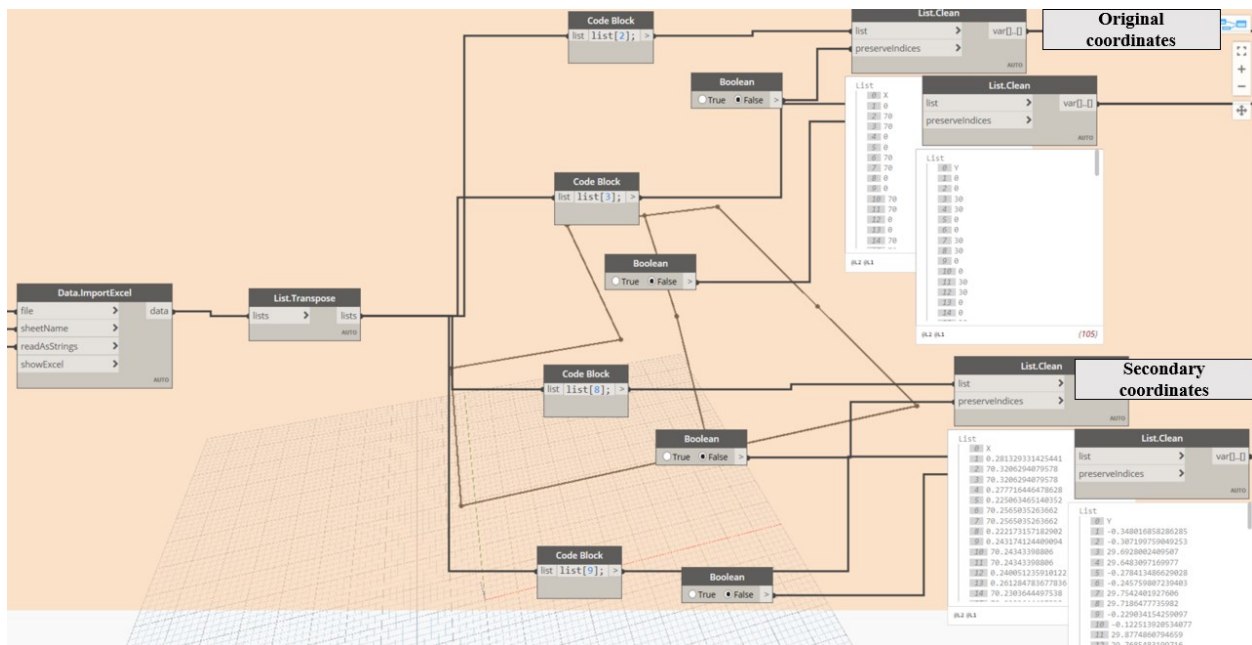


Figure 4. 25. The inputting process of the original and secondary coordinate values of EV building in Dynamo Studio from the relational database (code block module 1)

Subsequently, code block module 2 reads all the input coordinates and sorts the corresponding original and secondary coordinates of the second-floor slab. Then, according to the sorted coordinates, two floor slabs are formed in Autodesk Revit. The first slab is constructed from the original coordinates which represents the original position of the second-floor slab. However, the second slab is fed from the secondary coordinates which represents the movements imposed to the second-floor slab through the first mode shape. At the second-floor levels, each slab is constructed

from seven measured nodes (corner points). Figure 4.26 shows the process of sorting the input coordinates and constructing the corresponding floor slabs at the second floor through the code block module 2. Figure 4.27 shows the constructed floor slabs with both the original and secondary coordinates in Autodesk Revit, respectively.

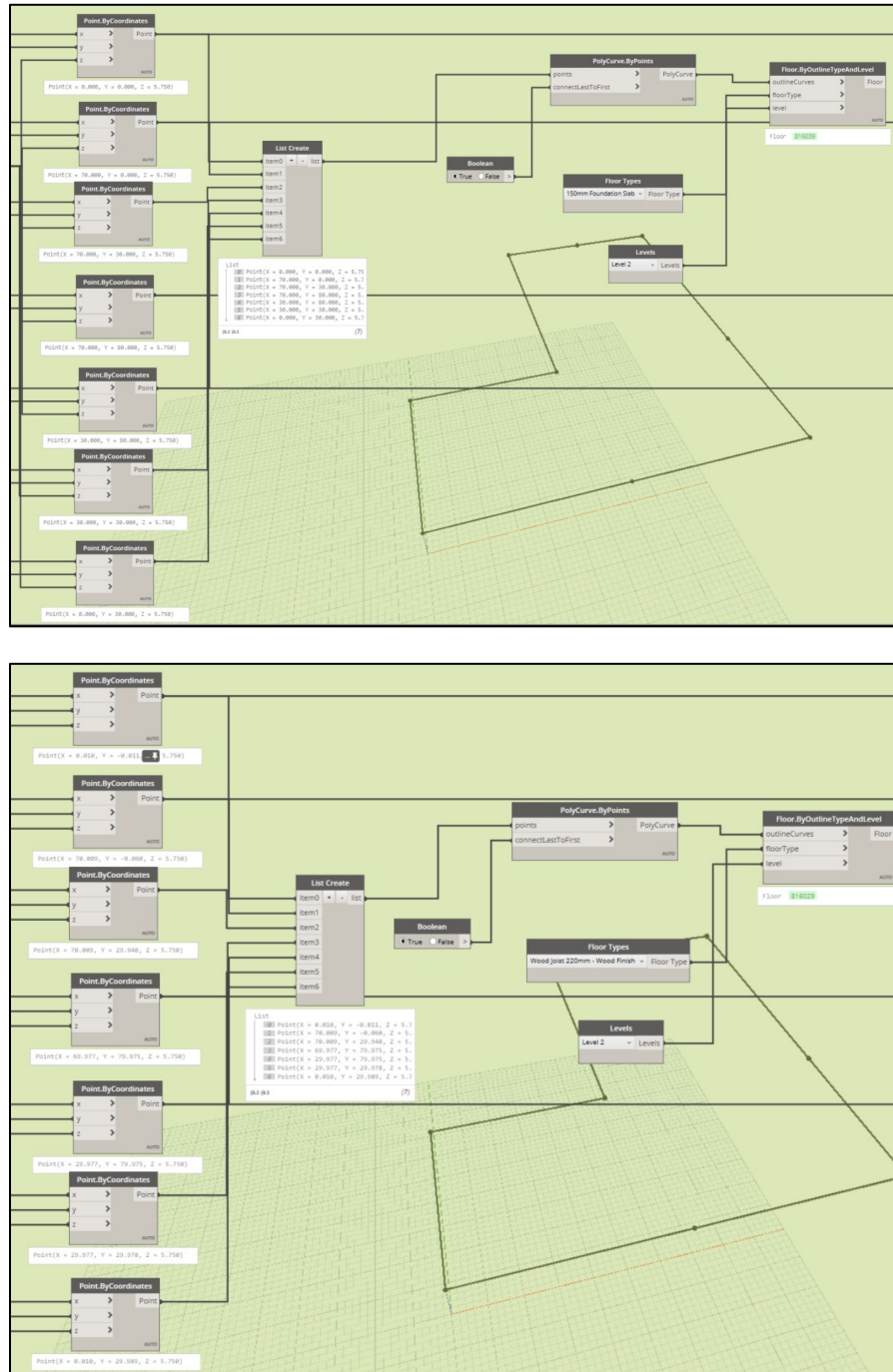


Figure 4. 26. The formation process of the floor slabs at the second floor from with the corresponding input original (up) and secondary coordinates (bottom), respectively (code block module 2)

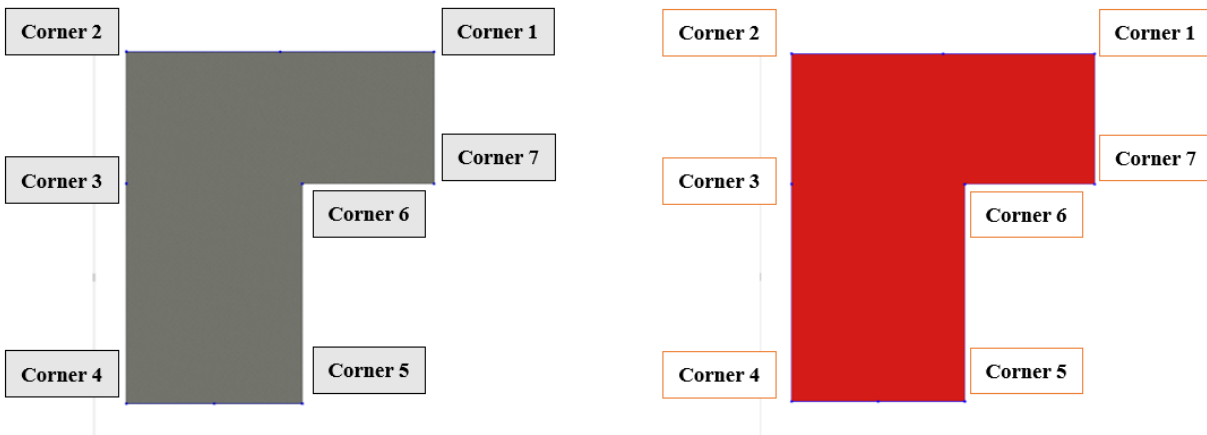


Figure 4. 27. The constructed floor slabs with the original (left) and secondary coordinates (right) in Autodesk Revit, respectively

Figure 4.28 shows the identified movements that the second-floor slab experiences during the first mode shape at each corner. Moreover, the movements are listed in Table 4.3.

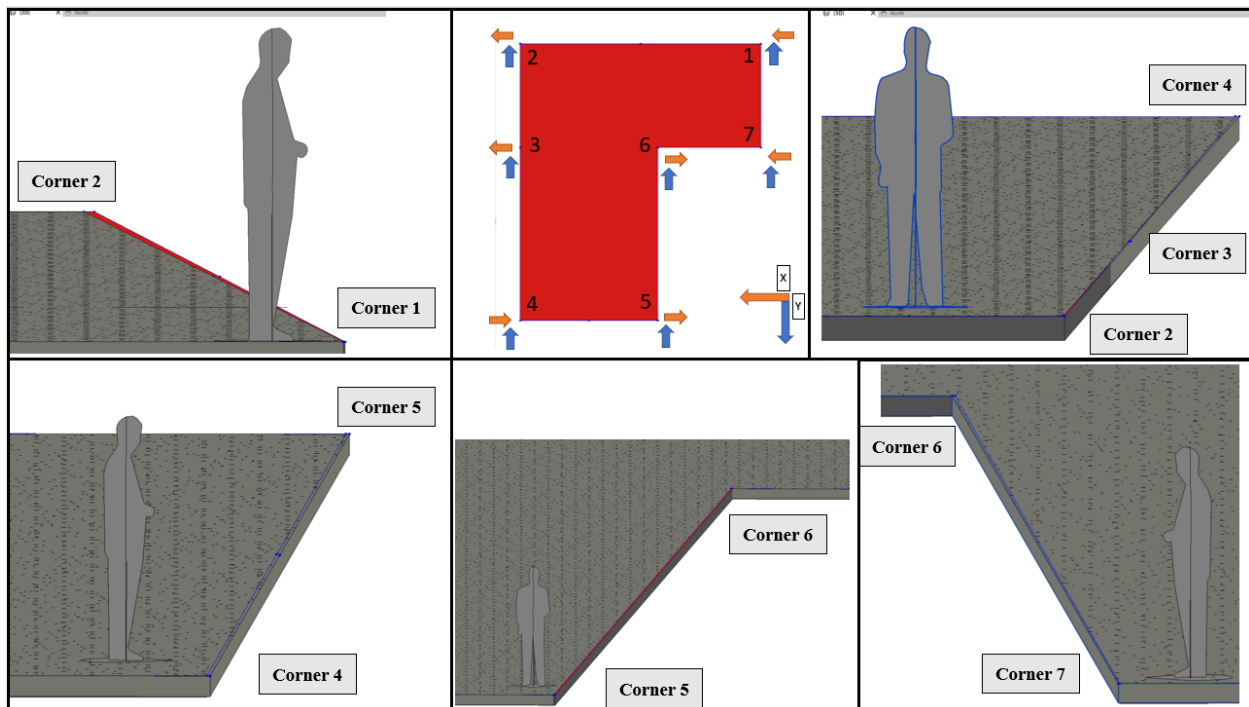


Figure 4. 28. The identified movements of the second-floor slab, imposed by the first mode shape at each corner

Corner number	Horizontal movement (X direction)	Horizontal movement (Y direction)
1	0.007485594	-0.032369062
2	0.006325471	-0.006897998
3	0.006325471	-0.006897998
4	-0.018611461	-0.01041162
5	-0.018611461	-0.01041162
6	-0.018611461	-0.01041162
7	0.007485594	-0.032369062

Table 4. 3. The identified movements of the second-floor slab, imposed by the first mode shape at each corner

Next, by adopting the code block module 3 in algorithm “MSOT” over EV building BIM model, initially the C.M. of both the original and secondary floor slabs are calculated. Moreover, the horizontal movements of the C.M. in both the directions (X and Y) as well as its in-plane rotation between the original and the transformed floor slabs are calculated. Figure 4.29 shows the computed horizontal movements of the C.M. between the original and the secondary (transformed) floor slabs at the second-floor level of EV building.

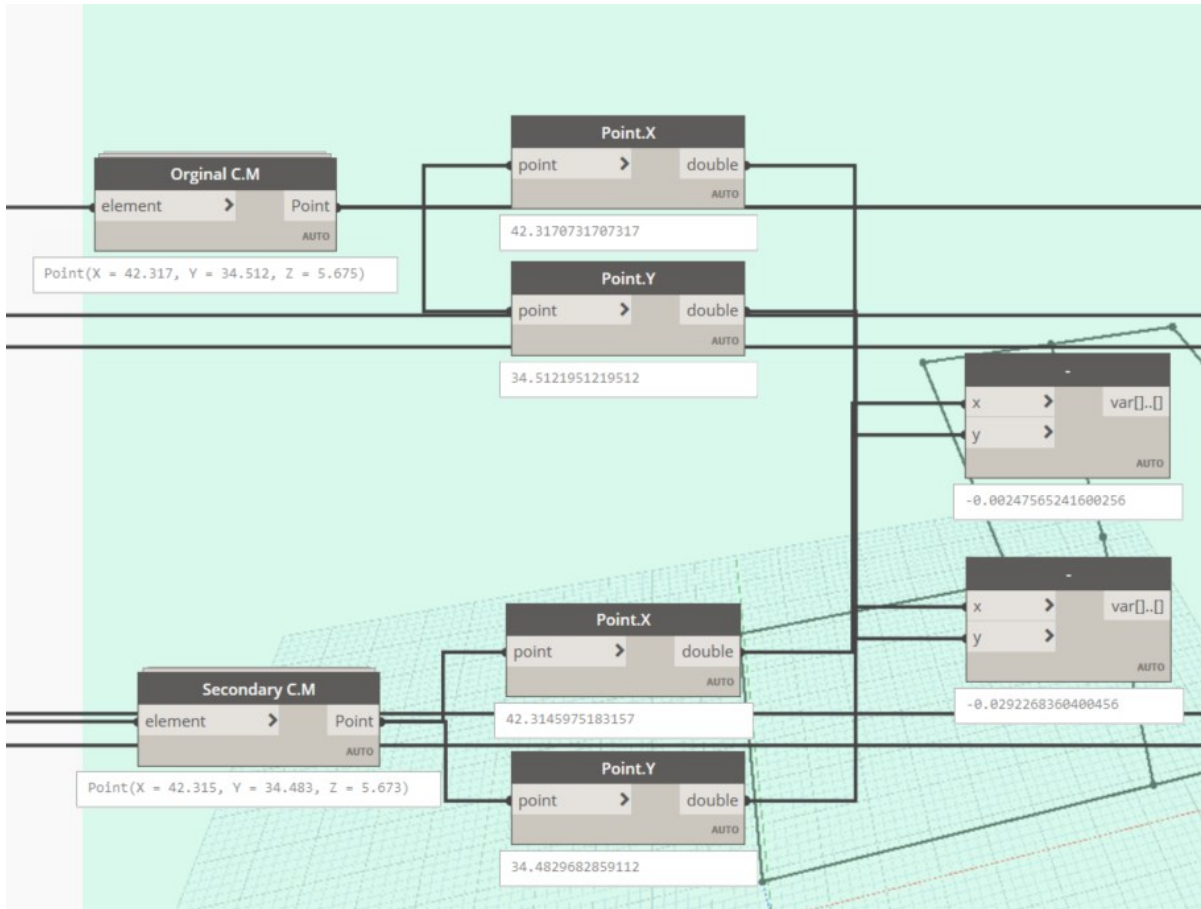


Figure 4. 29. The computing process of the horizontal movements of the C.M. between the original and the secondary (transformed) floor slabs at the second-floor level of EV building (code block module 3)

Figure 4.30 shows the calculation of the in-plane rotation at the C.M. location between the original and the transformed floor slabs at the second-floor level of EV building. The indicated rotation is in radians.

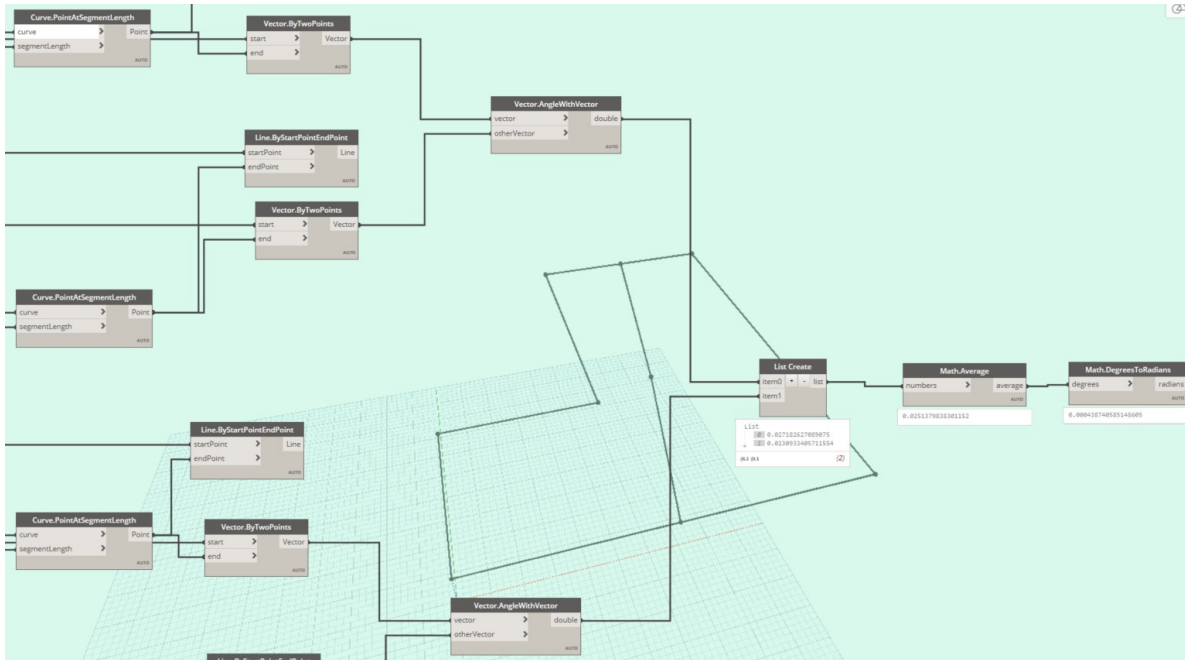


Figure 4. 30. The computing process of the in-plane rotation of the C.M. between the original and the transformed floor slabs at the second-floor level of EV building (code block module 3)

Table 4.4 shows the computed horizontal movements of the C.M. in both the directions (X and Y) as well as its in-plane rotation of the second-floor slab in the first mode shape.

Movement (X direction)	Movement (Y direction)	In-plane rotation (radians)
-0.0024756	-0.029226836	0.000436332

Table 4. 4. The computed displacements and in-plane rotation of the C.M. of the second-floor slab in the first mode shape

Finally, the computed mode shape values are transferred automatically from Dynamo to the relational database through the code block module 4. Figure 4.31 shows the process of exporting the computed mode shape values to the relational database through the code block module 4.

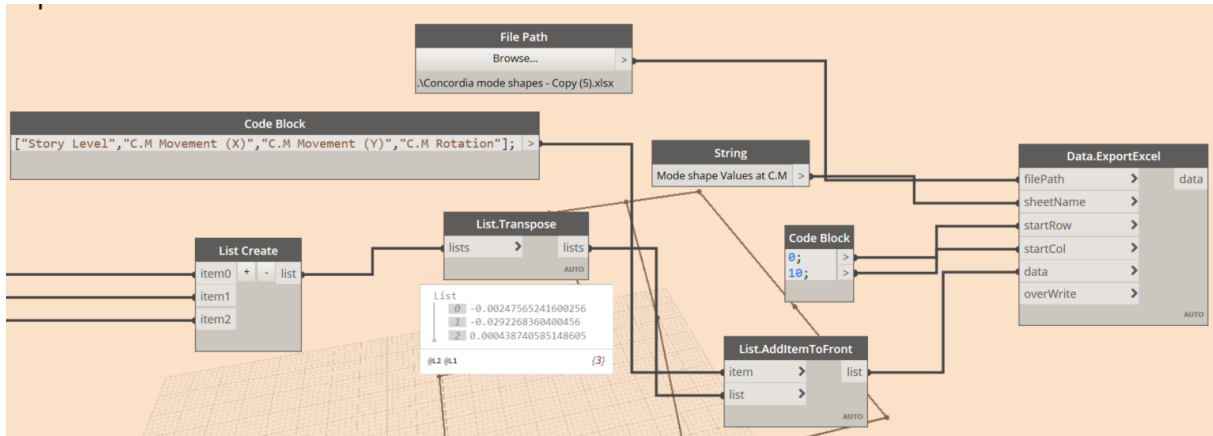


Figure 4. 31. The exporting process of the computed mode shape values from Dynamo to the relational database (code block module 4)

The same process is repeated for all the floor levels at each six mode shapes and consequently, leads to the formation of the mode shape matrix, including two horizontal movements and one in-plane rotation at each floor's C.M. location of EV building. Table 4.5 shows the collected mode shape values for the first mode shape.

Story Level	U(x)	U(y)	U(Θ) radians
Roof	0.217606384	-0.517649418	0.021375836
16 th Floor	0.174085107	-0.414119534	0.017126346
15 th Floor	0.175787925	-0.33609486	0.015178522
14 th Floor	0.177507093	-0.258091093	0.013229748
13 th Floor	0.154068707	-0.261569014	0.012471582
12 th Floor	-0.018467612	-0.179429956	0.00519793
11 th Floor	-0.010508949	-0.157018732	0.004492526
10 th Floor	-0.002563321	-0.134609645	0.003787325

9 th Floor	-0.030198505	-0.102054138	0.003249161
8 th Floor	-0.010978004	-0.05746431	0.00166591
7 th Floor	0.004056332	-0.075686027	0.002231443
6 th Floor	-0.002876772	-0.067662639	0.001868908
5 th Floor	-0.005224055	-0.052739602	0.001434338
4 th Floor	0.005079797	-0.041311572	0.000999553
3 rd Floor	-0.009939873	-0.026032122	0.000666577
2 nd Floor	-0.0024756	-0.029226836	0.000436332
Ground Floor	0	0	0

Table 4. 5. The collected mode shape values of the first mode shape of EV building

As a result of performing both the algorithm “SMMIC” and “MSOT” all the structural input parameters that were required to perform the simplified three-dimensional experimental response spectrum modal analysis were collected at the relational database. These structural input parameters are automatically organized in the form of both the mass matrix and the real mode shape matrices (at the C.M. of each floor). The mass matrix includes the seismic weight of all the floors and the associated moment of inertias in the relational database. Therefore, by inputting the aforementioned matrices and the target spectra defined by NBCC 2015 for Montreal (City Hall) with 2% probability of exceedance in 50 years into the formulated relational database, the experimental response spectrum modal analysis is performed and the desired EDPs are its final product. Figure 4.32 shows the input target spectra for Montreal (City Hall) defined by NBCC 2015. Moreover, the computed desired EDP values such as peak absolute floor accelerations, and peak story drift ratios are sorted at the relational database as shown in Figure 4.33. Microsoft Excel was used as the relational database in this example.

Target response spectra Montreal (City hall) NBCC 2015

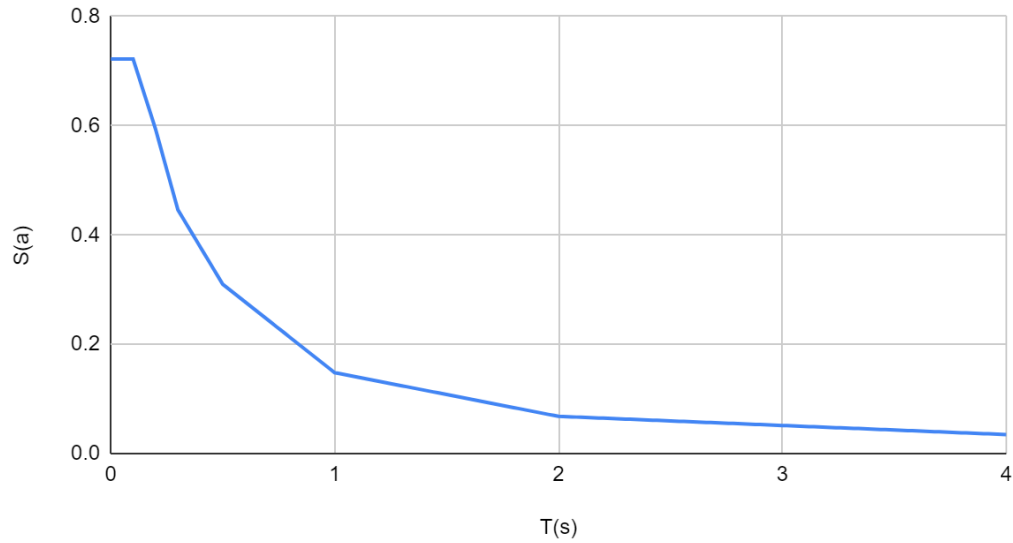


Figure 4. 32. The inputted target response spectra for Montreal (City Hall) defined by NBCC 2015

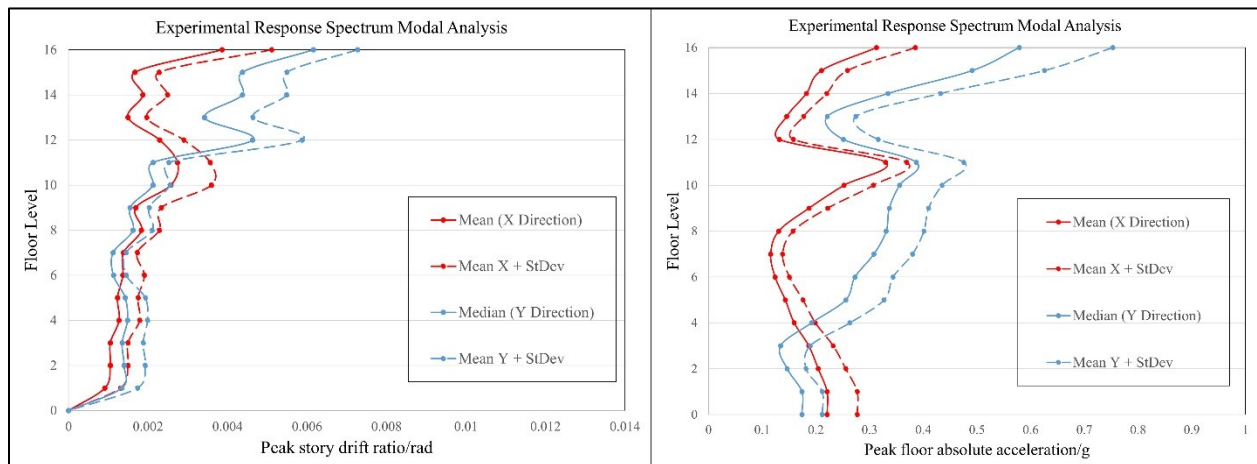


Figure 4. 33. Structural responses of EV building: peak story drift ratios (left) and peak floor absolute accelerations (right), (nonmodel-based approach)

4.4.3 EDP result comparison between the proposed approaches

With respect to the derived sets of EDPs from both the nonlinear time history analysis and experimental modal response spectrum analysis, Figure 4.34 and Figure 4.35 show the comparison of the peak absolute floor accelerations and peak story drift ratios. It can be seen that, the range of computed EDPs from the nonmodel-based method is relatively lower than the model-based

method. This is mostly due to the fact that, the experimental modal response spectrum analysis adopted in the nonmodel-based approach does not take into account the nonlinear relations. Moreover, the nature of the modal response spectrum analysis is a linear-dynamic statistical analysis method, whereas the nonlinear time history analysis employed in the model-based approach is a nonlinear-dynamic analysis that demonstrates the dynamic performance of a structure which may vary with time. Also, considering the fact that the adopted case study in this study, EV building is an irregular structure, nonlinear time history analysis demonstrates the potential structural performance of the building more precisely.

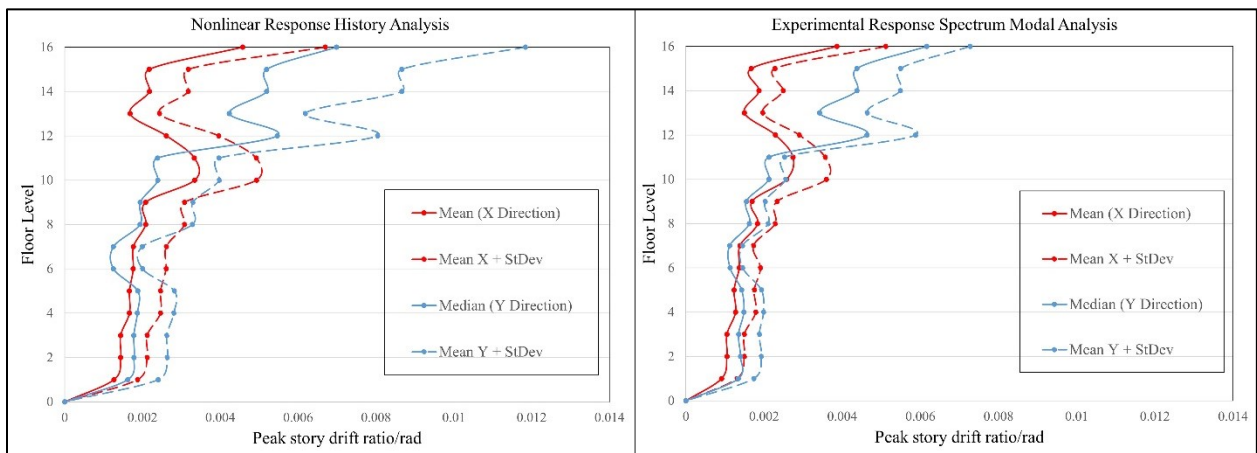


Figure 4. 34. Peak story drift ratios of EV building: model-based approach (left), nonmodel-based approach (right)

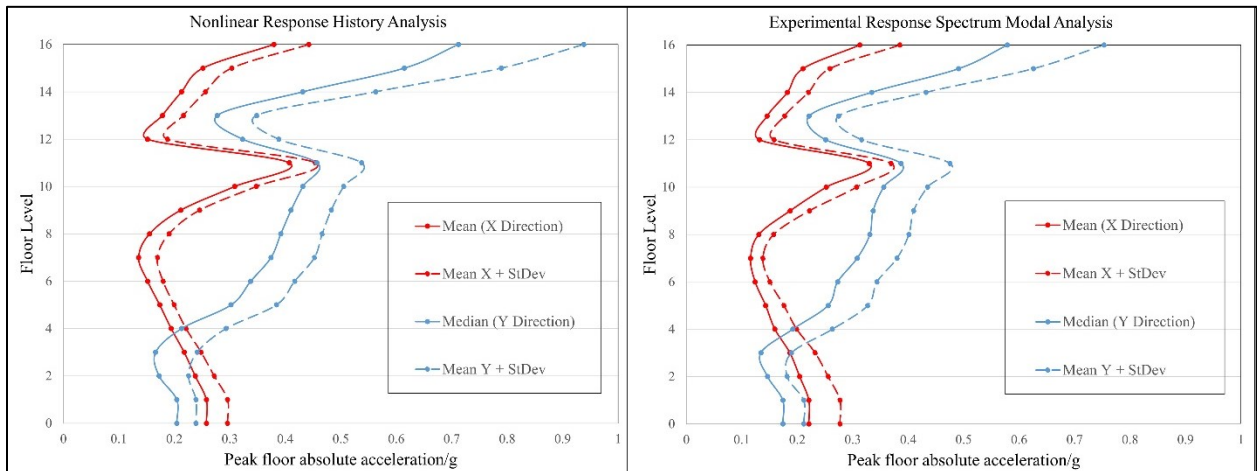


Figure 4. 35. Peak floor absolute accelerations of EV building: model-based approach (left), nonmodel-based approach (right)

The sudden changes in the amounts of the peak absolute floor acceleration and peak story drift ratio around the 11th floor indicate the distributed irregularity of the building in terms of the height.

4.5 BIM-based seismic loss analysis

As demonstrated in Section 3.4, in order to evaluate the induced physical damage and the associated loss consequence predictions of EV building against the probable seismic events, seismic loss analysis is required to be conducted. With respect to the latest generation of PBEE, FEMA P-58 or PEER-PBEE framework is adopted for this example. Therefore, regardless of the method of EDP determination (model-based and nonmodel-based approach), the conducted seismic loss analysis can predict the induced-loss of a building at the given intensity of Maximum Considered Earthquake (MCE). However, to demonstrate the impact of both the model-based and nonmodel-based approaches on the predicted seismic performance, two different seismic loss analyses schemes were applied to the EV building based on FEMA P-58 procedure. The only key distinction between these loss analyses schemes is the utilized EDPs. With respect to FEMA P-58, the output of each conducted loss analysis scheme indicates the predicted performance measures in terms of repair cost and repair time. Finally, to facilitate the interpretation of loss consequence predictions and subsequent decision-making process, the derived performance measures of both approaches are visualized independently through a framework of developed algorithms in Dynamo Studio.

4.5.1 Loss analysis based on FEMA P-58 (in PACT software)

4.5.1.1 Development of Building Performance Model

Regardless of the adopted approach to derive the desired EDPs (model-based or nonmodel-based approach), similar procedure based on FEMA P-58 is respected to perform the seismic loss analysis. This section discusses the considered inputs for developing the building performance model of EV building, which is utilized to run the seismic loss analysis in PACT software (Fema, 2012). Moreover, to better demonstrate the impact of the EDP determination approach (model-based and nonmodel-based) on the seismic loss analysis, two different performance models are developed. Although, the procedure of EDP acquisition in the building performance models are

quite different, the rest of input parameters and model characteristics remain the same. The EDP acquisition procedure is elaborated more in the following section.

As shown in previous sections, The BIM model of EV building is constructed in Autodesk Revit software, which includes all the implemented structural and non-structural components and systems according to the drawing plans. Therefore, all the geometric information (such as floor's area, height and so on), required to build the performance model of EV building are based on its BIM model. Also, it is noteworthy to mention that the average LOD of all the structural and non-structural components in the 3D model is close to 300, which has a significant impact on reducing the uncertainties in developing of the building performance model of EV building as well as the associated seismic loss analysis. Figure 4.36 shows the developed details of the wall-partitions, HVAC system etc. in the BIM model.

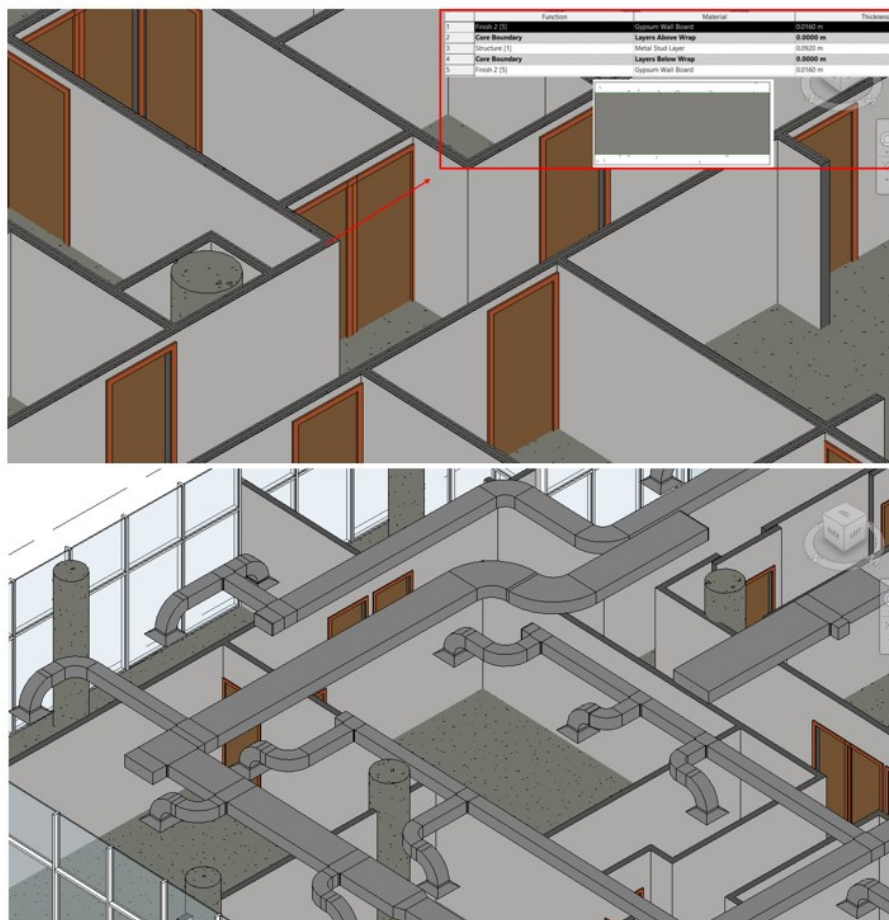


Figure 4. 36. The developed details of the wall-partitions, HVAC system etc. demonstrated in EV building BIM model in Autodesk Revit

Based on the BIM model, the total replacement cost and time estimated for EV building are (\$148 million) and two years (720 days), respectively.

Moreover, considering that the database of FEMA P-58 for the typical structural and non-structural components provided in PACT are based on Northern California region in the year of 2011, *Region Cost Multiplier* and *Date Cost Multiplier* are employed to adjust the repair costs to Montreal region in 2020. For this purpose, *Region Cost Multiplier* and *Date Cost Multiplier* are 0.82 and 1.25, respectively based on the RS Means Cost Index system (Mewis, 2019).

Although the irreparability level in FEMA P-58 is set at 40% of replacement cost (FEMA, 2012), the *Total Loss Threshold* in this study is set at 1.0 to completely evaluate the maximum consequence information before being labeled as irreparable.

With respect to identifying the probable structural non-structural components in risk, all the structural and non-structural system and components are extracted and listed from the BIM model based on FEMA P-58 fragility collection. As a result, Table 4.6 and Table 4.7 provide the description of all the identified structural and non-structural components in EV building, which are participating in the seismic loss analysis. It is noteworthy to mention that the average PACT values provided in the tables, represent the average quantity of all the identified vulnerable categories of components available in the EV building’s 3D model. Also, with respect to those categories of non-structural components that has no information included in the 3D model, Normative Quantity Spreadsheet (provided by FEMA P-58 collection) is utilized to quantify the non-structural components, conditioned on the occupancy and the floor area of each story.

Structural component type	Fragility classification number	PACT value (1 st to 11 th floor)	PACT value (12 th to 16 th floor)	Demand parameter
Concrete shear wall	B1044.021	13.29	5.42	Story Drift Ratio
Flat slab-column joint	B1049.042b	57	25	Story Drift Ratio

Table 4. 6. The identified structural component fragilities used in PACT software for EV building

Non-structural component type	Fragility classification number	PACT value (1 st to 11 th floor)	PACT value (12 th to 16 th floor)	Demand parameter
Curtain wall	B2022.002	225	180	Story Drift Ratio
Wall partition	C1011.001a	20.71	10.80	Story Drift Ratio
Wall partition	C3011.001a	3.14	1.43	Story Drift Ratio
Wall partition	C3011.002a	3.14	1.43	Story Drift Ratio
Suspended ceiling	C3032.001d	14.94	6.80	Acceleration
Pendant lighting	C3034.001	124	56	Acceleration
Traction Elevator	D1014.011	8	6	Acceleration
Hot Water Piping	D2022.012a	5.23	2.29	Acceleration
Hot Water Piping	D2022.022a	1.83	0.85	Acceleration
Sanitary Piping	D2031.022a	2.31	1.08	Acceleration
HVAC ducting	D3041.011b	3.05	1.42	Acceleration
HVAC ducting	D3041.012b	0.81	0.38	Acceleration
HVAC drops	D3041.031b	36.54	17.01	Acceleration
(VAV) box	D3041.041b	20.3	9.45	Acceleration
Fire sprinkler water piping	D4011.022a	8.12	3.78	Acceleration
Fire sprinkler drop	D4011.032a	3.65	1.70	Acceleration
Bookcase	E2022.105b	81.21	37.79	Acceleration
Lateral Filing Cabinet	E2022.125b	32.48	15.12	Acceleration

Table 4. 7. The identified non-structural component fragilities used in PACT software for EV building

However, it is evident that due to enormous scale of EV building and the corresponding vulnerable non-structural systems and components, some minor categories of non-structural components might be neglected unintentionally.

4.5.1.2 EDP acquisition for building performance model

With respect to the identified structural and non-structural components at risk in EV building (Table 4.6 and Table 4.7), the peak story drift ratios and peak floor accelerations are the only required EDPs (demand parameters) for the loss seismic analysis in this example. Therefore, regardless of the adopted approach for EDP determination (model-based or nonmodel-based approach), peak values of story drift ratios as well as peak floor accelerations in both two orthogonal directions throughout all the stories of EV building should be acquired in both the building performance models. Intensity-based assessment is adopted for both the building performance models. However, different EDP acquisition procedure (also known as structural analysis result input) are utilized. Non-linear analysis type was used to input the derived EDPs for the model-based approach, whereas, simplified (linear) analysis type for the nonmodel-based approach. Eleven sets of demand vectors are considered for the Non-linear analysis type (refer to section 4.4.1), whereas the simplified (linear) analysis type is limited to only one set of demand vector with dispersion.

Five hundred Monte Carlo samples are employed through PACT software (using inferred statistical distributions of building response based on limited suites of analyses) to stabilize the predicted loss analysis outcome, where it is presumed that the building remains free of any potential collapse and residual drift (Fema, 2012; Yang et al., 2009). It is to be noted that prior studies have used common simplifying assumptions (Cremen and Baker, 2018). Consequently, the result of the seismic loss analysis would be given in the form of repair cost and repair time. Moreover, for better realization of the outcome of the seismic loss analysis over EV building, 10th, 50th and 90th percentiles (90%, 50% and 10% chances of exceedance, respectively) from the cumulative loss distribution of repair cost and repair time are selected, extracted, and sorted into different standard format templates at the relational database.

4.5.1.3 Seismic loss analysis result

With respect to the performed FEMA P-58 seismic loss analysis over EV building through the PACT software, the outcome of the loss analysis is extracted and provided for both the approaches in the form of the cumulative loss distribution of repair cost and repair time. Total repair costs and repair time of 10th, 50th and 90th percentiles of the model-based and nonmodel-based approaches

are shown in Table 4.8 and Table 4.9, respectively. The derived total repair time for both the methods listed in Table 4.8 and Table 4.9 are directly derived from PACT software without considering the “maximum worker per square foot” parameter. Moreover, these percentiles are also exported from PACT software and demonstrated in Figure 4.37, where the allocations of the 10th, 50th and 90th percentiles can be compared between the model-based and nonmodel-based approaches. Overall, it can be seen that the allocation of the percentiles in the nonmodel-based approach is relatively more packed and focused close to the 90th percentile. Whereas, in the model-based approach, a considerable distance exists between the 10th, 50th and 90th percentiles. This is mostly due to the fact that the model-based approach is utilizing the nonlinear time history analysis which leads to the adoption of a wider range of the EDPs that support nonlinear relations in the analysis. Whereas the experimental modal response spectrum analysis employed in the nonmodel-based approach is more limited to the maximum seismic response of an essentially elastic structure. As a result, the distribution of the total repair costs in model-based approach is more spread out than the nonmodel-based approach, which looks reasonable.

Percentile	Total repair cost (CAD \$)	Total repair time (days)
10 th	670,000.00	508
50 th	1,300,000.00	942
90 th	3,800,000.00	2279

Table 4. 8. Total repair cost & repair time of the model-based approach (10th, 50th and 90th percentiles)

Percentile	Total repair cost (CAD \$)	Total repair time (days)
10 th	765,000.00	486
50 th	925,000.00	661
90 th	1,100,000.00	866

Table 4. 9. Total repair cost & repair time of the nonmodel-based approach (10th, 50th and 90th percentiles)

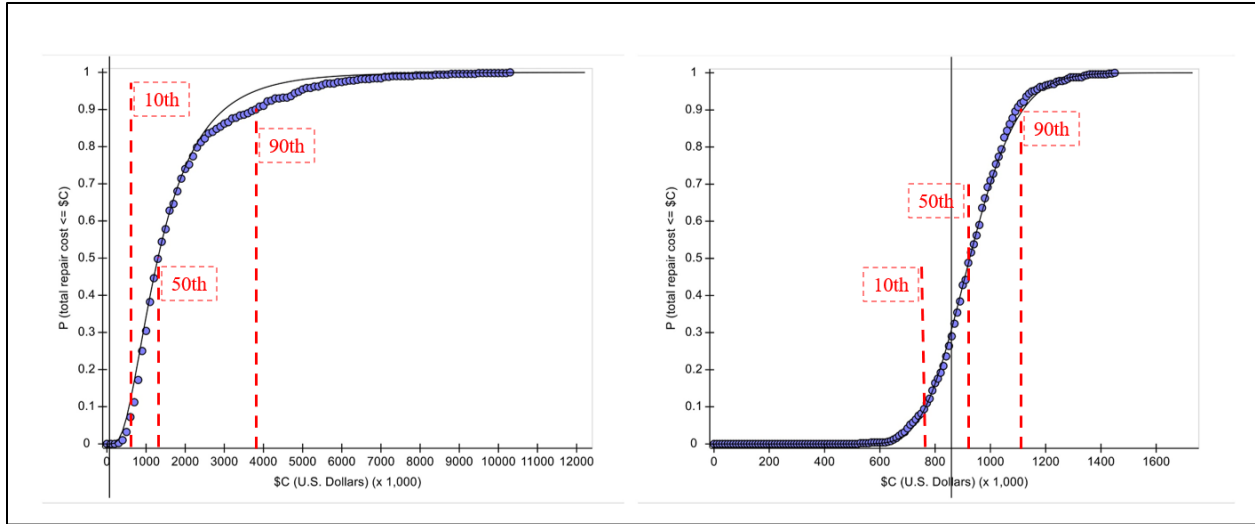


Figure 4. 37. The cumulative loss distribution of repair cost of EV building: model-based approach (left), nonmodel-based approach (right)

Concerning to Figure 4.38, it could be concluded that, regardless of the adopted approach, the dominant total repair costs in all the selected percentiles including 10th percentile (50th largest cost among the 500 realizations), 50th percentile (250th largest cost) and 90th percentile (450th largest cost) are only caused by the non-structural components. However, the rate of the vulnerable structural components is growing from the 10th to the 90th percentile in each approach.

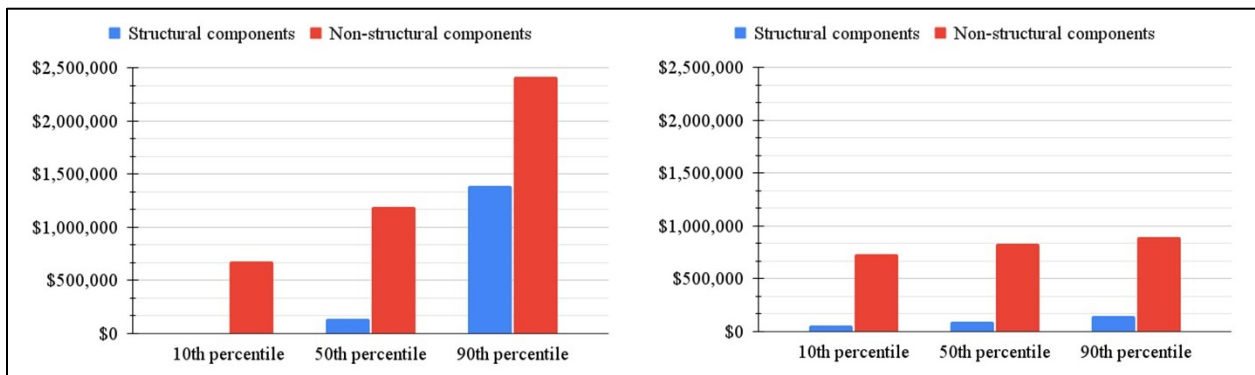


Figure 4. 38. Participation of the structural and non-structural components in the total repair cost: model-based approach (left), nonmodel-based approach (right)

With regards to the decomposition of the total repair cost at the 10th percentile in Figure 4.39, the Traction elevator and the wall partition (includes both the wall partitions and the wall finishes) are the dominant categories of the non-structural components that sustain the total repair cost,

respectively in both the approaches. However, minor structural damage can be predicted through the contribution of the flat slab-column joints and concrete shear walls in the nonmodel-based approach, which is not the case in the model-based approach. With regards to the 50th percentile in Figure 4.40, it could be seen that the similar pattern to the 10th percentile is repeated, where the majority of the total repair cost is caused by the Traction elevator and the wall partition categories, respectively. However, unlike the 10th percentile, the contribution of the structural damage in the total repair cost is more evident in both the approaches. With regards to the 90th percentile in Figure 4.41, it can be seen that nearly a third of the total repair cost in the model-based approach comes from the wall partition, while the remaining two-thirds of the total repair cost is distributed with an average of 20% among the Traction elevator, concrete shear walls and flat slab-column joints. Moreover, the contribution of the suspend ceiling and curtain wall categories are more apparent than the previous percentiles. On the other hand, the Traction elevator and the wall partition categories still significantly dominate the total repair cost in the nonmodel-based approach. However, a minority of the total repair cost comes from the contribution of the structural components such as the flat slab-column joints and concrete shear walls.

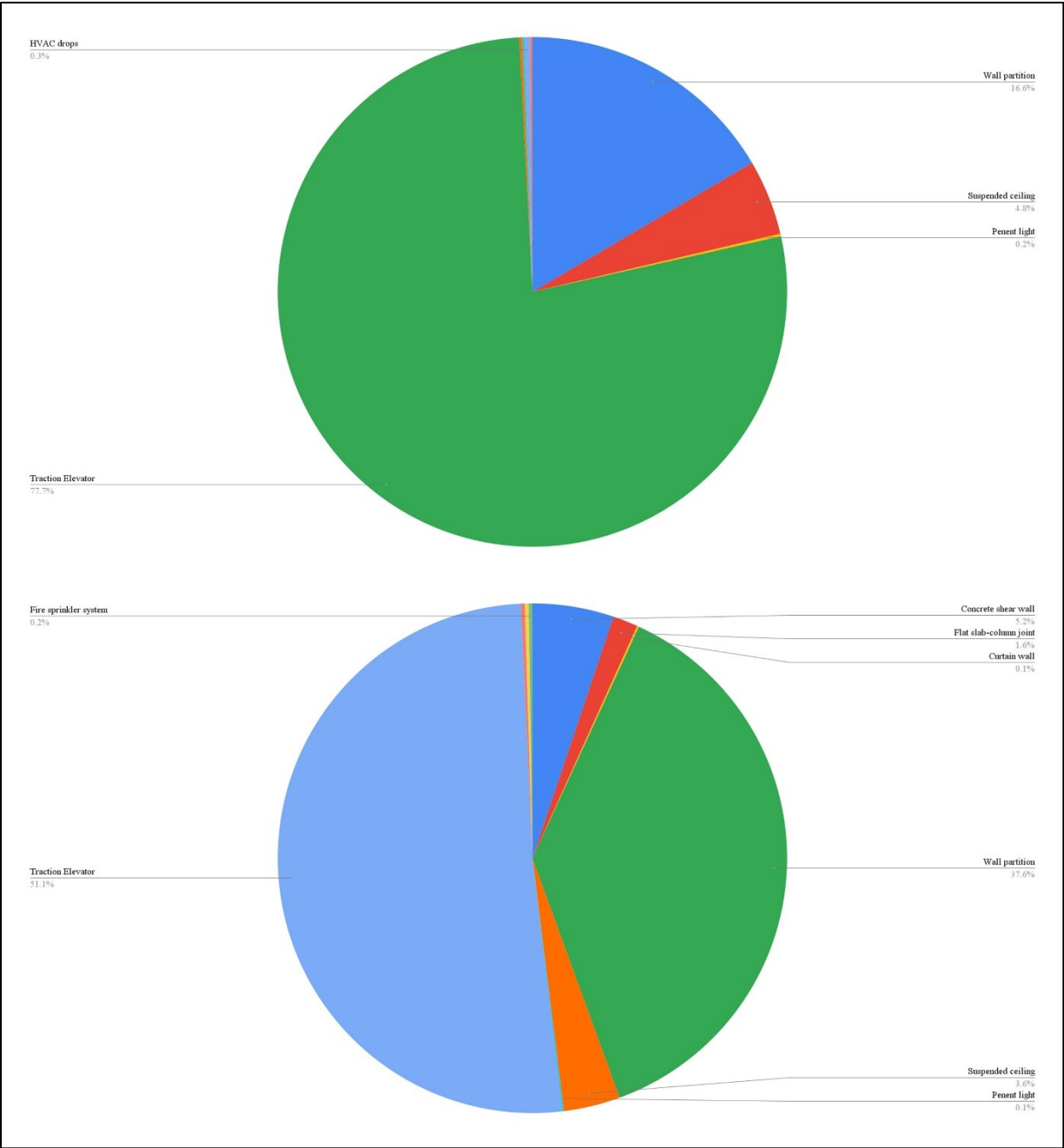


Figure 4. 39. Decomposition of the total repair cost in the 10th percentile: model-based approach (top), nonmodel-based approach (bottom)

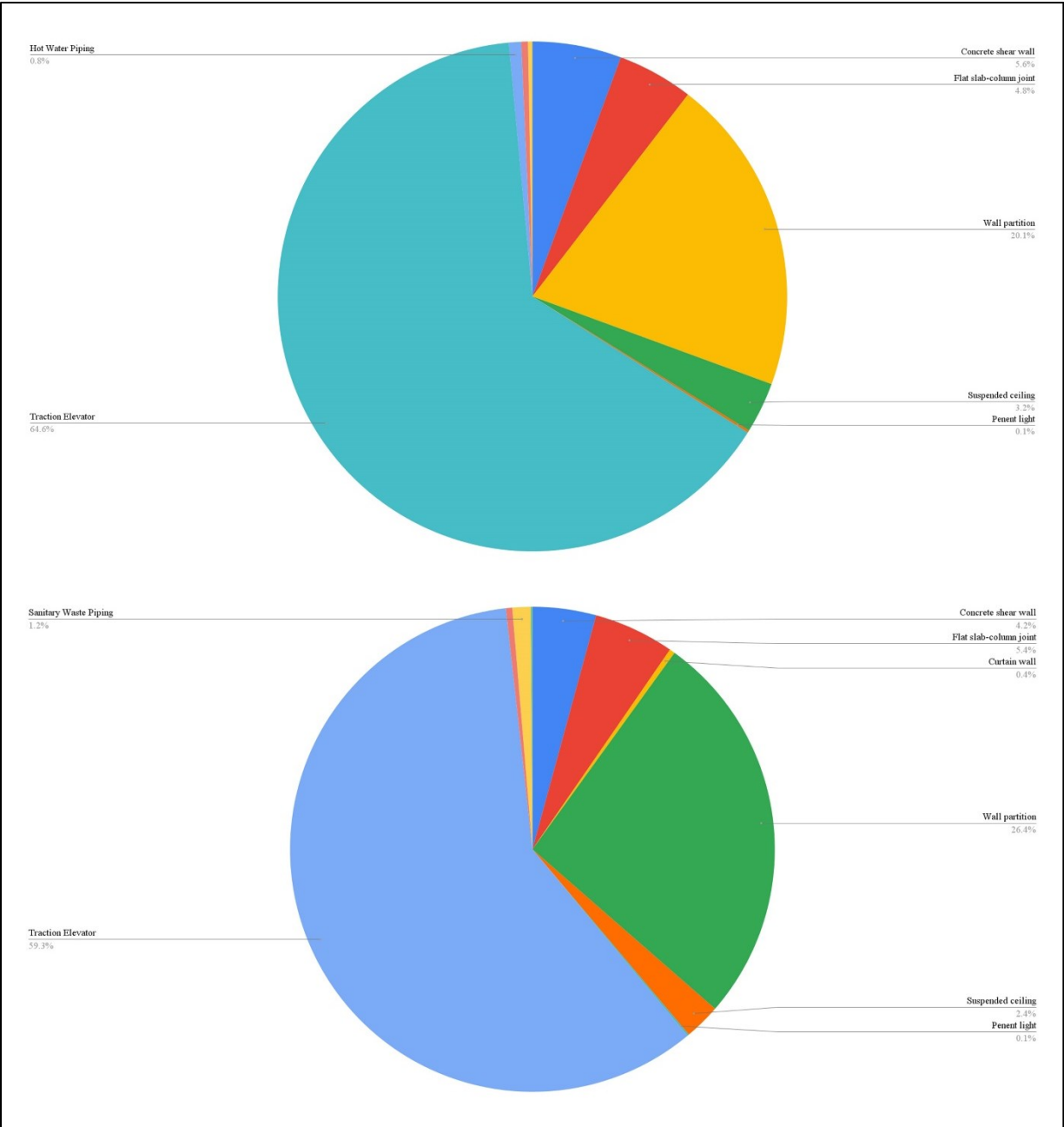


Figure 4. 40. Decomposition of the total repair cost in the 50th percentile: model-based approach (top), nonmodel-based approach (bottom)

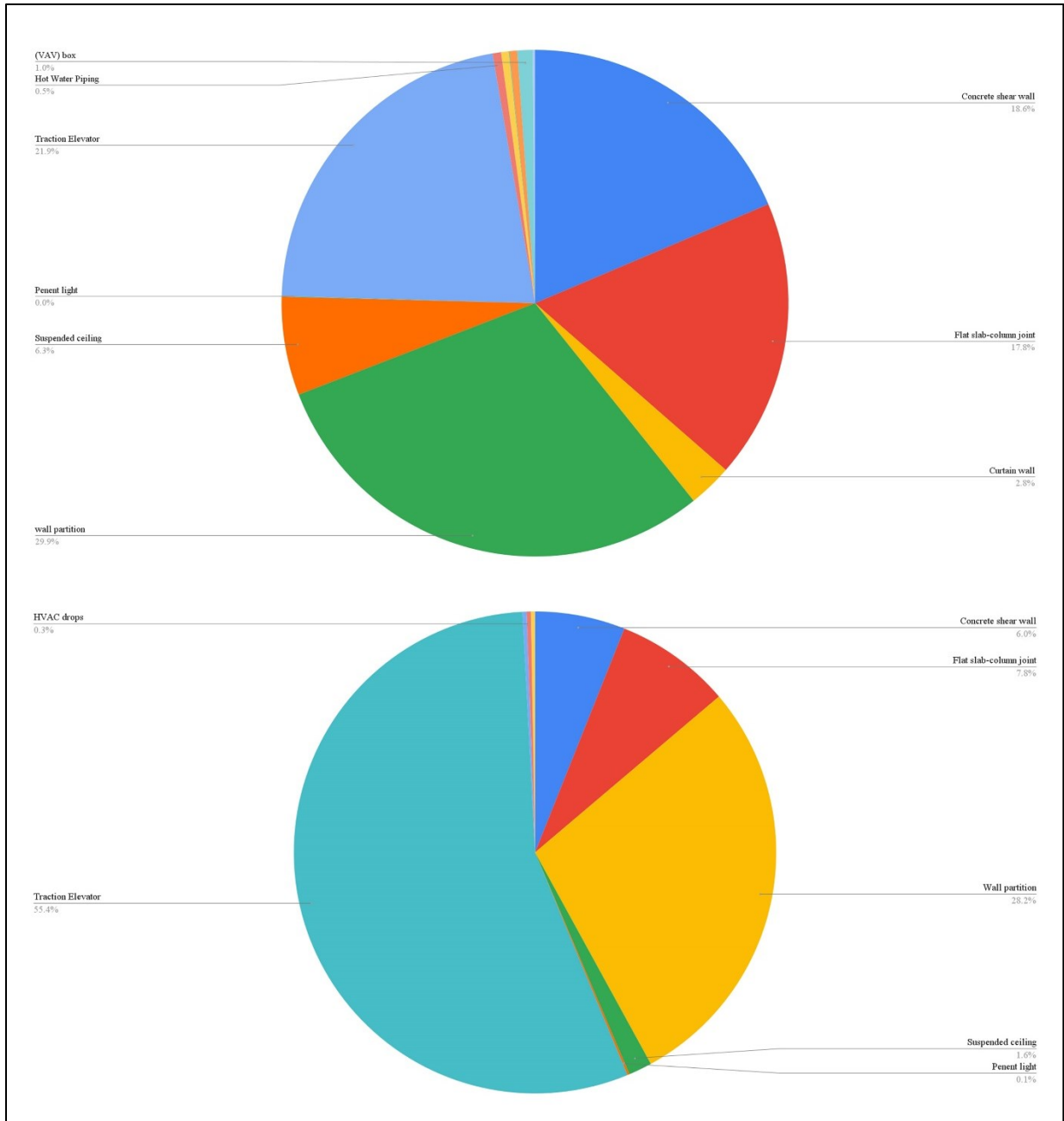


Figure 4. 41. Decomposition of the total repair cost in the 90th percentile: model-based approach (top), nonmodel-based approach (bottom)

4.5.2 Loss data visualization Dynamo algorithms (results)

With respect to the sorted loss data of EV building in the relational database, the loss data visualization Dynamo algorithms are employed to visualize them over the highly detailed spatial model in color code fashions. Therefore, initially, with the intention of visualizing the categories of components with the most contribution to the induced loss in terms of repair cost and repair time, Algorithm “FGVT” is performed over the 3D model of EV building. This process is demonstrated for the estimated repair cost and repair time at the 50th percentile (median) derived from the seismic analysis with the model-based approach. For this purpose, initially, all the required information about the most vulnerable categories of components for the 50th percentile, including category code (based on UNIFORMAT II) along with the corresponding estimated repair cost and repair time are automatically, extracted in Dynamo from the corresponding template at the relational database. The aforementioned information is provided in Table 4.10. Figure 4.42 shows the inputting process of repair cost and repair time of the most vulnerable categories of components (at the 50th percentile) from the relational database through the algorithm “FGVT”, adopted for the BIM-based loss data visualization.

Category code	Category name	Repair cost (CAD)	Repair time (Days)	Presented color in PACT software
D1014.011	Traction Elevator	660370.00	669	Brown
C3011.002a	Wall partition	221191.00	206	Blue
C3011.001a	Wall partition	71401.00	67	Yellow

Table 4. 10. The obtained repair cost and repair time (loss data) of the most vulnerable categories of components (at the 50th percentile) for EV building

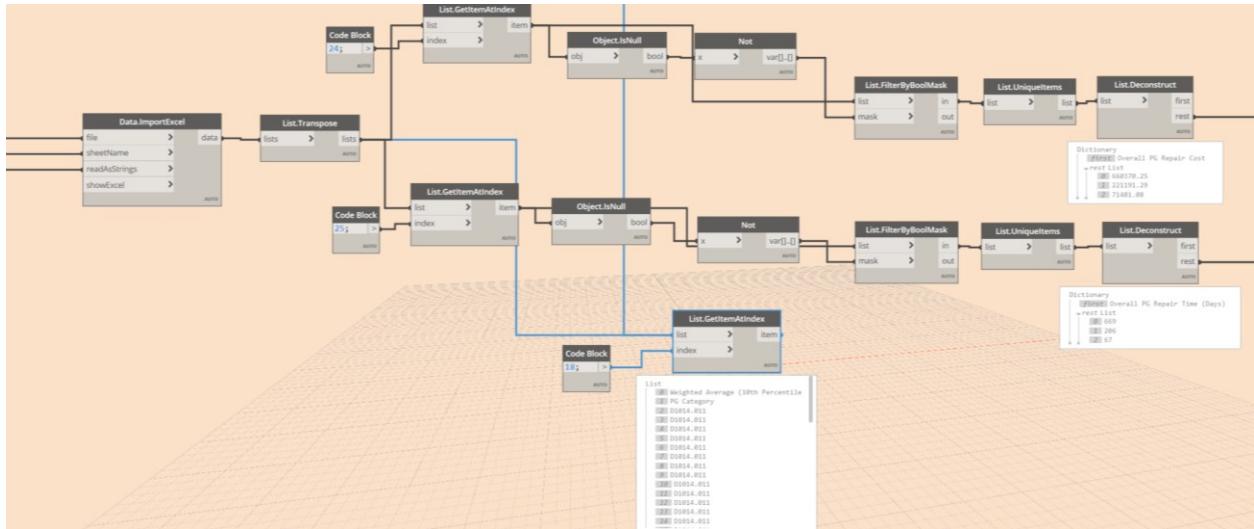


Figure 4. 42. The inputting process of repair cost and repair time of the most vulnerable categories of components of EV building (at the 50th percentile)

Next, the developed Dynamo script automatically selects and sorts all the components in the BIM model, having the matched category codes with the inputted loss data from the corresponding template (Figure 4.43).

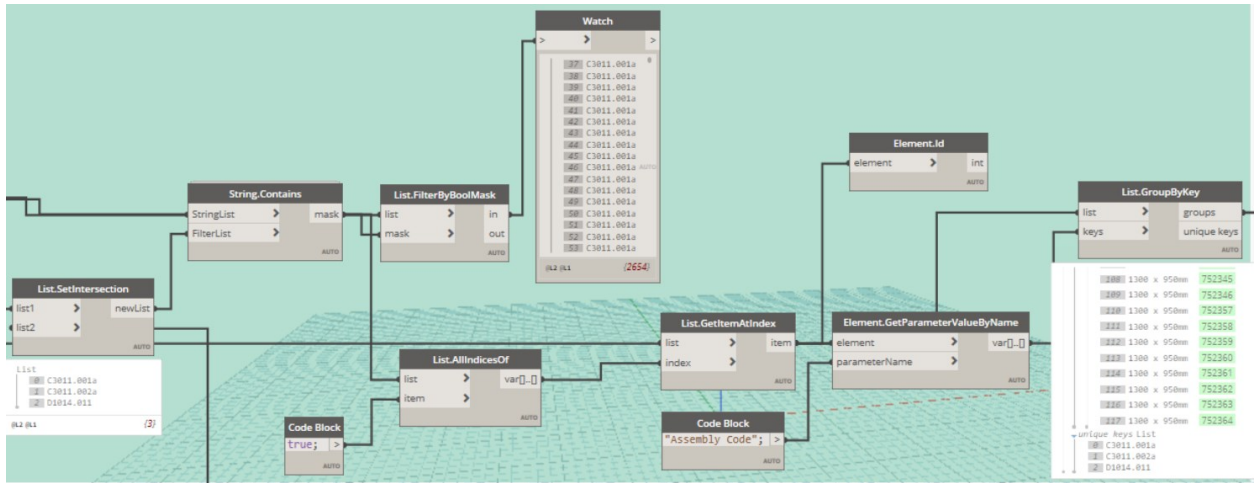


Figure 4. 43. Automatic selection of the vulnerable groups of components in EV building, based on the matched category codes with the inputted loss (at the 50th percentile)

Finally, all the identified components associated with the matched category codes in the entire building are assigned with the corresponding repair cost and repair time of their corresponding category. Furthermore, each group of components with the common category is color coded based

on the same color fashion presented in PACT software at 50th percentile (Figure 4.44). It is noteworthy to mention that the same visualization procedure is repeated for all the templates representing different percentiles (10th, 50th and 90th) with different approaches (model-based and nonmodel-based).

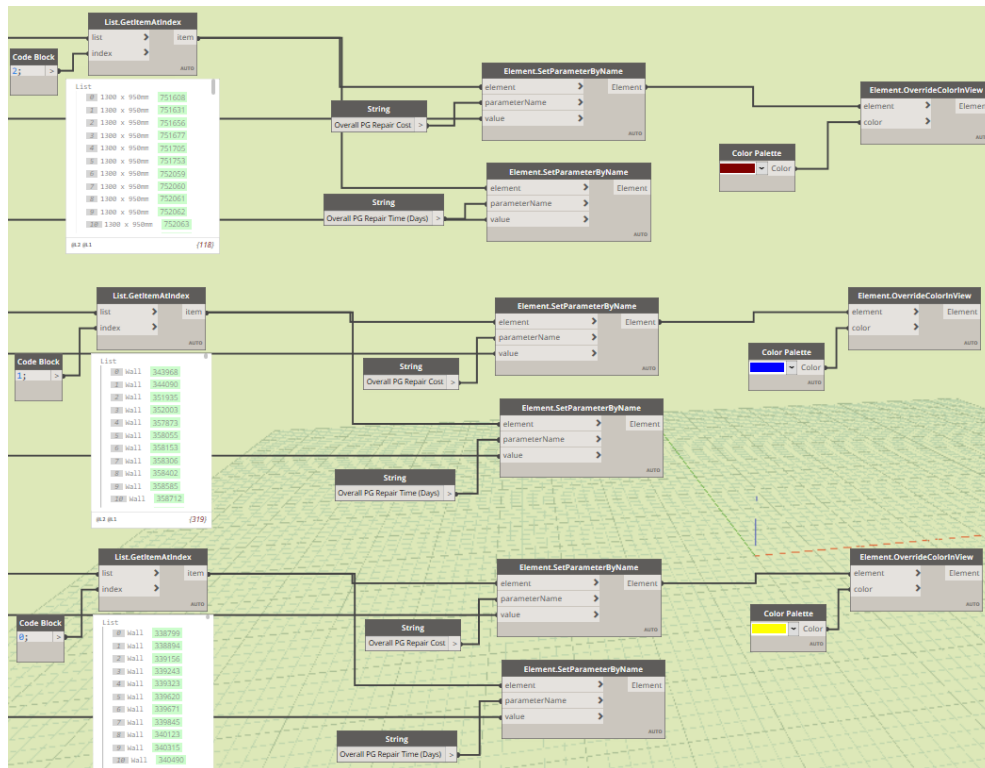


Figure 4.44. The automatic assignment process of the vulnerable groups of components in EV building with the corresponding obtained repair cost, repair time and color code (at the 50th percentile)

Figure 4.45 to Figure 4.47 show the most contributed vulnerable categories of components for the 50th percentile along with the corresponding estimated repair cost and repair time.

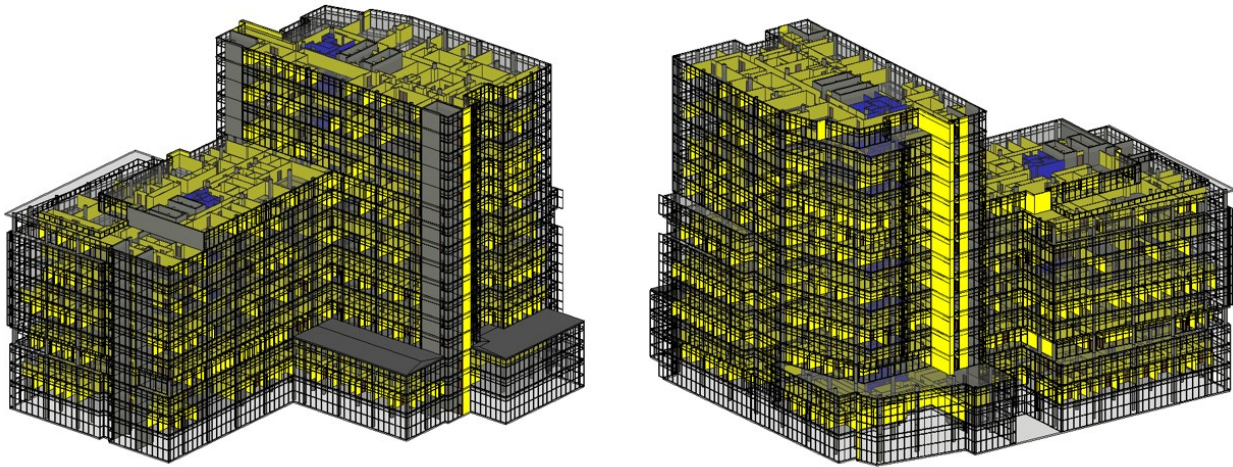


Figure 4. 45. The most contributed vulnerable categories of components of EV building (at the 50th percentile)

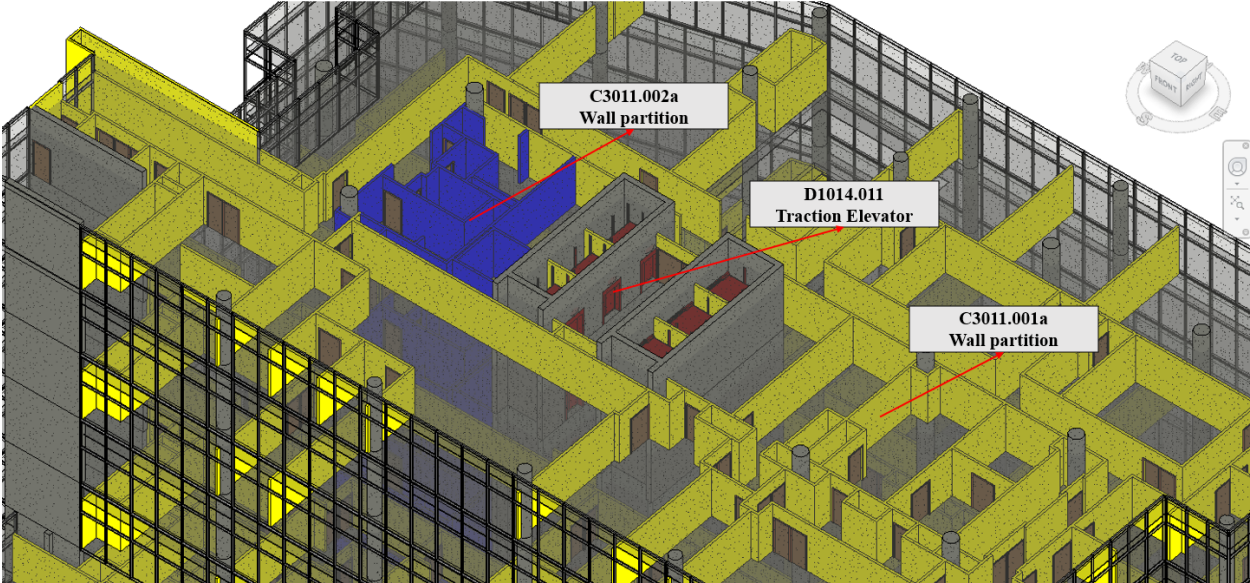


Figure 4. 46. The most contributed vulnerable categories of components of EV building (at the 50th percentile): traction elevator (D1014.011), wall partition (C3011.002a) and wall partition (C3011.001a)

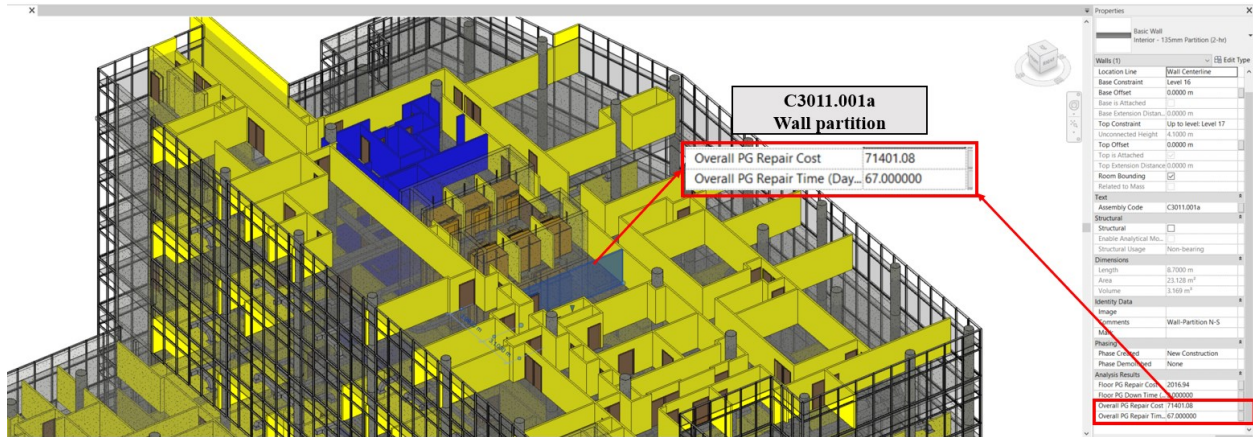


Figure 4. 47. The most contributed vulnerable categories of components of EV building (at the 50th percentile) along with the corresponding estimated repair cost and repair time

Moreover, to bring the loss data visualization to the next level, where the corresponding group of components of particular categories throughout different stories are automatically mapped and assigned with the distributed induced loss data, Algorithm “PGVT” is employed. It is to be noted that the induced loss data refers to the estimated repair cost and repair time in this example. To demonstrate the practicality of the algorithm “PGVT” over the EV building BIM model, the loss data outcome of the 50th percentile (median) derived from the seismic analysis with the model-based approach is chosen to be visualized. For this purpose, initially, all the required information about the most vulnerable categories of components for the 50th percentile, including category code (based on UNIFORMAT II) along with the corresponding estimated repair cost and repair time of each group of components with a common category and level are automatically extracted in Dynamo from the corresponding template at the relational database. A key distinction between the input information between algorithm “FGVT” and algorithm “PGVT” is that, in algorithm “PGVT”, the repair cost and repair time of all the contributed group of components in different stories are provided per each identified category, whereas, in algorithm “FGVT” the total repair cost and repair time are provided for the identified categories with no further distribution. Figure 4.48 and Figure 4.49 show the input process of the distributed repair cost and repair time of the most vulnerable categories of components among all the stories (at the 50th percentile) from the database.

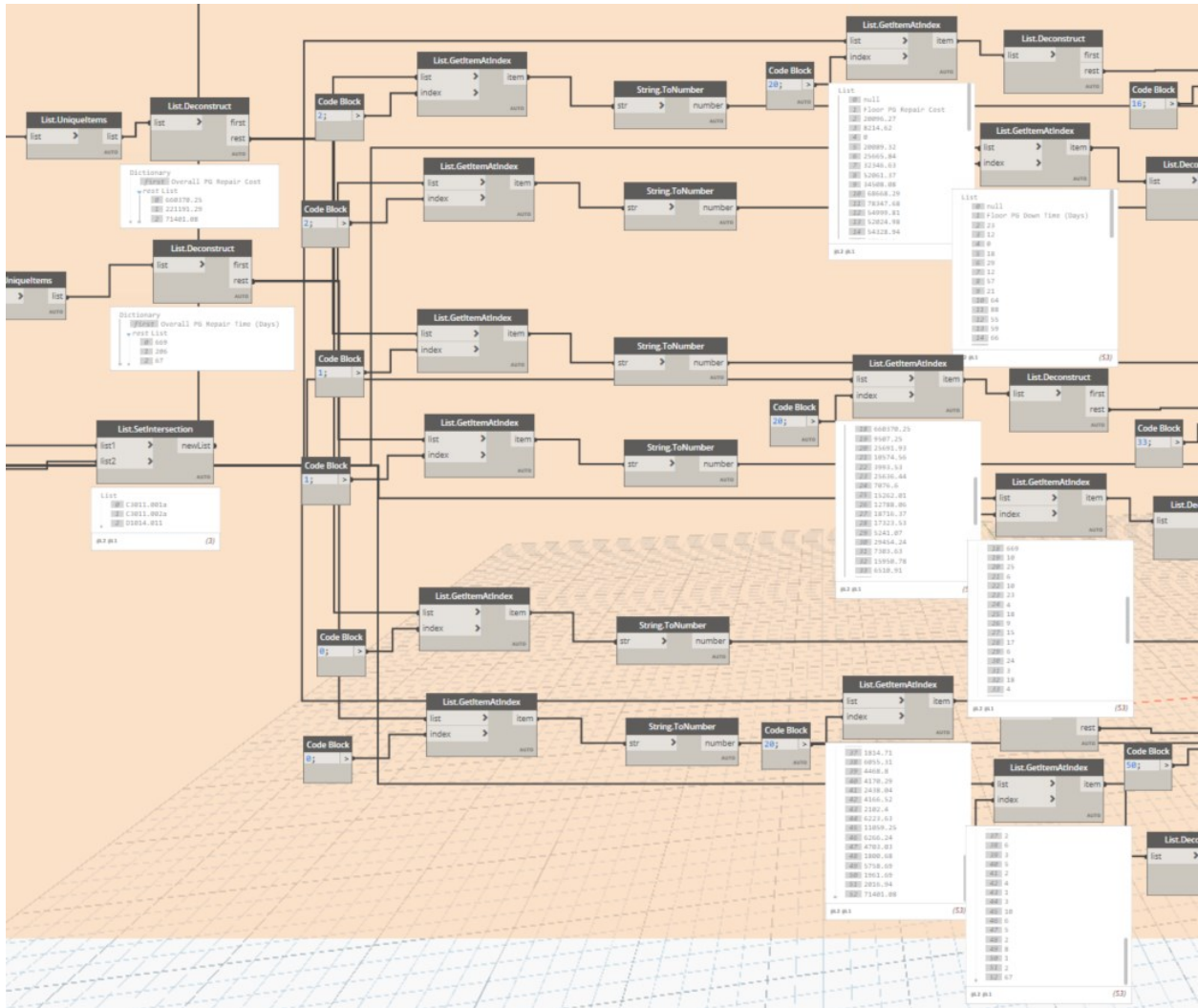


Figure 4. 48. the input process of the distributed repair cost and repair time of the most vulnerable categories of components among all the stories in EV building at the 50th percentile (code block module 1)

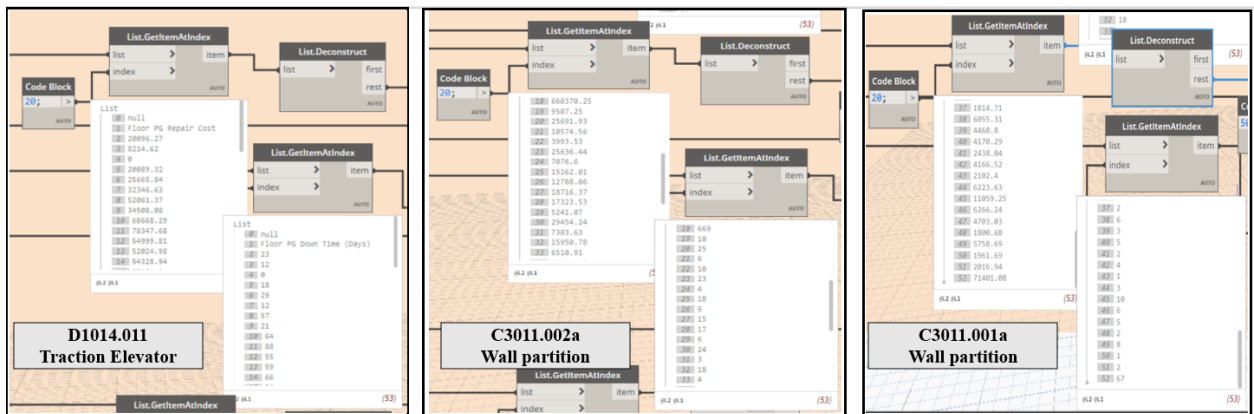


Figure 4. 49. The most vulnerable categories of components of EV building (at the 50th percentile): traction elevator (D1014.011), wall partition (C3011.002a) and wall partition (C3011.001a)

Similar to the aforementioned process in the algorithm “FGVT”, at this step, the developed Dynamo script automatically selects and sorts all the components in the BIM model, having the matched category codes with the inputted loss data from the corresponding template (Figure 4.50).

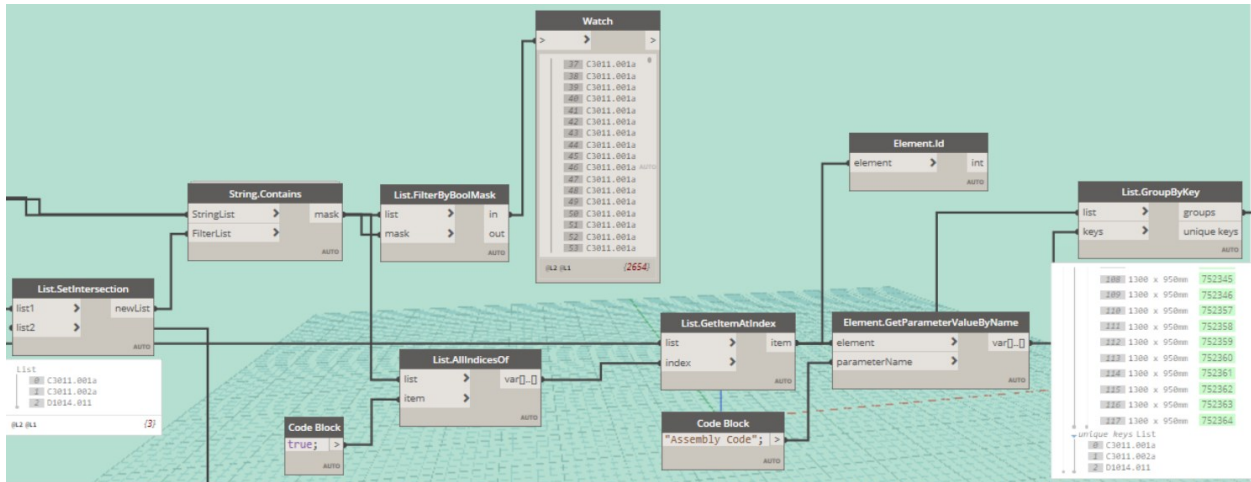


Figure 4. 50. Automatic selection of the vulnerable groups of components in EV building, based on the matched category codes with the inputted loss at the 50th percentile (code block module 2)

Subsequently, all the corresponding group of components of each category located at various stories of the building are automatically assigned with the corresponding repair cost and repairs time portions associated with their story. Figure 4.51 shows the assignment of the most vulnerable categories of components predicted at the 50th percentile with the corresponding repair cost and repair time at the 16th story. This information is also listed in Table 4.11.

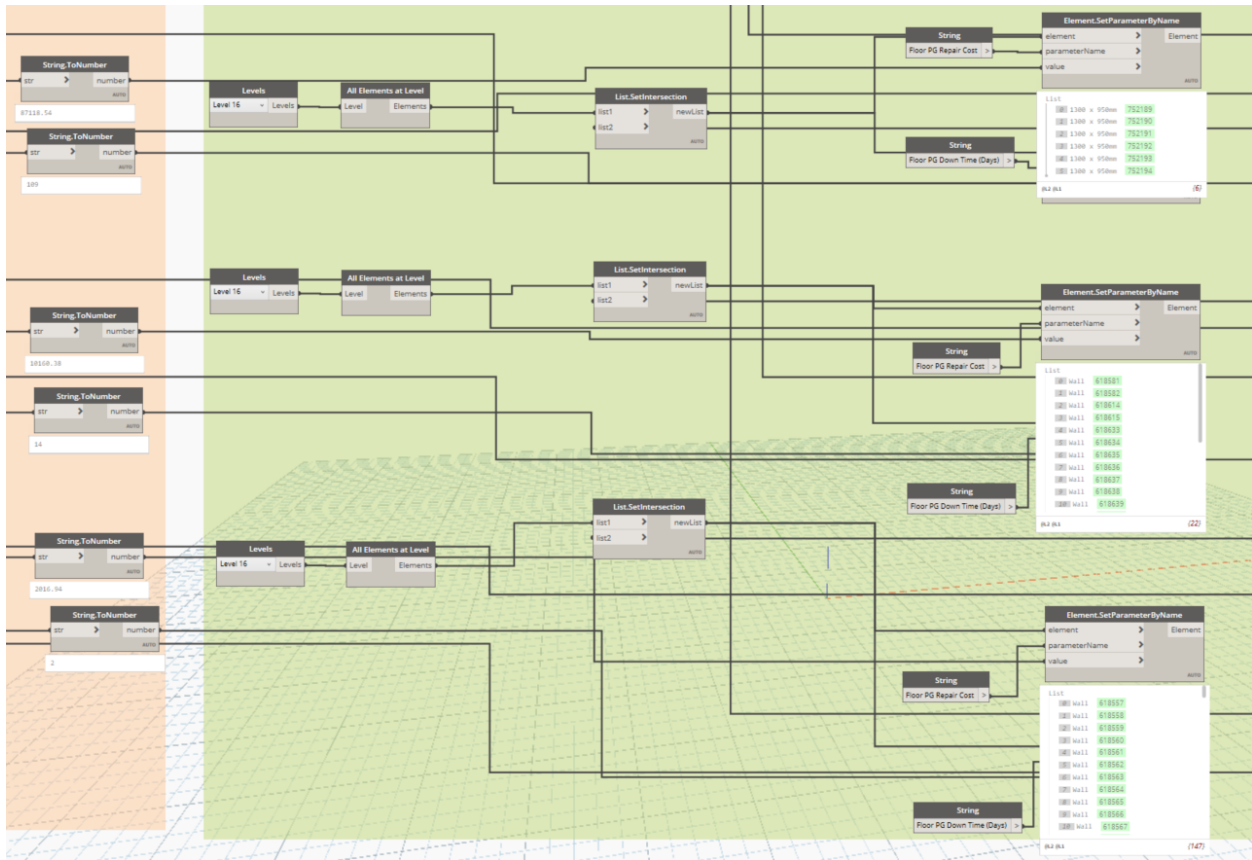


Figure 4. 51. Th automatic assignment process of the most vulnerable group of components of EV building (at the 50th percentile) with the corresponding repair cost and repair time portions associated with the 16th story (code block module 3)

Category code	Category name	Repair cost (CAD)	Repair time (Days)	Story Level
D1014.011	Traction Elevator	\$87118.54	109	16 th story
C3011.002a	Wall partition	\$10160.00	14	16 th story
C3011.001a	Wall partition	\$2016.00	2	16 th story

Table 4. 11. The most vulnerable group of components of EV building (at the 50th percentile) with the corresponding repair cost and repair time portions associated with the 16th story

Next, desired constrain functions are defined to first identify the repair cost and repair time of all the contributed group of components in different stories for all the selected categories. Then,

according to the distribution of all the repair costs or repair time, various ranges are automatically defined. It is also to be noted that, these ranges can be either limited to only a group of components under one specific category or it can be expanded to different categories simultaneously. Figure 4.452 shows the process of automatic range assignment between the identified vulnerable categories of components at the 50th percentile.

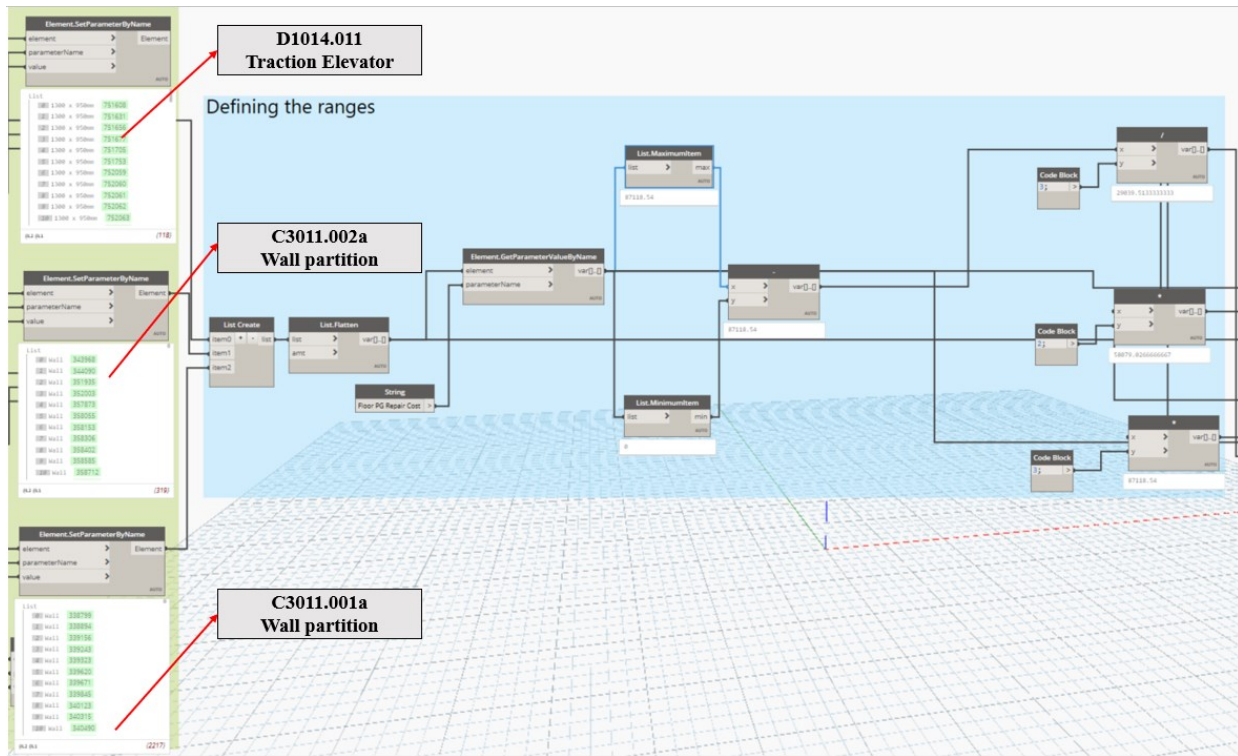


Figure 4.52. The automatic process of range identification between the considered vulnerable categories of components at the 50th percentile (code block module 4)

It can be seen that initially, the predicted repair costs of all the selected vulnerable components at the 50th percentile are automatically identified and then accordingly, four ranges of the repair costs are defined to cover all the repair costs. These ranges are provided in Table 4.12.

Range num	Range values (CAD)	Range color
1	Repair costs = 0	Green
2	0 < Repair costs < 29,039.51	Yellow
3	29,039.51 < Repair costs < 58,079.02	Orange
4	58,079.02 < Repair costs < 87,118.54	Red

Table 4. 12. Defined ranges of the predicted repair costs of the most vulnerable components of EV building (at the 50th percentile)

Finally, Dynamo, automatically, sorts and maps all the identified group of components among the corresponding pre-defined ranges based on the corresponding portion of repair cost or repair time at each story. Moreover, a color code scheme is also defined per each range corresponding to each percentile. However, in this example, the ranges are adjusted based on the estimated repair costs. Figure 4.53 shows the workflow of the assignment of the mapped group of components in various pre-defined ranges in Dynamo.

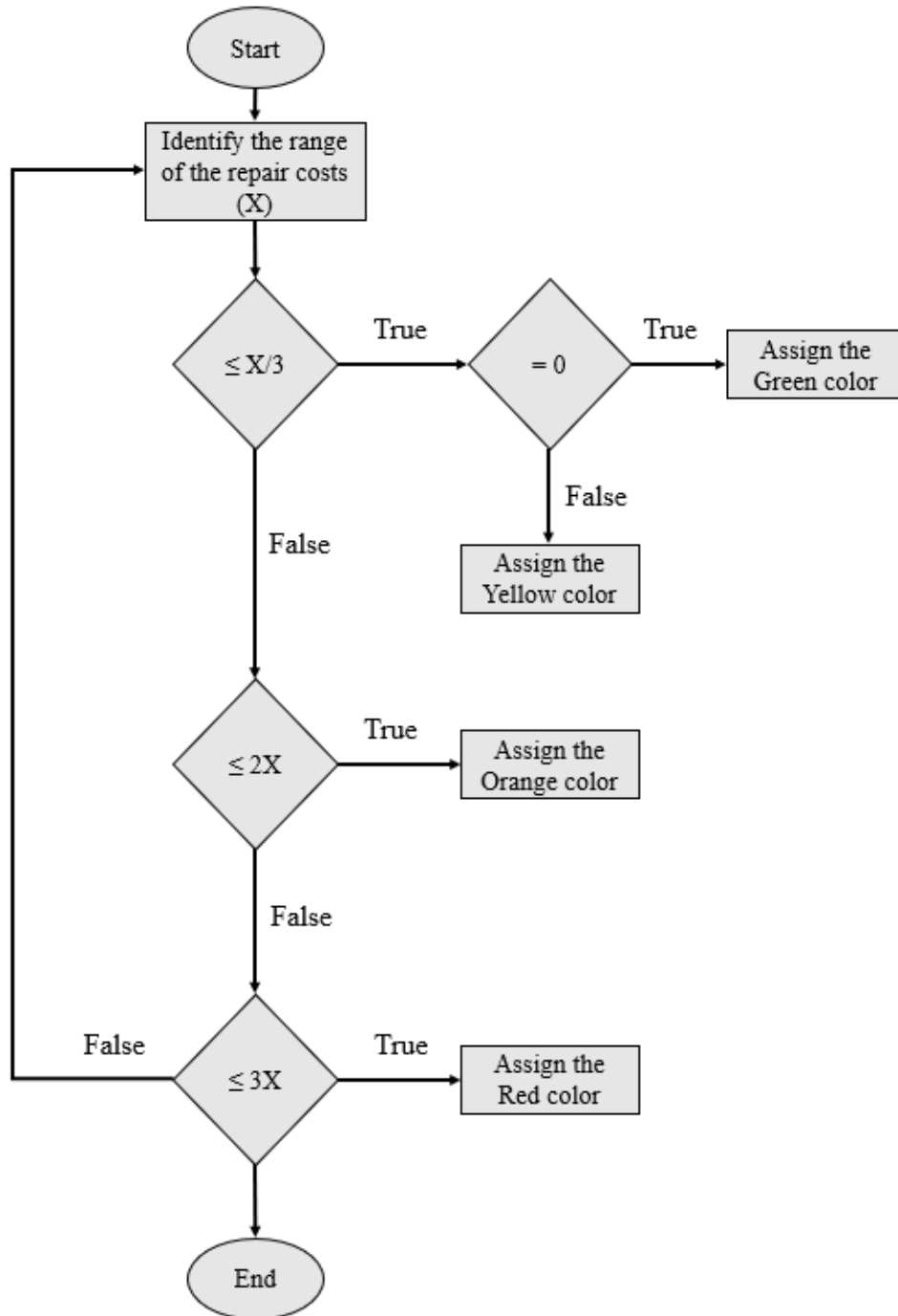


Figure 4. 53. the assignment workflow of the mapped groups of components of EV building in various pre-defined ranges adopted in code block module 5

Figure 4.54 shows the process of the automatic assignment of the mapped group of components in corresponding ranges through the code block module 5 of the algorithm “PGVT” of the BIM-based seismic loss visualization.

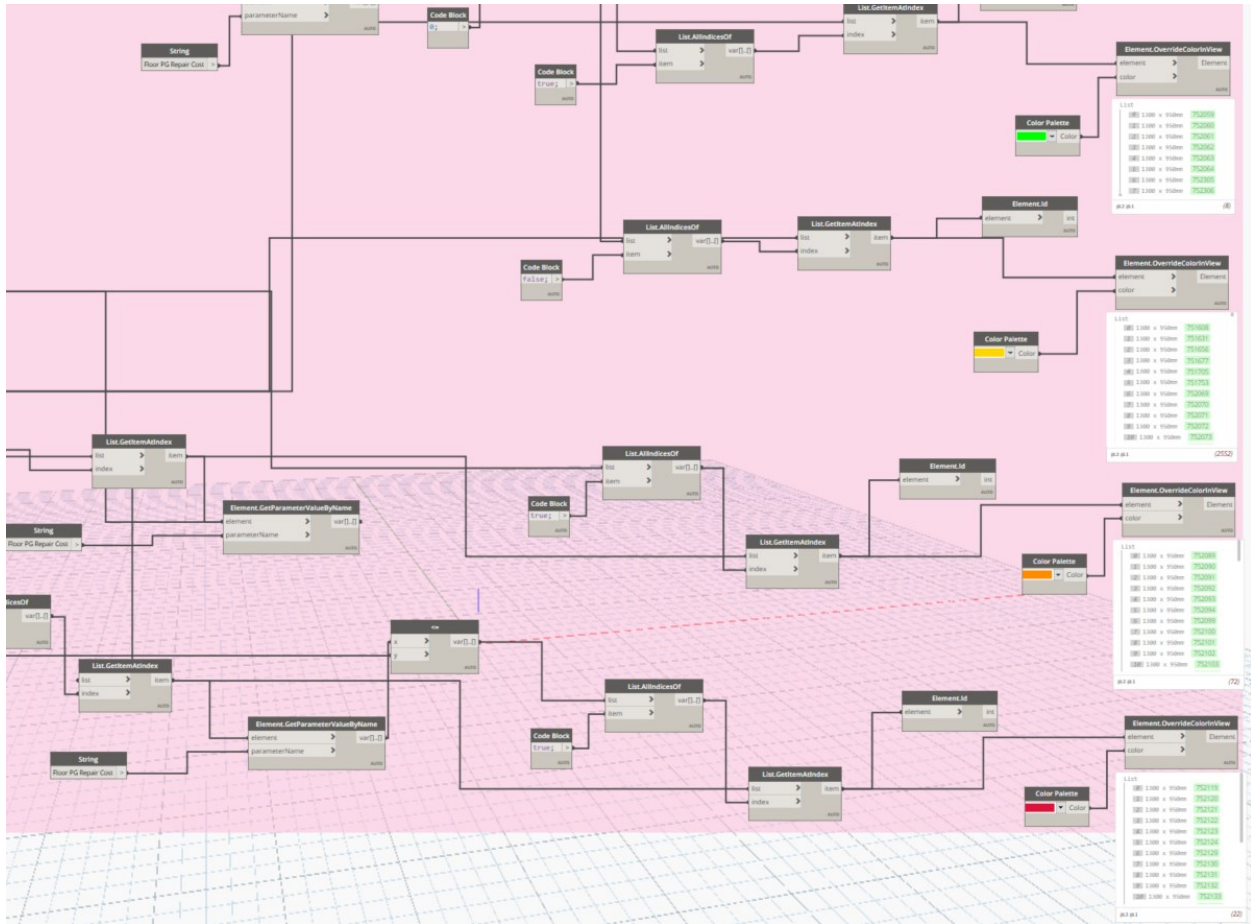
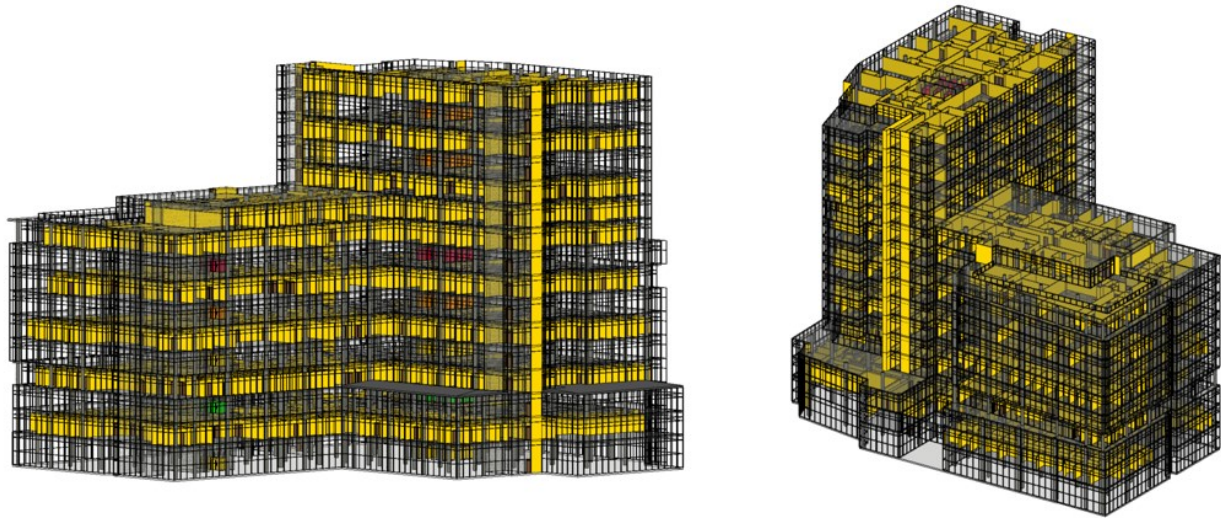


Figure 4. 54. the automatic assignment process of the mapped group of components of EV building in corresponding ranges through the code block module 5 of the algorithm “PGVT” (BIM-based seismic loss visualization)

Figure 4.55 and Figure 4.56 show the most contributed vulnerable group of components of EV building at the 50th percentile along with the corresponding estimated repair cost and repair time distributed among all the stories.



Ranges (CAD)	Color codes
Repair costs = 0	Green
0 < Repair costs < 29,039.51	Yellow
29,039.51 < Repair costs < 58,079.02	Orange
58,079.02 < Repair costs < 87,118.54	Red

Figure 4. 55. An overview of the most contributed vulnerable group of components of EV building at the 50th percentile, sorted by the corresponding estimated repair cost between all the stories

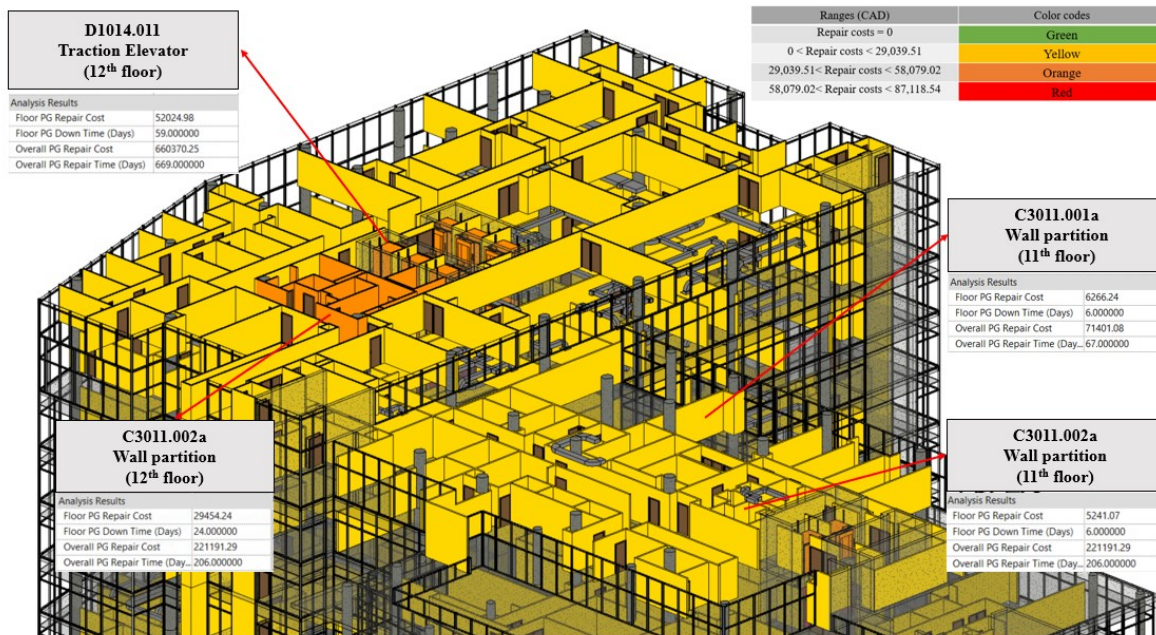


Figure 4. 56. Another view of the most contributed vulnerable group of components of EV building at the 50th percentile with the corresponding estimated repair cost and repair time at different stories

Also, it is noteworthy to mention that these ranges can be also limited to only groups of components with the common category rather than including all the vulnerable categories. Figure 4.57 shows the visualized distribution of the estimated repair costs only for the Traction elevators.

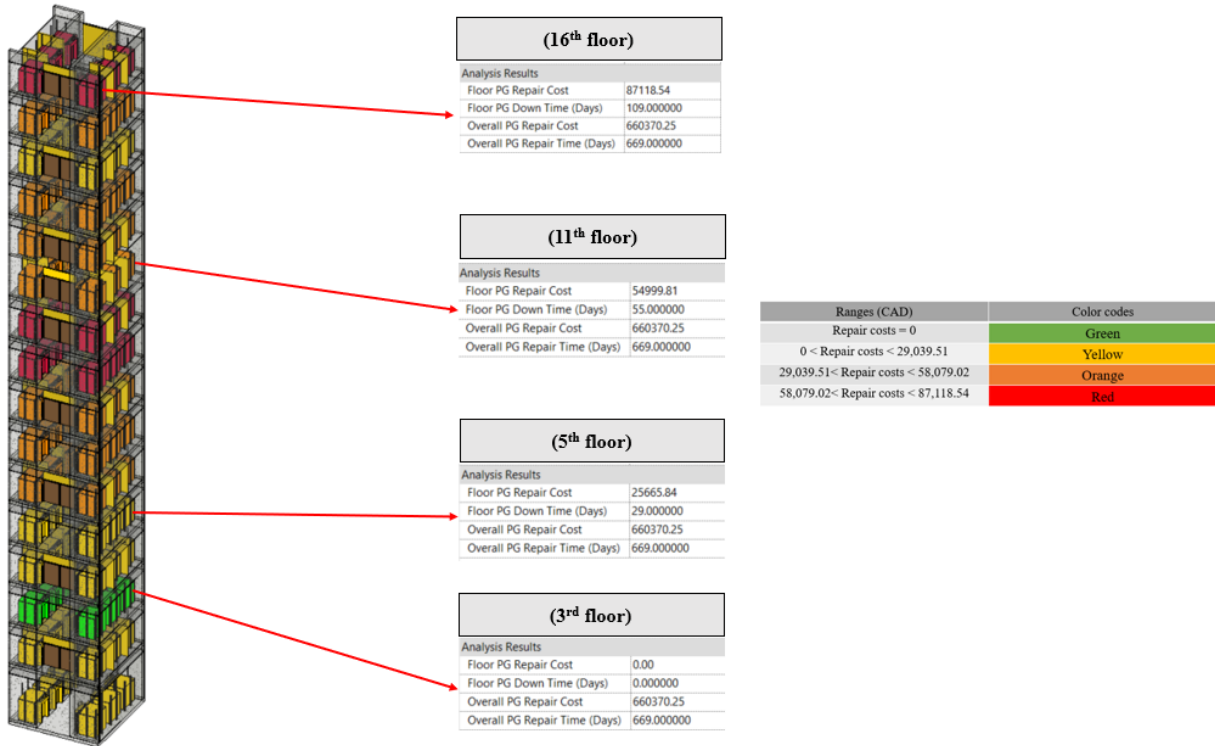


Figure 4. 57. An overview of the Traction elevators of EV building at the 50th percentile, sorted by the corresponding estimated repair cost between all the stories

4.6 Summary

This chapter investigated the rationality of the proposed methodology through a case study analysis with detailed examination over the 16-storey Engineering and Visual arts (EV Building) complex of Concordia University located in Montreal, Canada. Considering the outcome of the seismic loss analyses, it was verified that the proposed systematic methodology can be an efficient framework to determine and translate the actual seismic performance of buildings into potential damage, loss and corresponding performance metrics (such as repair cost and repair time), based on FEMA P-58 procedure. Utilizing innovative technologies such as seismic instrumentation of buildings and

integrated BIM tools in PBEE loss assessment frameworks were fully demonstrated through the proposed case study under the two main approaches of the model-based and nonmodel-based. Estimating the loss consequence predications of the building through the adoption of the model-based and nonmodel-based approaches, demonstrated the comparison and correlation of the proposed approaches. Moreover, it was also, proved that the BIM-based API tools can have a major role in the automation and enhancement of the PBEE-based seismic loss assessment frameworks.

By adopting (EV Building) complex of Concordia University as the case study of the proposed framework, it was found that at the given intensity of MCE, regardless of the adopted approach, the dominant induced-damage and loss could cause by the non-structural components rather than the structural components. While the majority of the vulnerable non-structural components among all the identified percentiles were the traction elevators and the wall partitions, the concrete shear walls and the flat slab-column joints were the most contributed among the structural components.

CHAPTER 5 Summary and Conclusions

5.1 Summary

Review of the literature on PBEE-based loss assessment frameworks indicated that the current generation framework, PEER-PBEE (Also known as FEMA P-58) provides the capability to predict the seismic loss estimation of buildings in terms of repair cost, downtime, and other decision variables. However, despite its many advantages, the lack of accurate structural performance characteristics (structural analysis) and ineffective details of the building components (damage analysis) are largely, affecting the application of the FEMA P-58 framework, and the quality of the results suffers from significant sources of uncertainties. For this purpose, employing innovative technologies such as seismic instrumentation and integrated BIM tools are suggested in literature to overcome the caused uncertainties in structural and damage analysis of the FEMA P-58 framework, respectively. However, yet, no comprehensive systematic methodology has been developed and demonstrated with the employment of seismic instrumentation and integrated BIM tools in PBEE-based loss assessment frameworks.

This thesis aimed to develop a systematic methodology to address some limitations of a refined PBEE-based loss assessment framework, PEER-PBEE, by employing innovative technologies such as, seismic instrumentation of buildings and integrated BIM tools. For this purpose, a workflow of seismic loss estimation was developed for buildings, where initially, the operational modal analysis was conducted to experimentally obtain the actual performance characteristics of the structure through the measurement of structural dynamic response (ambient vibration test) as well as subsequent output-only system identification. Next, by employing the derived structural performance characteristics into experimental structural analysis, refined structural response parameters were computed. The structural response parameters were then, utilized in the seismic loss analysis based on FEMA P-58 framework to estimate the loss consequence predications of the building into appropriate performance metrics such as economic losses, downtime and other decision variables. Finally, a loss data visualization algorithm was developed and implemented in Dynamo Studio in Autodesk Revit software program (BIM software) to visualize the predicated loss data in a more understandable fashion with a color-coding scheme. It is noteworthy to mention that two different methodological approaches (model-based and nonmodel-based) were developed

for the experimental structural analysis. The key difference between the model-based and nonmodel-based approach is the manner to compute the structural response parameters (also known as EDPs); the model-based approach uses finite element model (FEM), while the nonmodel-based approach is FEM free and is developed through a BIM-based API tool in Dynamo Studio. The functionality of the proposed systematic methodology is validated in the case study analysis over a building located in Montreal, Canada.

A real case study analysis was performed over the 16-storey Engineering and Visual arts (EV Building) complex of Concordia University. In this case study analysis, the following main steps were taken: (1) the data from an operational modal analysis, conducted earlier over the EV building, where the actual performance characteristics of the structure were obtained through the ambient vibration test and subsequent output-only system identification (i.e. using Frequency Domain Decomposition (FDD) technique) were harvested and processed; (2) the extracted structural performance characteristics were used in the experimental structural analysis (by both the model-based and nonmodel-based approaches) to obtain refined structural response parameters; (3) the seismic loss analysis based on FEMA P-58 framework was conducted to estimate the loss consequence predications of the building in terms of repair cost and repair time; (4) the predicted loss data of the building was visualized and interpreted by the loss data 3D visualization algorithm, developed in Dynamo Studio in Autodesk Revit software program (BIM software). Overall, the outcome of the proposed seismic loss analysis framework over the EV building, indicates a slight level of damage, including in both the structural and non-structural components of the building. Moreover, 10th, 50th and 90th percentile values (90%, 50% and 10% chances of exceedance, respectively) from the cumulative loss distribution of repair cost and repair time, are benchmarked in this study for the further decision-making process.

5.2 Contributions

The aim of this research was to develop a systematic methodology to mitigate the current limitations of PEER-PBEE loss assessment framework by employing innovative technologies such as seismic instrumentation of buildings and integrated BIM tools. Following are the project's objectives and contributions to achieve this goal:

(1): Identifying the real structural performance characteristics of a building based on the operational modal analysis (RO 1): acquiring accurate structural performance characteristics of buildings is essential to reduce the sources of uncertainties associated with the structural analysis in PBEE-based loss assessment frameworks. Although, employing seismic instrumentation of buildings is a practical solution towards achieving this goal, but critical challenges such as performing proper ambient vibration test and subsequent modal properties extraction exist within this procedure. For this purpose, an efficient operational modal analysis workflow is developed in this study, that collects the real structural performance characteristics required for the proposed seismic loss analysis. This workflow contains, performing the ambient vibration test with limited number of sensors as well as subsequent output-only system identification using the most common technique in frequency domain called, Frequency Domain Decomposition (FDD).

(2): Developing an experimental structural analysis workflow based on the model-based approach (RO 2): employing the actual structural performance characteristics of a building into the experimental structural analysis can result in obtaining the refined structural response parameters. Moreover, it could reduce the sources of uncertainties associated with the structural analysis in PBEE-based loss assessment frameworks as well. For this purpose, a workflow of experimental structural analysis based on model-based approach, including FE model calibration and nonlinear time history analysis is developed in this study, to obtain the refined structural response parameters required for the proposed seismic loss analysis.

(3): Developing an experimental structural analysis workflow based on the nonmodel-based approach (RO 3): Obtaining the structural response parameters from the nonmodel-based approaches is becoming a frequently discussed topic (i.e. utilizing ambient vibration monitoring data to predict the structural response parameters of a building without the use of FE models). For this purpose, a simplified three-dimensional response spectrum modal analysis is developed in this study, that uses the experimentally, obtained structural performance characteristics of the building (from the operational modal analysis) to compute the refined structural response parameters required for the proposed seismic loss analysis. The major advantage of this method compared to the procedure adopted in the model-based approach is to be free of FE modeling.

(4): Automating the simplified three-dimensional response spectrum modal analysis through the BIM-based API tool (RO 4): Although BIM adoption has been significantly increased in the AEC industry, however very limited research has been dedicated to the development of the BIM-enabled tools by using API. Developing BIM-based API tools can be a great step towards automating the associated workflows in the proposed seismic loss analysis framework such as experimental structural analysis. For this purpose, a combination of the BIM-based API tool and a relational database is developed in this study, to automate the application of the nonmodel-based experimental structural analysis (i.e. the simplified three-dimensional response spectrum modal analysis). The BIM-based API tool refers to the set of algorithms developed in Dynamo Studio in Autodesk Revit software program (BIM software).

(5): Performing the seismic loss analysis based on FEMA P-58 framework using the refined structural response parameters from the adopted approaches (model-based and nonmodel-based) (RO 5): with respect to the employment of the refined structural response parameters, the seismic loss analysis is integrated with both the model-based and nonmodel-based approaches. The result in this study shows the compatibility of the predicted loss data between both the adopted approaches, while different methods are employed in obtaining the structural response parameters. Model-based approach utilizes nonlinear time history analysis, whereas nonmodel-based approach uses response spectrum modal analysis. Also, it is to be noted, that PACT software (provided by FEMA P-58 framework) is utilized to perform the seismic loss analysis, which leads to the formation of the cumulative loss distribution of repair cost and repair time. Finally, 10th, 50th and 90th percentiles (90%, 50% and 10% chances of exceedance, respectively) are benchmarked in this study to cover the most range of typical acceptance criteria.

(6): Automating the predicted loss data visualization through the BIM-based API tool (RO 6): A combination of the BIM-based API tool with a relational database is developed in this study to extract, collect, and visualize the predicted loss data from the performed seismic loss analysis based on FEMA P-58 procedure. The BIM-based API tool is developed in Dynamo Studio with two different visualization strategies, where the predicted loss data can be visualized and interpreted in a more understandable fashion (color code scheme). More information regarding the visualization strategies can be found in “Chapter 3 Methodology).

5.3 Conclusions

The following conclusions are reached based on the work given in the research.

- With respect to the process of obtaining refined structural response parameters for the proposed seismic loss analysis, two main workflows of experimental structural analysis, model-based and nonmodel-based were developed. Adopting (EV Building) complex of Concordia University as the case study of the proposed framework, proved that the range of the computed EDPs from both the approaches are reasonably compatible. However, due to the fact that, the nonmodel-based workflow did not take into account the nonlinear relations, the model-based workflow resulted in a wider range of the EDPs compared to the nonmodel-based workflow.
- The generated cumulative loss distribution of repair cost and repair time from the performed seismic loss analysis based on FEMA P-58 framework, demonstrated the impact of the adopted approach (model-based and nonmodel-based) over the quality of the results. In the other words, adopting the nonmodel-based approach in the case of EV building led to the generation of relatively more packed and focused percentiles close to the 90th percentile, whereas in the model-based approach, notable distance was evident among the 10th, 50th and 90th percentiles. Therefore, the distribution of the total repair costs and repair time in the model-based approach were reasonably more widespread compared to the nonmodel-based approach.
- With respect to the nonmodel-based experimental structural analysis, a combination of the developed Dynamo algorithms, called “SMMIC” and “MSOT” with the formulated relational database are integrated to perform the simplified three-dimensional experimental response spectrum modal analysis and provide the desired EDPs as its final product. The functionality of the developed Dynamo scripts employed in the nonmodel-based approach was proved through the case study of EV building.
- To ease the decision-making process for the engineers and non-engineers, another combination of the developed Dynamo algorithms, called “FGVT” and “PGVT” with the

relational database are employed to visualize the predicted performance measures such as repair cost and repair time with different complementary strategies. The case study over EV building was an appropriate example to demonstrate the capability of the developed Dynamo scripts in collecting, sorting, mapping, and visualizing the induced-loss data over the highly detailed spatial model in color-coding schemes.

5.4 Limitations and future work

The main purpose of this section is to highlight the limitations that are identified throughout the present research. These limitations are worthy of the future investigations and are listed as following:

- (1) An efficient operational modal analysis workflow is developed in this study to collect the real structural performance characteristics required for the proposed seismic loss analysis. This workflow contains, performing the ambient vibration test as well as the subsequent output-only system identification using FDD method. However, more advanced methods of system identification techniques such as parametric method (Time Domain) and Time-Frequency Analysis can be adopted to enhance the reliability of the extracted structural performance characteristics of structures as future studies.
- (2) With respect to the proposed model-based experimental structural analysis workflow, iterative process for FE model updating is utilized to calibrate the FE model based on the derived structural performance characteristics from the operational modal analysis. However, more advanced FE model updating techniques such as hybrid model updating technique and Artificial Neural Networks (ANN) can be adopted in future studies.
- (3) Nonlinear time history analysis is utilized in the model-based experimental structural analysis to obtain the structural response parameters. However, only material nonlinearities are taken into account in the performed structural analysis. Therefore, to enhance the quality of the nonlinear time history analysis, geometric nonlinearities as well as further modification over the structural connections can be adopted.

- (4) With respect to the proposed nonmodel-based experimental structural analysis workflow, the simplified three-dimensional response spectrum modal analysis is developed to obtain the required structural response parameters for the seismic loss analysis. Although, the main advantage of this method is to perform the structural analysis without using the FE models, however, only one set of structural response parameters (also known as EDPs) required for the subsequent seismic loss analysis can be extracted from this method. Considering this, only simplified (linear) analysis type can be utilized to perform the loss analysis in PACT software. However, to obtain various sets of EDPs which, consequently, leads to the enhancement of the proposed seismic loss analysis, nonlinear time history analysis is recommended to be used. Therefore, the simplified three-dimensional response spectrum modal analysis can be upgraded into the nonlinear time history analysis using the nonmodel-based approach (i.e. free of FE modeling techniques).
- (5) A real case study analysis is provided in this study over the 16-storey Engineering and Visual arts (EV Building) complex of Concordia University which validates the functionality of both the proposed model-based and nonmodel-based approaches. However, to demonstrate an approximation of how much each approach can contribute to the improvement of the associated sources of uncertainties with structural analysis, sensitivity analysis with more real case studies has to be conducted.
- (6) With respect to the proposed seismic loss analysis based on FEMA P-58 framework, fragility specifications based on the FEMA P-58 extensive database are utilized in this study to identify the probable physical damage associated with each category of the vulnerable components in a building. Although this database contains so many categories of the existing vulnerable structural and non-structural components, however, yet so many categories might be existing in the loss analysis that the provided fragility curves by the FEMA P-58 database could not be a great match for them. Therefore, utilizing more accurate and comprehensive database of the fragility specifications can certainly increase the quality of the proposed seismic loss analysis.

- (7) With regards to the proposed seismic loss analysis, the occurrence of the potential collapses and residual drifts are not considered in this study. Consequently, the extracted performance measures of this seismic loss analysis are only given in the form of repair cost and repair time. However, to provide more performance measures such as potential fatalities, injuries and risk of building closure correspond to the identified collapse modes, developing collapse fragility curves by incremental dynamic analysis (IDA) can be investigated.
- (8) Two different BIM-based API tools are developed in this study to perform the nonmodel-based experimental structural analysis and visualizing the predicted loss data, respectively. Although the BIM-based API tools has enhanced the automation of these two workflows in the proposed seismic loss assessment framework, however, yet so many manual operations are associated with the other workflows such as model-based experimental structural analysis in this framework. Therefore, developing a fully adopted BIM-based API which can perform all the proposed workflows in this framework is to be investigated.

CHAPTER 6 References

References

Anon 2021. *FEMA P-58*. [online] Available at: <<https://femap58.atcouncil.org/>> [Accessed 8 Mar. 2021].

Anon 2021. *Sensequake Larzé*. [online] Available at: <<https://www.sensequake.com/larze>> [Accessed 9 Jan. 2021].

Atkinson, G.M. and Goda, K., 2011. Effects of seismicity models and new ground-motion prediction equations on seismic hazard assessment for four Canadian cities. *Bulletin of the Seismological Society of America*, 101(1), pp.176–189.

Bagchi, A., 2005. Updating the mathematical model of a structure using vibration data. *Journal of Vibration and Control*, 11(12), pp.1469–1486.

Bahmanoo, S., Bagchi, S., Sabamehr, A. and Bagchi, A., 2021. Seismic loss analysis of Buildings using sensor-based measurements. 10th International Conference on Structural Health Monitoring of Intelligent Infrastructure. Porto, Portugal.

Bahmanoo, S., Valinejadshoubi, M., Sabamehr, A., Bagchi, A. and Bagchi, S., 2019. Enhancing the efficiency of structural condition assessment by integrating building information modeling (BIM) into vibration-based damage identification (VBDI). Proceedings of the 12th International Workshop on Structural Health Monitoring. .

BIMForum, 2020. *LOD Spec*.

Calvi, G.M., Sullivan, T. and Welch, D., 2014. A seismic performance classification framework to provide increased seismic resilience. In: *Perspectives on European earthquake engineering and seismology*. Springer, Cham.pp.361–400.

Çelebi, M., Sanli, A., Sinclair, M., Gallant, S. and Radulescu, D., 2003. Real-Time seismic monitoring needs of a building owner and the solution. Proceedings of 1st International Conference on Structural Health Monitoring and Intelligent Infrastructure, Tokyo, Japan, AA Balkema. pp.1011–1016.

Charette, R.P. and Marshall, H.E., 1999. *UNIFORMAT II elemental classification for building specifications, cost estimating, and cost analysis*. US Department of Commerce, Technology Administration, National Institute of

Christodoulou, S.E., Vamvatsikos, D. and Georgiou, C., 2010. A BIM-based framework for forecasting and visualizing seismic damage, cost and time to repair. In: *8th European Conference on Product and Process Modelling (ECCPM)*, Cork, Ireland.

- Cimellaro, G.P., Reinhorn, A.M. and Bruneau, M., 2006. Quantification of seismic resilience. Proceedings of the 8th US National conference on Earthquake Engineering. pp.1–10.
- Council, B.S.S., 1997. NEHRP guidelines for the seismic rehabilitation of buildings. *FEMA-273, Federal Emergency Management Agency, Washington, DC*, pp.2–12.
- Cremen, G. and Baker, J.W., 2018. Quantifying the benefits of building instruments to FEMA P-58 rapid post-earthquake damage and loss predictions. *Engineering Structures*, 176, pp.243–253.
- Eastman, C.M., Eastman, C., Teicholz, P., Sacks, R. and Liston, K., 2011. *BIM handbook: A guide to building information modeling for owners, managers, designers, engineers and contractors*. John Wiley & Sons.
- Extractor, Art., 1999. Structural vibration solutions. *Aalborg, Denmark*.
- Fajfar, P. and Krawinkler, H., 2004. Performance-based seismic design concepts and implementation. Proceedings of the International Workshop, Bled, Slovenia. pp.2004–05.
- FEMA, 2012. Seismic Performance Assessment of Buildings Volume 1-Methodology. *Rep. No. FEMA P-58-1. Federal Emergency Management Agency, Washington*.
- Filiatrault, A. and Sullivan, T., 2014. Performance-based seismic design of nonstructural building components: The next frontier of earthquake engineering. *Earthquake Engineering and Engineering Vibration*, 13(1), pp.17–46.
- Fischinger, M., 2014. *Performance-based seismic engineering: Vision for an earthquake resilient society*. Springer.
- Gulati, B., 2006. Earthquake risk assessment of buildings: applicability of HAZUS in Dehradun, India. ITC Enschede.
- Günay, S. and Mosalam, K.M., 2013. PEER performance-based earthquake engineering methodology, revisited. *Journal of Earthquake Engineering*, 17(6), pp.829–858.
- Hamburger, R., 2014. FEMA P-58 seismic performance assessment of buildings. Proc., 10th National Conf. in Earthquake Engineering, Earthquake Engineering Research Institute, Anchorage, AK. .
- Hazus, 2020. *HAZUS 4.2 SP3: Hazus Earthquake Model Technical Manual*.
- Hazus, M.H., 2011. *Multi-hazard loss estimation methodology: earthquake model hazus-MH MR5 technical manual*.
- Hong, Y., Hammad, A.W. and Akbarnezhad, A., 2019. Forecasting the net costs to organisations of Building Information Modelling (BIM) implementation at different levels of development (LOD). *ITcon*, 24, pp.588–603.

- Hwang, S.-H. and Lignos, D.G., 2018. Nonmodel-based framework for rapid seismic risk and loss assessment of instrumented steel buildings. *Engineering Structures*, 156, pp.417–432.
- Jin, Z. and Gambatese, J., 2019. Bim for temporary structures: Development of a revit api plugin for concrete formwork. In: *Proceedings of the CSCE Annual Conference Growing with Youth, Laval, QC, Canada*. pp.12–15.
- Kensek, K., 2014. Integration of Environmental Sensors with BIM: case studies using Arduino, Dynamo, and the Revit API.
- Kolarić, S., Mandičák, T., Vukomanović, M. and Mesároš, P., 2018. BIM training in construction management educational practices in Croatia and Slovakia. Creative Construction Conference 2018. Budapest University of Technology and Economics. pp.1002–1009.
- Lee, T.-H., 2005. *Probabilistic seismic evaluation of reinforced concrete structural components and systems*. University of California, Berkeley.
- Lim, C., 2016. Application of vibration-based techniques for modal identification and damage detection in structures.
- Lu, X. and Guan, H., 2017. *Earthquake disaster simulation of civil infrastructures*. Springer.
- Mewis, R., 2019. *Building Construction Costs With RSMeans Data 2020*. Means Building Construction Cost Data. [online] Gordian Group Incorporated. Available at: <<https://books.google.ca/books?id=6fJSzAEACAAJ>>.
- Mirshafiei, F., 2016. *A novel three-dimensional seismic assessment method (3D-SAM) for buildings based on ambient vibration testing*. McGill University (Canada).
- NATSPEC, 2013. Natspec bim paper nbp 001 bim and lod - building information modelling and level of development. [online] Available at: <https://bim.natspec.org/images/NATSPEC_Documents/NATSPEC_BIM_LOD_Paper_131115.pdf>.
- Oti, A.H., Tizani, W., Abanda, F., Jaly-Zada, A. and Tah, J., 2016. Structural sustainability appraisal in BIM. *Automation in Construction*, 69, pp.44–58.
- Parrott, B.C. and Bomba, M.B., 2010. delivery and building information modeling. *PCI journal*.
- Perrone, D. and Filiatrault, A., 2017. Automated seismic design of non-structural elements with building information modelling. *Automation in construction*, 84, pp.166–175.
- Ploeger, S., Atkinson, G. and Samson, C., 2010. Applying the HAZUS-MH software tool to assess seismic risk in downtown Ottawa, Canada. *Natural hazards*, 53(1), pp.1–20.
- Porter, K., Mitrani-Reiser, J. and Beck, J.L., 2006. Near-real-time loss estimation for instrumented buildings. *The Structural Design of Tall and Special Buildings*, 15(1), pp.3–20.

- Porter, K.A., 2003. An overview of PEER's performance-based earthquake engineering methodology. Proceedings of ninth international conference on applications of statistics and probability in civil engineering. pp.1–8.
- Porter, K.A., Beck, J.L. and Shaikhutdinov, R.V., 2002. Sensitivity of building loss estimates to major uncertain variables. *Earthquake Spectra*, 18(4), pp.719–743.
- Ranjbar, P.R. and Naderpour, H., 2020. Probabilistic evaluation of seismic resilience for typical vital buildings in terms of vulnerability curves. *Structures*. Elsevier.pp.314–323.
- Ren, W.-X. and Chen, H.-B., 2010. Finite element model updating in structural dynamics by using the response surface method. *Engineering structures*, 32(8), pp.2455–2465.
- Sabamehr, A., 2018. *Development of Efficient Vibration-based Techniques for Structural Health Monitoring*. PhD dissertation. Concordia University.
- Standard, I., 2010. ISO 29481-1: 2010 (E): Building Information Modeling-Information Delivery Manual-Part 1: Methodology and Format.
- Timir Baran Roy, Bagchi, S., Sabamehr, A. and Bagchi, A., 2019. Operational modal analysis of Concordia university EV building using ambient vibration response. Proceeding of the 7th International Congress on Computational Mechanics and Simulation. India.
- Uma, S., 2007. Seismic Instrumentation of Buildings-A promising step for performance based design in New Zealand. NZSEE conference proceedings. .
- Valinejadshoubi, M., Bagchi, A. and Moselhi, O., 2019. Development of a BIM-based data management system for structural health monitoring with application to modular buildings: Case study. *Journal of Computing in Civil Engineering*, 33(3), p.05019003.
- Wang, Y., Pejmanfar, S. and Tirca, L., 2019. Intensity-based performance assessment of middle-rise steel office buildings. Proceedings of the 12th Canadian Conference on Earthquake Engineering. Quebec.
- Xu, X., Ma, L. and Ding, L., 2014. A framework for BIM-enabled life-cycle information management of construction project. *International Journal of Advanced Robotic Systems*, 11(8), p.126.
- Xu, Z., Lu, X., Zeng, X., Xu, Y. and Li, Y., 2019a. Seismic loss assessment for buildings with various-LOD BIM data. *Advanced Engineering Informatics*, 39, pp.112–126.
- Xu, Z., Zhang, H., Lu, X., Xu, Y., Zhang, Z. and Li, Y., 2019b. A prediction method of building seismic loss based on BIM and FEMA P-58. *Automation in Construction*, 102, pp.245–257.
- Yang, T., Moehle, J., Stojadinovic, B. and Der Kiureghian, A., 2009. Seismic performance evaluation of facilities: Methodology and implementation. *Journal of Structural Engineering*, 135(10), pp.1146–1154.

Yang, X., Koehl, M. and Grussenmeyer, P., 2018. Automating Parametric Modelling From Reality-Based Data by Revit API Development.

Appendix A - Publications

Conference Papers

- **Bahmanoo, S.**, Bagchi, S., Sabamehr, A. and Bagchi, A., 2021. Seismic loss analysis of Buildings using sensor-based measurements. 10th International Conference on Structural Health Monitoring of Intelligent Infrastructure. Porto, Portugal (published).
- **Bahmanoo, S.**, Valinejadshoubi, M., Sabamehr, A., Bagchi, A. and Bagchi, S., 2019. Enhancing the efficiency of structural condition assessment by integrating building information modeling (BIM) into vibration-based damage identification (VBDDI). Proceedings of the 12th International Workshop on Structural Health Monitoring (published).

Journal Papers

- **Bahmanoo, S.**, Bagchi, A. “BIM-Based Seismic Loss Assessment For Instrumented Buildings”, Journal of Computing in Civil Engineering, ASCE (under preparation).

Awards

- MITACS Accelerate Fellowship in collaboration with Sensequake company and Concordia university, 2020
- Split Concordia Merit Scholarship, 2018